ISSN: 2754-4753

Journal of Physics & Optics Sciences

SCIENTIFIC Research and Community

Research Article

Open Access

Periodic System of Isotopes

AS Magula

Ukrainian Nuclear Society, Kharkiv, Ukrainian

ABSTRACT

With the help of a special algorithm being the principle of multilevel periodicity, the periodic change of properties at the nuclear level of chemical elements was discovered and the variant for the periodic system of isotopes was presented. The periodic change in the properties of isotopes, as well as the vertical symmetry of subgroups, was checked for consistency in accordance with the following ten types of the experimental data: mass ratio of fission fragments; quadrupole moment values; magnetic moment; lifetime of radioactive isotopes; neutron scattering; thermal neutron radiative capture cross-sections (n, γ); α-particle yield cross-sections (n, α); isotope abundance on Earth, in the Solar system and other stellar systems; features of ore formation and stellar evolution. For all the ten cases, the correspondences for the proposed periodic structure of the nucleus were obtained. The system was formed in the usual 2D table, similar to the periodic system of elements, and the mass series of isotopes was divided into 8 periods and 4 types of "nuclear" orbitals: s_n, d_n, p_n, f_n. The origin of "magic" numbers as a set of filled charge shells of the nucleus was explained. Due to the isotope system, the periodic structure is shown at a new level of the universe and the prospects of its practical use are opened up.

***Corresponding author**

A.S. Magula, Ukrainian Nuclear Society, Kharkiv, Ukrainian, Tel: +380675721418; E-Mail: magula@karazin.ua; carbon6@ukr.net

Received: May 14, 2021; **Accepted:** May 21, 2021; **Published:** June 07, 2021

Keywords: Periodic System, Isotope, Period, Subgroup, Nuclear Orbital, Nuclear Reaction.

Table of contents

Issues

A time is coming when the methods and technologies allowing nuclear reactions to be carried out at low energies will appear and the periodic system of isotopes will be in demand not only for a narrow circle of nuclear specialists. The periodic system of isotopes allows looking at a new level of the universe, into the atomic nucleus.

Today, there are at least 12 known models of atomic nucleus. Among them there are three models describing the existence and parameters of nuclear shells: the nuclear shell model, cluster model and statistical model. The nuclear shell model (D.D. Ivanenko, E.N. Gapon (1932); Maria Goeppert-Mayer, Johannes Hans Daniel Jensen, Eugene Wigner (1963), etc.) supports the concept that periodicity of the nucleus is not explicitly expressed due to the influence of particle interaction in a dense nucleus, but still exists on the basis of nucleon numbers called magic. Magic numbers for protons are 2, 8, 20, 50, 82, 114, 126, 164; for neutrons – 2, 8, 20, 28, 50, 82, 126, 184, 196, 228, 272, 318. The model shows that the most stable nuclei contain a specified number of protons and/or neutrons, similar to inert gases in the periodic system of elements.

In the cluster model, it is suggested that the nucleus consists of an α-particle and smaller clusters rotating towards the common gravity center of the nucleus. Also, the cluster model is used to explain the properties of light nuclei. In the statistical model (Jacob Frenkel, 1936; Lev Landau, 1937), the nucleus is considered to be a Fermi liquid of nucleons. The statistical model is used to describe the energy level distribution and the probability distribution of quanta emission at the transition between the high-lying excited states of the nucleus; it allows taking into account the corrections related to the presence of shells in the nucleus. As a rule, periodic systems of isotopes are constructed using the nuclear shell model.

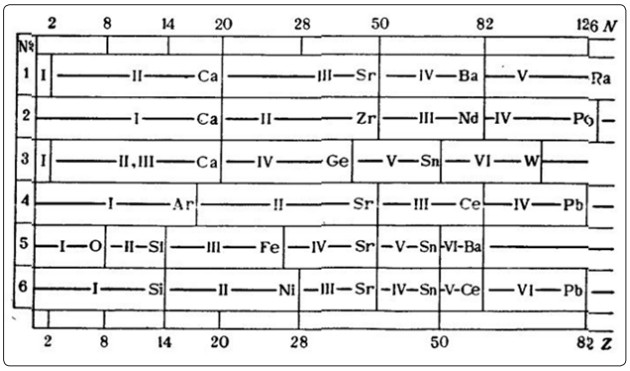

Figure 1: 6 variants for the periodic system of isotopes [1]

Nowadays, there are over 60 variants of construction for *periodic systems of isotopes*. These variants of consruction differ depending on the following nuclear characteristics: *A* is the mass number of isotopes; *Z* is the ordinal number of the element; *N* is the number of neutrons. When constructing the isotope system, the composite indicators of nuclear differentiation are also used: I_d=A-2Z is the number of excess neutrons; Z/A is the specific charge of the nucleus; N/Z; N/A, etc. The use of such composite indicators as Id, Z/A, N/Z, N/A, as a rule, makes the systems more complicated without giving any new information about the structure. When using separately the charge number *Z* and/or the number of neutrons *N* for system construction, as a rule, a series of "magic" numbers completing the shells is distinguished. In 1933-1934, Walter Elsasser concluded that the nuclei with the number of protons or neutrons equal to 2, 8, 20, 50, 82, 126 have special stability. These numbers were later called "magic numbers". While trying to give a theoretical justification for the abovementioned regularities, Elsasser suggested that each nucleon of the nucleus moved in the averaged field of other nucleons, considered the quantum-mechanical problem of nucleon motion in a quantum well of rectangular shape and found the order of filling the levels for the nuclear shell structure.

Almost all the periodic systems are constructed empirically on the basis of the analysis of such properties as: abundance, stability, binding energy, reaction cross-section, etc. In many cases, the outer shells are smaller than the internal ones (fig. 1). This is unusual for the spherically organized systems. The criteria of "magicalness" for mass numbers are also not obvious. In the paper of M. Goeppert-Mayer, J.H.D. Jensen, "The elementary theory of nuclear shell structure", the following criteria of "magicalness" are highlighted: prevailing adundance of one isotope in the natural mixture; cosmic nuclear abundance; small cross-section of neutron absorption; greater number of stable nuclei; increased resistance to various types of decay. If the abundance of one isotope in the natural mixture is determined with sufficient accuracy, the cosmic abundance is rather inaccurate because of the limited methods of calculation and selective temporal coverage in comparison with the lifetime of the universe [2]. Many isotopes have a small neutron absorption cross-section and the increased resistance to various types of decay, but they are not "magic". When using this approach, it is possible to only partially classify the nuclei by properties, and it is impossible to correctly identify the shell type – period, orbital. As a result of such confusion, a sufficiently large number of variants for the isotope system was created (60). Thus, the current situation on the periodic system of isotopes can be explained by the statement of V.I. Semishin [3]: "There is a number of attempts to create the periodic system of isotopes, which, similar to the periodic system of chemical elements, would explain the connection of various characteristics of isotopes with their mass number and nuclear charge, and also would allow predicting the properties of not yet discovered isotopes. However, the system that could be considered successful, at least in the first approximation, does not exist to date".

It became possible to overcome the confusion and construct the periodic system of isotopes by solving the following two issues:

1. Discovering the principle of multilevel periodicity, which made it possible to determine the magnitude of nuclear periods and orbitals (for more detail, see Section 3).
2. Defining a clearer (numerical) criterion for "magicalness" of mass numbers (see Section 10).

The periodic system of isotopes is formed similarly to the Mendeleev's periodic system of elements as a 2D table. The mass sequence of stable isotopes is divided into 8 periods of 2, 12, 40 and 100 isotopes. Each of them is repeated twice. The periods consist of the following nuclear orbitals: s_n, p_n, d_n, f_n of 2, 10, 28, 60 nucleons, respectively.

With the help of the periodic nuclear structure, it became possible to explain the following phenomena:

1. The mass asymmetry of fragments (2:3) formed at heavy nuclear fission (A>230) is the consequence of the periodic nuclear structure. At fission, the "double-humped barrier" isotopes are formed. These isotopes are arranged in the same subgroups of dn-orbitals, but in different periods.
2. The values of the quadrupole moment *Q* are anomalous within the following nuclear ranges: 150<A<190 and A>220. The qadrouple moment of isotopes within the described nuclear ranges is on average 10 times greater than of other isotopes. This phenomenon corresponds to the periodic structure and is caused by the beginning of filling the massive nuclear orbital: f_n-orbitals of the period 7 (148≤A≤208) and d_n-orbitals of the period 8 (220≤A≤248).
3. Nowadays, there is a number of papers showing that cosmic abundance of isotopes is determined by nuclear properties rather than by astrophysical ones (for example, O. Korobkin et al. 2012, and others; for more detail, see Sections 6 and 7) [4]. When comparing the astronomical observations to the periodic structure of the nucleus, it is established that the mass boundaries of isotope synthesis in stars correspond to the periodic structure (for more detail, see Section 7).
4. A distinctive feature of ore formation for the planetary material formed by the stellar matter ejection is the joint concentration of minerals, the main isotopes of which are located in the same or adjacent subgroups.
5. Distribution in accordance with the periodic structure of the nucleus is demonstrated by the nuclear magnetic moment.
6. It was established that the magnitude and sign of the coherent neutron scattering length depend on the period number.
7. The increased values of thermal neutron capture in the isotopes with A=113 and A>148 are the consequence of structural transitions to the massive nuclear shells.

The knowledge on the periodic structure of the nucleus opens up the prospects similar to those of inorganic chemistry at the end of the nineteenth century.

The Principle of Multilevel Periodicity of the Atom

The periodic law has no expression in the form of a formula, so the dimensions of the shells are established empirically. The number of electron quantum states is fixed for each shell of the orbital or period. In modern physics, such a fixed number is calculated using a combination of 4 quantum numbers: n, l, ml,

ms. The angular momentum of a particle is related to the last three numbers. The spatial distribution of momentum is calculated with the help of operators; the Hamiltonian operator, which has 3 spatial coordinates, is the most commonly used. The meaning of the periodic law is similar to that of the Hamiltonian operator in quantum mechanics. The Hamiltonian shows the spectrum of quantum parameters for the system and its evolution in space and time. Considering that the universe becomes heavier as a result of the synthesis of new elements, the periodic law shows the evolution of chemical element charge in the universe in a "discrete spectrum" (table) on a large time scale. In both cases, a common task is to show the evolution of atomic structures in space and time.

Construction of the isotope periodic system became possible due to the discovery of a special algorithm for determining the size of atomic shells – the principle of multilevel periodicity. It is noted that the binomial coefficients included in the Pascal's numerical triangle show the number of possible quantum states for a pair of electrons in different shells, and arrangement of the coefficients in the triangle corresponds to a particular shell — orbital or period (fig. 1a).

This algorithm is formed on the basis of the following observations:
- by now, several types of resonance receiving electric or magnetic signals from various substances have been detected (nuclear magnetic resonance (NMR), nuclear quadrupole resonance (NQR), electron magnetic resonance (EMR), paramagnetic (EPR), ferromagnetic (FR), antiferromagnetic resonance (PRA), as well as optical resonance, paraelectric resonance, resonance absorption of γ-radiation, etc.). All these types of resonance have multiplet signals. A multiplet in spectroscopy is a series of closely spaced spectral lines that appear as a result of splitting one line, for example, under the influence of electron spin. The area of signals or the width of multiplet lines is proportional to the numbers in the rows of the Pascal's triangle, their sum or other combination. In nuclear physics, the multiplet has a more general meaning: it is a group of hadrons having approximately the same mass and similar properties;

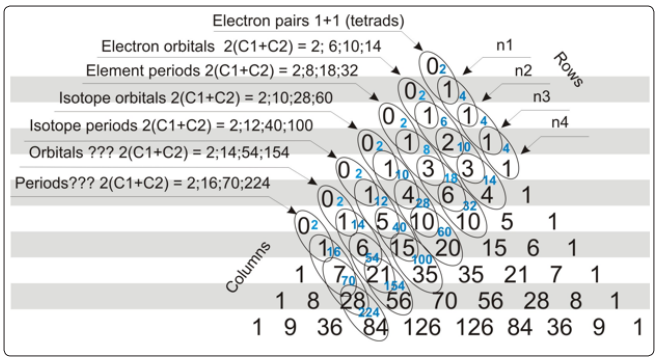

Figure 1a: The Pascal's triangle. The principle of multilevel periodicity

- in the well-known experiments on the diffraction of photons, electrons and more massive particles (photons in the Jung experiment, 1803, electrons in the Davisson-Germer experiments, 1927, and Jensen, 1961, fullerenes C60 in the Zeilinger experiment, 1999) in the absence of an "observer", when the particles behave like a wave, the trace of interference fringe pattern appears on the screen [5, 6]. The fringes of the pattern are proportional to the binomial coefficients of the Pascal's triangle;
- based on the fact that many processes in physics and nature in general (probability distribution, wave processes, quantum processes) are modulated by the normal distribution, it is assumed that within the normal distribution function, there is an algorithm of matter differentiation into the evolutionary stages.

The binomial distribution is the closest to the normal distribution having a simple decomposition algorithm. The binomial distribution is considered to be the most common type of discrete distribution.

The multiplet nature of signals at such different levels of atomic composition as electron and nucleus shows that at these levels there are general regularities caused by similar conditions or environment. It should be assumed that the proportionality to the binomial coefficients in the abovementioned experiments and cases of electron and nuclear magnetic resonance is a result of changes in the properties and degrees of freedom for the configuration spaces at different levels of atomic structure. Taking into account the observation that during interference, the fringe intensity on the screen is proportional to the binomial coefficients, it should be assumed that the configuration spaces are formed by the wave processes inside the atom. The assumption on the change in the configuration spaces also follows from the observation that the numbers in the rows of the Pascal's triangle reflecting the proportionality of multiplet signals show the number and dimensions of geometric figures involved in the Cartesian coordinate system at the increase of the degrees of freedom (dimensions) *n*. The row 1: 1 1, 1 point, 1 line, n=1; the row 2: 1 2 1, 1 point, 2 lines, 1 plane, n=2; the row 3: 1 3 3 1 – 1 point, 3 lines, 3 planes, 1 3D space, n=3, etc. (for more detail on n>3, see paper) [7]. Thus, the multiplet nature of signals for the electron and nuclear magnetic resonances can be the result of appearing wave spatial structures with the degree of freedom n at different levels of atomic composotion, where configuration spaces form the multipulse system of several levels and are fundamental in the formation of shells and signals from them. In accordance with the principle of multilevel periodicity, the nuclear shell should be considered as a superposition of the systems with the degrees of freedom changing from 2 to 7 (2-7 are the rows of the Pascal's triangle, fig. 1-a). There is nothing unexpected or surprising in the fact that the multilevel periodicity can follow from the numerical table; quantum mechanics of electron shells is based on the following 4 sequences of numbers: n, l, m_l, m_s.

The Hamiltonian type depends on the coordinate system composition. In this connection, it should be assumed that the solution spectrum of the Schrödinger equation for nucleons can be brought nearer to the periodic regularities by bringing the Hamiltonian type into correspondence with the configuration space of the studied nuclear (atomic) structures. A separate study is devoted to this assumption. In this study, a quantum-mechanical justification is given for the principle of multi-level periodicity [8]. However, the extensive calculations included in the description of the method for checking the assumption using the mathematical physics equations may reduce the initial interest. Therefore, it is more convincing to start directly with checking the final results. As in case of periodic law, the results follow from the empirical assumption that the periods for the system of elements have duration of 2, 8, 18, 32, as well as vertical connections in the subgroups. For the periodic system of isotopes, this assumption is somewhat more justified and is such that the development of the Pascal's triangle shows the number of possible quantum states for the pairs of nucleons in accordance with the principle of multilevel periodicity (fig.1-a).

In addition to the numbers showing the number of elements in the electron orbitals and periods, the numbers that determine the number of nucleons in the nuclear periods and orbitals can be

obtained from the Pascal's triangle. The Pascal's triangle should be represented as a table of slanted columns and rows. The corresponding rows and columns are the same. If the number of adjucent columns $2*(C_1+C_2)$ is doubled, the number of allowed states for the particles in periods and orbitals will be the result. Each row shows a certain level of atom constitution (fig. 1-a). For example, paired sums of the slanted column 3 (1, 4, 9, 16) are the sequence of squares for the principal quantum number *n*. Doubled sums of numbers in the column (2, 8, 18, 32) are equal to the number of elements in the periods for the system of elements. The sequence 1, 4, 9, 16 is found in the formulas of Bohr orbits for a hydrogen-like atom: $r_n=n^2a_0$; $r_1=1a_0$; $r_1=4a_0$; $r_1=9a_0$; $r_1=16a_0$; in the expressions for determining the potential energy of electron in a hydrogen-like atom $E = -kz^2/n^2$, etc. The number of nucleons in the orbitals and periods of isotopes is show by the paired sums of slanted columns 4 and 5. To calculate the number of elements (isotopes) for different periodic structures of the atom, the numbers of the adjucent rows should be summed up in pairs and the result should be doubled: $2*(C_1+C_2)$, where n is the number of slanted columns, 1 is the electron pairs; 2 is the atomic orbitals; 3 is the periods for the Mendeleev's system of elements; 4 is the nuclear orbitals; 5 is the periods for the system of isotopes. The following calculation results will be obtained: column 1:2 (electron pairs); column 2: 2, 6, 10 and 14 – the number of electrons in the orbitals *s*, *p*, *d*, *f*; column 3:2, 8, 18, 32 – the number of chemical elements in the periods; column 4: 2, 10, 28, 60 – the number of nucleons in the nuclear orbitals; column 5: 2, 12, 40, 100 – the number of nucleons in the nuclear periods. This algorithm is called the principle of multi-level periodicity of the atom.

The Principle of Multi-Level Periodicity: *The doubled sum of the adjacent numbers from the slanted row of the Pascal's triangle $2*(C_1+C_2)$ shows the number of possible states for the quantum system at different levels of atomic structure. The number of slanted row determines the level of atomic structure: 1 – electron pairs; 2 — electron orbitals (2, 6, 10, 14); 3 – periods of elements (2, 8, 18, 32); 4 — nuclear orbitals (2, 10, 28, 60); 5 – nucleus periods (2, 12, 40, 100), etc. The number of horizontal row shows the degree of freedom for the system from 1 to n.*

In accordance with the fundamental principle of quantum mechanics, the Pauli exclusion principle, two or more identical fermions (electron and other particles with a half-integral spin) cannot simultaneously be in the same quantum state. If the principle is applied to the synthesis and decay processes of elements and nuclei, then this principle can be rephrased: *any quantum system in the course of its evolution goes through the discrete stages, the number of which is determined by the number of non-repeating combinations of quantum numbers for the total number of possible*. The number of possible evolutionary combinations can be determined using the Pascal's triangle as a numerical figure showing the development of spaces with the dimension n [7]. The Pauli principle refers not only to the "prohibition", but also to the principle of "non-repeating combinations" for the evolutionary cycles of quantum systems. From the point of view of understanding, the term "prohibition" is not completely well-fitting and leads away from studying the evolution of quantum systems as a whole. In this aspect, the periodic system of isotopes shows the synthesis and decay cycles of isotopes in nature only for stars so far.

The properties of the Pascal's triangle known as a table of binomial coefficients are well described by the American mathematician and writer Martin Gardner: "*the Pascal's triangle is so simple that even a ten-year-old child can write it out. At the same time, it harbors inexhaustible treasures and binds together various aspects of mathematics, which, at first glance, have nothing in common with each other. Such unusual properties make the Pascal's triangle one of the most elegant schemes in all mathematics*".

The Periodoc System of Isotopes

For convenience of analysis, the periodic system of isotopes is constructed in the usual flat form. It should be noted that the shape of nuclear orbitals and the properties of the Pascal's triangle, which are described below, show that there may be other forms. The slanted column 5 of the Pascal's triangle shows that in the periods of the isotope system there are 2, 12, 40, 100 nucleons (protons and neutrons). As in the Mendeleev's periodic system, each of the periods of the same length is repeated twice (8, 8, 18, 18, 32, 32). The periods 1 and 2 consist of one s-nuclear (s_n) orbital of 2 nucleons each; the periods 3 and 4 consist of s_n (2) and p_n (10) orbitals of 12 nucleons each; the periods 5 and 6 consists of s_n (2), p_n (10) and d_n (28) orbitals of 40 nucleons each; the periods 7 and 8 consist of s_n (2), p_n (10), d_n (28) and f_n (60) orbitals of 100 nucleons each. The period 8 (A = 209-308) is not completely filled, since stable isotopes heavier than U^{238} do not exist in nature.

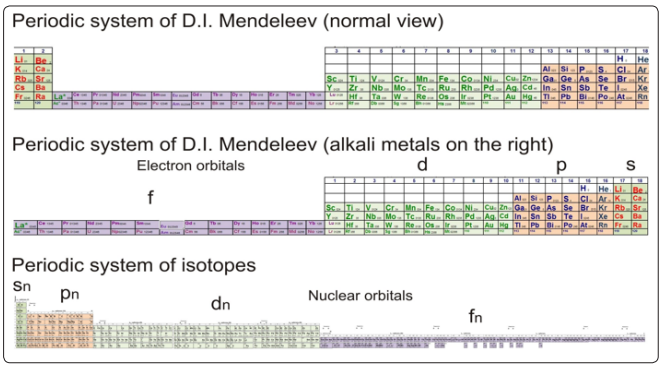

Figure 1-b: The similarity of periodic systems

It is important to note that there are two logical inconsistencies in the usual form of the periodic system of elements:

1. All the periods are repeated twice, except for the first one.
2. Electron orbitals are filled in the following order: *s*, *f*, *d*, *p*, i.e. the smallest orbital is arranged at the beginning of the period; the smallest orbital is followed by the largest f-orbital, and then – by d and p-orbitals.

Both logical inconsistencies can be overcome, if the first and second subgroup containing alkali metals are put in the table on the right, i.e. behind inert gases (fig. 1-b). The sequence of increasing atomic numbers and the periodic law are not violated, only the interpretation will be changed. Thus, the orbitals in the periodic system of elements can be represented in decreasing order: *f*, *d*, *p*, *s*. In the system of isotopes, the orbitals are arranged, on the contrary, in increasing order.

It is important to emphasize that the orbitals and periods (cycles) of nuclear isotopes in the system are formed under the influence of nuclear forces, in contrast to the periodic system of elements, where the periodicity of properties is based on the action of "electron" forces. Nuclear reactions mainly occur in stellar interior, in high-energy environments, with complete or almost complete ionization, where the electron shells are not formed or completely absent and do not affect the course of reactions. Therefore, in the subgroups of the isotope system, there are the elements with different chemical properties, and the chemist's usual way of thinking should be switched to the nuclear physicist's way of thinking. As it is shown is the analysis, the periodic structure of the nucleus can be observed when considering the following

nuclear characteristics and phenomena: nuclear quadrupole and magnetic moments; neutron scattering lengths for nuclei; natural abundance of isotopes; mass ratio of nuclear fission fragments; stages of stellar evolution, ore formation regularities, neutron capture cross-section and other nuclear reactions.

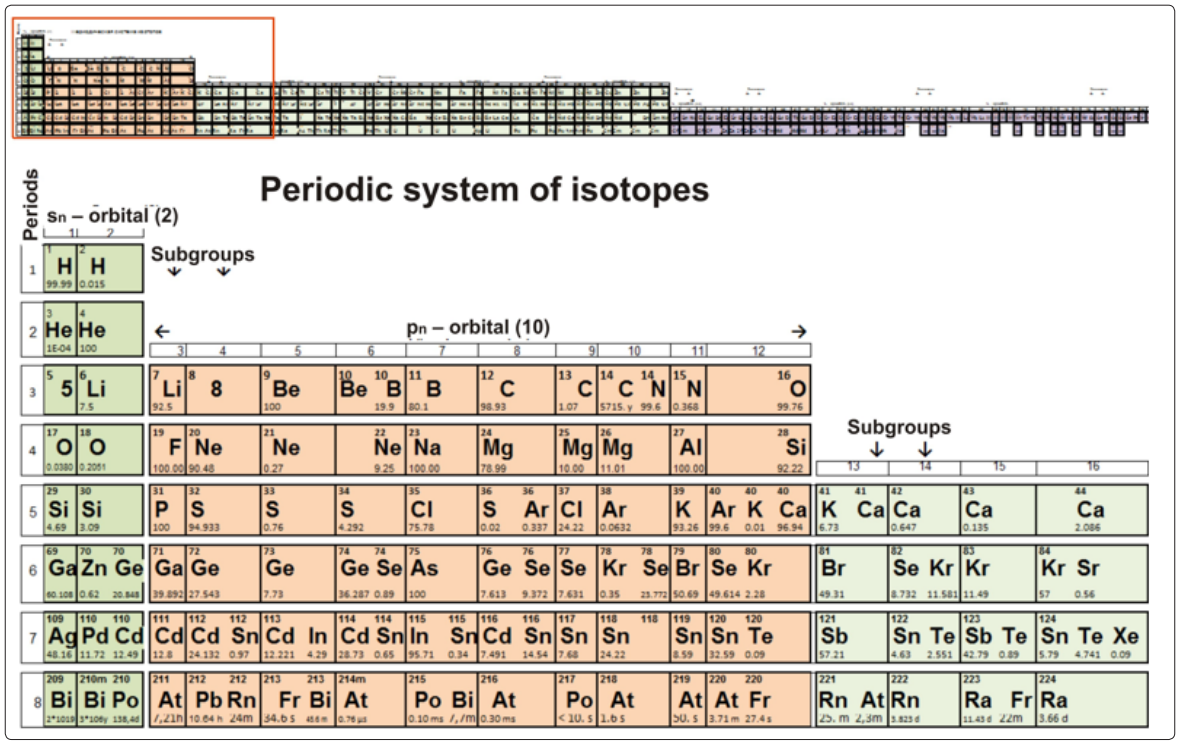

Figure 2-a: The periodic system of isotopes, sn, pn-orbitals and the beginning of dn-orbital. Sheet 1.

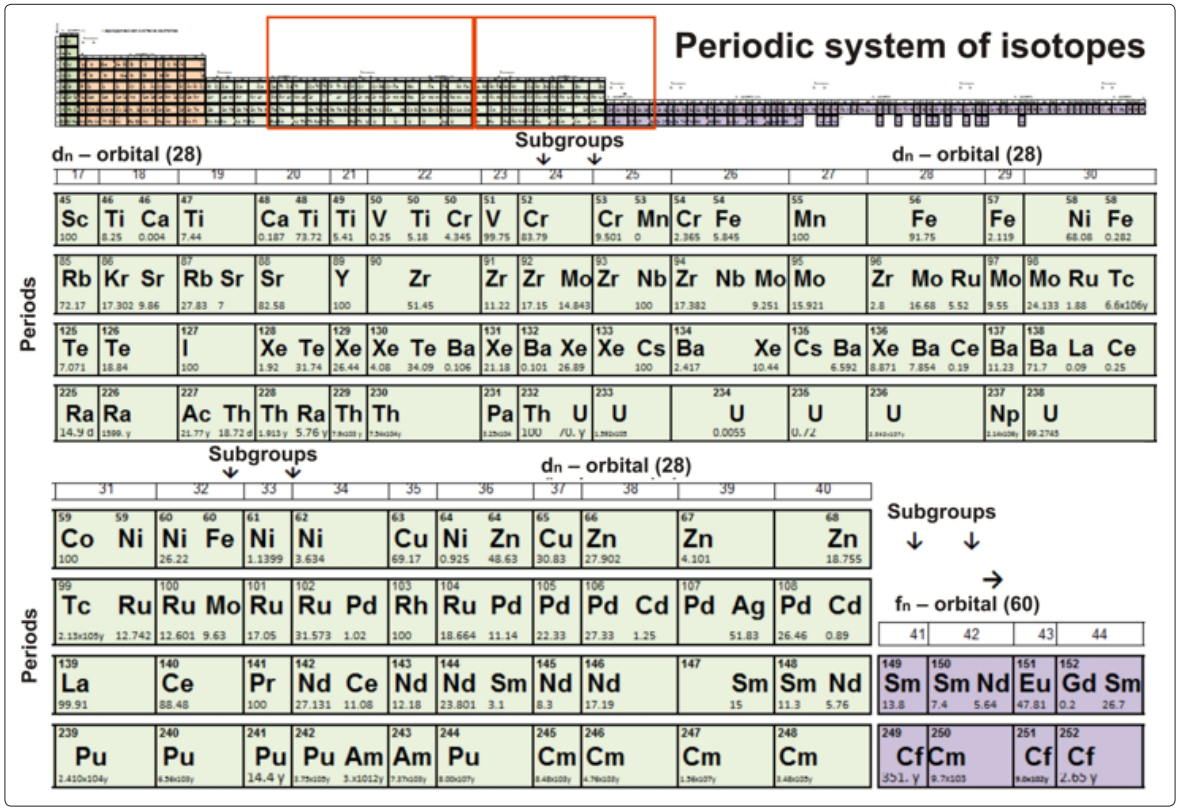

Figure 2-b: The periodic system of isotopes, dn-orbital (the beginning of fn-orbital). Sheet 2.

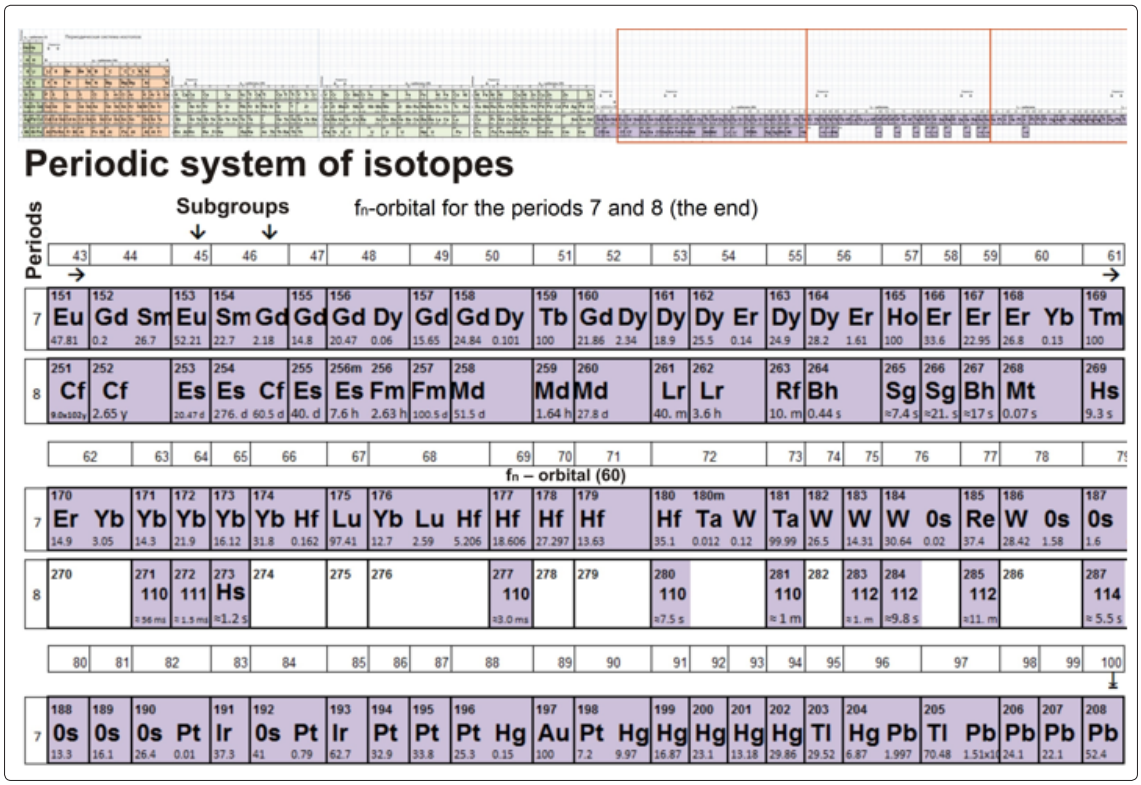

Figure 2-c: The periodic system of isotopes, fn-orbital (the end). Sheet 3.
As the fn-orbital has linear extension, it is presented in fragments to save space.

Fragment Mass Asymmetry at Nuclear Fission

It is interesting to start analyzing the regularities of the isotope periodic system by considering one of the unsolved issues of modern physics. Nuclear fission is a powerful source of energy that has been used by humanity for over 50 years. Among the fission products of heavy nuclei there are the atoms with nuclear mass numbers (A) within the intervals of 90-105 and 130-148. The nuclei of these fragments make up about 90% of all the fission products and are distributed within the mass ratio of 2:3. For modern nuclear models, such a distribution is anomalous. No satisfactory explanation for the mass asymmetry of fission fragments and, as a consequence, of fission mechanism itself has been found yet.

Due to the periodic system of isotopes, it becomes possible to explain why the fission fragments of heavy nuclei are distributed within the mass ratio of 2:3. The periodic system also makes it possible to understand the fission mechanism based on the structural features of the nucleus. In fig. 2-a, the mass distribution of fission fragments for heavy nuclei is shown: ^{234}U, ^{236}U, ^{240}Pu, ^{252}Cf, ^{256} Fm, as well as the boundaries of nuclear orbitals and periods. In fig. 2-b, the mass distribution of fission fragments for heavy nuclei is shown: ^{235}U and ^{241}Pu, depending on the kinetic energy of neutrons (thermal neutrons, fast neutrons and 14 MeV neutrons), as well as the boundaries of nuclear orbitals and periods. The peaks of the double-humped fission barrier for the nuclei described above are arranged within the d_n-orbitals for the periods 6 and 7 of the isotope system. If the peaks are arranged in accordance with the subgroups, they are arranged symmetrically, one below the other.

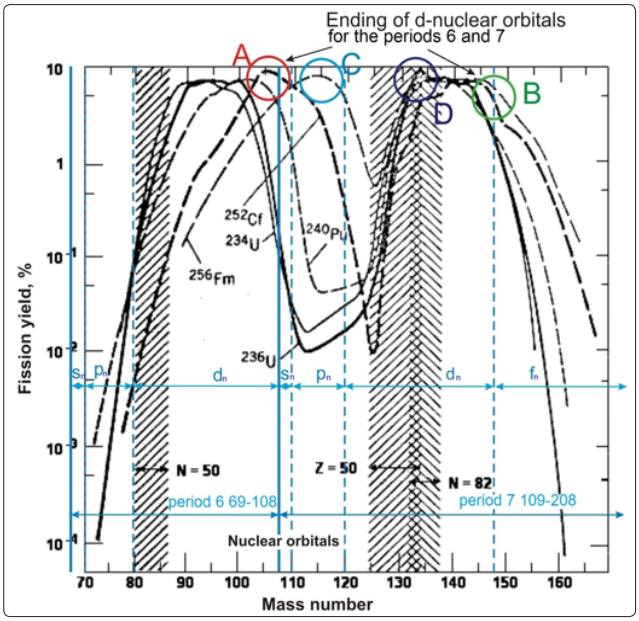

Figure 3-a: Analysis for the mass distribution of fission fragments by thermal neutrons ^{233}U, ^{235}U, ^{239}Pu, as well as for spontaneous fission of ^{252}Cf, ^{256}Fm together with the arrangement of the periods and orbitals for the isotope system [9].

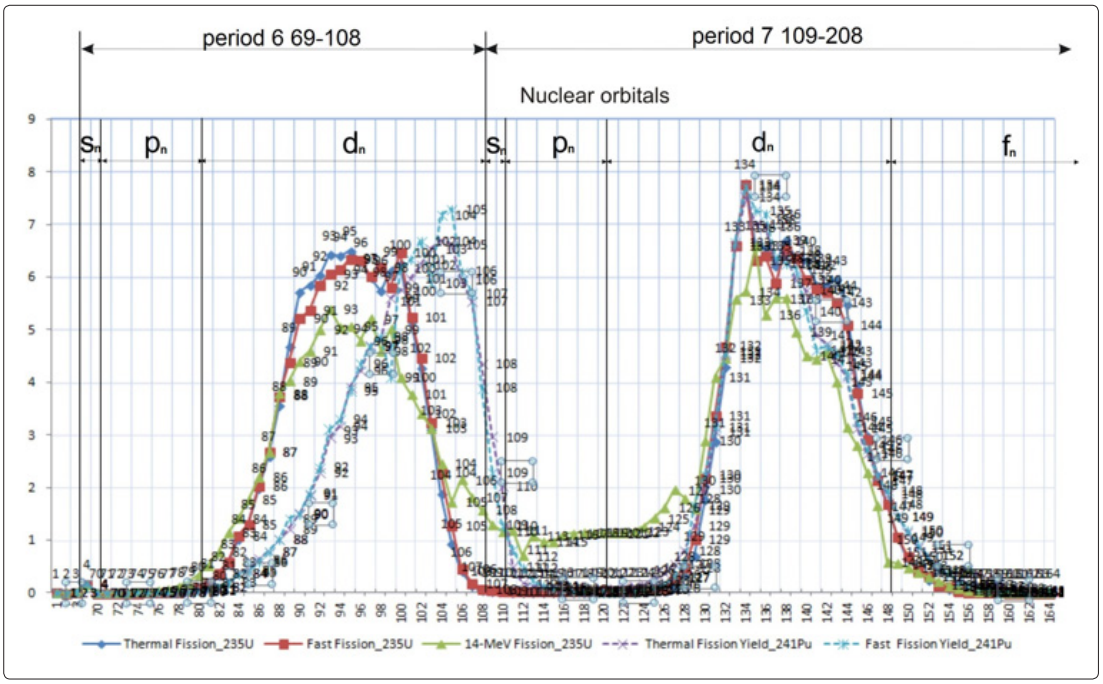

Figure 3-b: Fission products of U^{235} and Pu^{241} for different energy values and the periodic structure of the periods 6 and 7

In fig. 3, the graph for the "double-humped barrier" of ^{235}U nuclear fission is divided in two and arranged in the isotope system in accordance with the subgroups of the periods 6 and 7. Three curves correspond to the neutrons with different kinetic energy (thermal neutrons, fast neutrons and 14 MeV neutrons). The arrangement of nuclei for natural isotopes with the "magic" numbers *p* and *n* are shown with shaded regions in fig. 3. The symmetry of peaks for the fragment mass of the "double-humped" barrier is also observed in accordance with the periodic structure of the nucleus.

Analysis of the graphs for the fragment yield of the "double-humped" barrier together with the arrangement of the isotope system periods and orbitals (figs. 2 and 3) allows revealing the following main features of the fission mechanism:

1. In the process of fission, the nuclei of fragments consisting of completed nuclear shells (periods) and nucleon remnants are formed. Composition for the central part of the nucleus is formed by the completed periods. Asymmetry of the mass ratio for the "double-humped barrier" fragments ≈ 2/3 (0.6 (6)) is determined by the magnitude of periods. For the light part of the double-humped barrier, the central nuclear shell is formed by the period 5 (A=68), for the heavy part – period 6 (A=108), 68/108=0.629. The outer layers of the nucleus are formed by the nucleon remnant.
2. For the nuclei with the mass number of about A≤250 (^{233}U, ^{235}U, ^{239}Pu), the peaks of the "double-humped" barrier are distributed symmetrically in accordance with the periodic structure of the nucleus within the dn-orbitals in the subgroups 18–40 (figs. 2 and 3), for the light part of the barrier – in the period 6, for the heavy part – in the period 7. The graph, in which the yield of ^{235}U fission fragment is represented, has a more detailed resolution by mass numbers (fig. 3-b). It is also shown in the graph, that the double-humped barrier peaks for the periods 6 and 7 have different widths (fig. 4-b). The peak for the heavy group of fragments (period 7) is narrower than the peak for the light group of fragments (period 6) by the mass number of about 2, which corresponds to the yield of fast neutrons at the beginning of the fission process due to the outer (heavy) part of nuclear shells (first 10^{-14} s). Since the values of the periods are fixed and the value of the nucleon remnant depends on the nuclear mass of fission ancestor, for the nuclei with A ≥ 250, where the average constitution of the nucleon remnant for each barrier peak approaches the sum of s_n, p_n and d_n-orbitals – 40 nucleons (2 + 10 + 28), the gap in the "barrier" graph becomes narrower. For 252Cf nucleus, the average nucleon remnant at the peak is equal to: $A_{rem252}=(A_{252}-A_{7per}-A_{6per}-A_{free.n})/2=(252-108-68-2)/2=36-37$,

where A_{6per} and A_{7per} are the mass numbers of completed shells for the periods 6 and 7; $A_{free.n}$ is the mass of free neutrons escaping at fission.

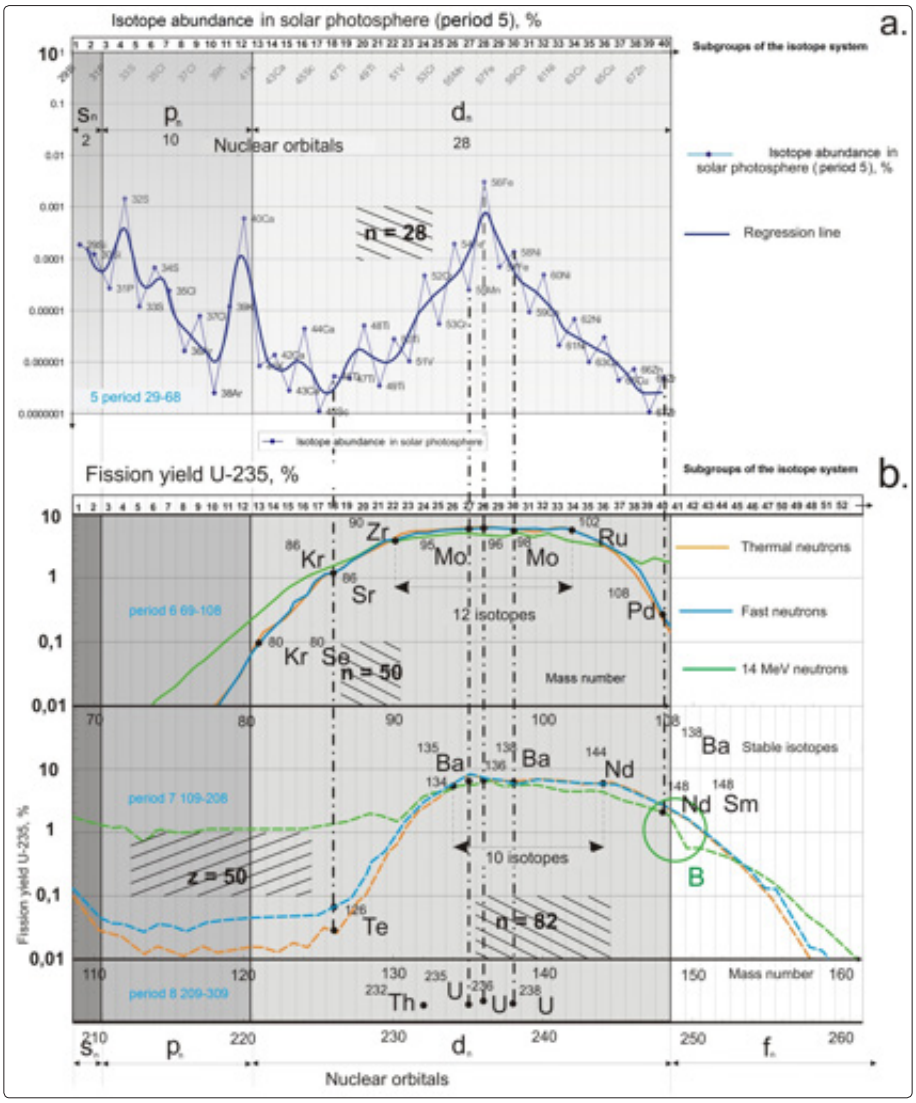

Figure 4: Symmetry for the periodic system of isotopes: distribution of 2 peaks for the mass numbers of fragments at fission of ^{235}U – the periods 6 and 7 (b); abundance of isotopes in the solar photosphere – the period 5, "iron peak" (a).

On the graph for the light part of fission fragments, a characteristic maximum is observed at the boundary of the periods 6 and 7 (the "A" region, fig. 3-a), the remnant tends to maintain the distribution within the completed d_n-orbital of the lighter period 6. For the heavy part of fission fragments, all the fission ancestors at the boundary of d_n- and f_n-orbitals for the period 7 have a sharp drop in the number of fission fragments (the "B" region, fig. 3-a), and the maximum is not observed. Presence of a maximum shows that the average distribution of nucleon remnant between the light and heavy parts of A≥250 nuclei is asymmetric. The formation of light fission fragments turned out to be more energy-efficient than the formation of heavy fission fragments in the massive fn-orbital for the period 7. At further increase in the mass number (^{256}Fm), the asymmetry of the nucleon remnant distribution is even stronger. The peak of the graph for the light part of the "barrier" is shifted abruptly beyond the boundaries of the period 6 to the beginning of the period 7 (the "C" region, fig. 2-a). It turns out that going beyond the dn-orbital of the period 7 (beyond the "B" region), as well as filling the fn-orbital, is less energy-efficient. Therefore, the excess of nucleon remnant is compensated due to the increase in the mass of fragments for the light part, and the barrier peaks approach each other. At fission of ^{235}U neutrons with the energy of 14 MeV, the boundary for dn or fn-orbitals is defined even more clearly than for fast and slow neutrons due to a sharp decrease in the graph (A=148), in which the yield of fission fragments drops by almost an order of magnitude (the "B" region, fig. 4-b)

The symmetry of the "two-humped" barrier, as well as the arrangement of "A", "B" and "C" extremes (figs. 4-a and 4-b), shows that the mass distribution of fission fragments occurs in accordance with the periodic structure of the nucleus. The "B" region is the boundary for the d_n and f_n-orbitals of the period 7; the "A" and "C" regions are the extremes which exist on both sides of the boundary for the periods 6 and 7. Such a structural organization corresponds to the division of the mass line of isotopes by the periods and orbitals in accordance with the principle of multi-level periodicity.

3. Periodicity of the peaks for the "double-humped" barrier is also shown in the period 5. In fig. 4-a, the graph of the isotope distribution for the period 5 in the solar photosphere is presented. In the period 5, there are no fission fragments, but the dn-orbital is included, just like in the periods 6, 7 and 8. It is easy to notice that within the d_n-orbital there is a region ("iron peak") that is symmetric to the peaks of the two-humped barrier, as well as to the fission ancestors. The top of the peak is ^{56}Fe isotope arranged in the center of the dn-orbital, in the subgroup 28. In accordance with the various estimates, ^{56}Fe takes the 1st-3rd place in terms of

isotope abundance on Earth. The isotopes 54Fe, 58Ni are arranged in the subgroups 26 and 30, and occupy the 5th and 6th place in the mass abundance scale.

4. Arrangement of natural isotopes, fission ancestors of ^{235}U and ^{238}U (fig. 4), is also symmetric with respect to the peaks of the "double-humped" barrier and the "iron" peak in the subgroups of the dn-orbital for the period 8 (figs. 4-a and 4-b). The nuclei ^{238}U and ^{235}U, together with ^{232}Th, are heavy, long-lived radioactive isotopes with a lifetime at the level of stable isotopes. Among the isotopes of the period 8, such nuclei are no longer present. Moreover, the heavy isotopes ^{238}U and ^{232}Th, among the elements presented in the period 8, have anomalously high abundance in the continental lithosphere – 0,000149% and 0,00073%, respectively. It is much higher than that of most light isotopes of the periods 7, 6, and 5. A long lifetime and high abundance shows that ^{238}U and ^{232}Th are the structurally advantageous nucleon configurations in the process of decay/synthesis of heavy nuclei in nature. ^{232}Th, ^{235}U and ^{238}U are arranged in the center of dn-orbital – the subgroups 24, 27 and 30.

5. Approximate arrangement of radioactive nuclei for the fission fragments with "magic" numbers is shown with cross hatching (Fig. 3-b) [9]. In the right part of the graph, this region covers the front, the first half of the peak and coincides with the maximum of the graph in the region of nuclei having 50 protons and 82 neutrons simultaneously (double hatching, z=50, n=82). In the left peak of the "double-humped" barrier, the regions in which the fission products are formed in the amount of only 0.1-1% of the total number correspond to the magic number of 50 neutrons (n=50). There are no magic numberts for about 70% of all the fission fragments of heavy nuclei. In fig. 4, the regions corresponding to the nuclei with "magic" numbers of neutrons or protons are shown with cross hatching. The heavy part of fission fragments is symmetric with respect to the region n=82. However, when forming the light part of the barrier, formation of the isotope with the magic number of protons and neutrons n=50 or z=50 is not a priority. The "light peak" is formed by the isotopes with n=50-60. The symmetry of the region with n=50 in relation to the center of the peak is not observed. A series of stable isotopes for the period 6 ("light peak") has 6 isotopes with n=50, 5 isotopes with n=58 and 60, and 4 isotopes with n=40 and 48. The difference in the abundance of 1-2 isotopes between the number of isotopes with the "magic" number 50 and the "non-magic" numbers (40, 48, 58, 60) is small and not obvious as a criterion of "magicalness". The isotopes with n=50 (^{86}Kr, ^{88}Sr, ^{90}Zr) are the most abundant among the nuclei of the period 6 (fig. 7, isotope abundance in the solar photosphere). At the same time, the most abundant isotope ^{56}Fe of the period 5 has no magic numbers (z=26, n=30). To solve the resulting contradictions, the nature of magic numbers and the degree of their influence on the nuclear structure should be clarified. Such contradictions do not allow accepting the "magic" numbers as the only determining criterion of stable nuclei formation. In section 10 (Origin of "magic" numbers), the numerical criteria for the "magic" numbers and shells obtained due to the principle of multilevel periodicity are analyzed and developed, their common features and differences are shown. The revealed characteristics of symmetry for the nuclei of the "double-humped" barrier, "iron" peak and natural isotopes of fission ancestors show that structural organization of the nucleus, in accordance with the principle of multi-level periodicity, is more consistent with the fission process of heavy nuclei.

The beginnings of the peaks for the double-humped barrier of the fission products at the mass number of A=90 and 134 are determined by the necessary minimum number of nucleons in the period for the formation of the closed shell around the core (completed shell of the previous period). For the period 6, the necessary minimum number is 22 nucleons, for the period 7, the necessary minimum number is 26 nucleons. The peaks of the "double-humped" barrier are shaped as a "table rock" with a flat upper section of 10-12 nuclei, with the maximum yield probability of ~5-6 % per isotope. In case of ^{235}U fission, A=90-102 for the light part and 134-144 for the heavy part (fig. 3). Distribution of natural isotopes within the "double-humped" barrier peaks and dn-orbitals has a pointed shape with clearly-defined peaks (iron peak), where the difference for the isotopes of the flat part is 1-2 orders of magnitude, and for the "bottom" of the peak – 2-3 orders of magnitude. Among the fission products, there are stable nuclei, but most nuclides are radioactive. Nuclides, in turn, undergo further radioactive transformations: the short-lived nuclides disappear and the new ones appear as a result of decay. The transformations are directed towards stable nuclei (^{88}Sr, ^{90}Zr, ^{92}Zr(Mo), ^{94}Zr, ^{96}Mo, ^{135}Ba, ^{136}Ba, ^{137}Ba, ^{138}Ba, ^{139}La, ^{140}Ce, ^{142}Nd), which are the structurally advantageous nucleon configurations. It should be assumed that the shape of the double-humped barrier peaks will be changed to a pointed one after a series of decays. The search for nucleon configurations within the period and orbital should be carried out via the study of isotope constitution in different realms of nature (bodies of planets, stars and galaxies). To determine the shape of nuclear shells, nucleon configurations should be identified. Preliminarily, it can be said that the most structurally advantageous nucleon configurations within the dn-orbital are the numbers of 24(12), 26(14), 28(16), 30(18) nucleons. These values are also the most probable mass numbers of the fragment yield at cluster radioactivity arising from the nuclei with A≥228 (see Section 12, Isotope lifetime, radioactivity and periodic structure of the nucleus). Different constitution and proportion of isotopes in the natural mixture shows that, along with structurally advantageous configurations, there are disadvantageous, less favorable and anomalous nucleon configurations (below).

Quadrupole Moment of the Nucleus and Periodic Structure

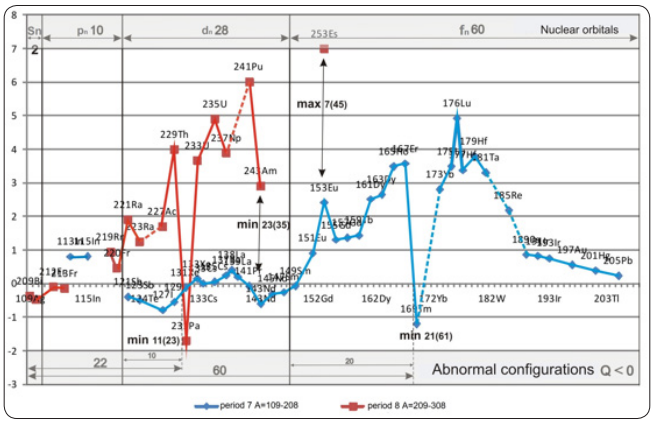

Figure 5: Quadrupole moment of the isotopes for the periods 7 and 8. Boundaries of the orbitals and abnormal configurations

As the mass is increased for a series of isotopes, the two clearly defined anomalies of the values for the external quadrupole moment of nuclei are observed. The quadrupole moment is observed for the isotopes having an odd mass number and unpaired nucleon. The exception is ^{176}Lu isotope, which has an odd number of both protons and neutrons. Outside the anomalies, the normal values of the quadrupole moment are within the range of -0.7-0.7 barn (1 barn=10-24 cm^2). Within the nuclear ranges of 150<A<190 and A>220, the values are on average 10 times greater than those of other isotopes. The magnitude and sign of the quadrupole moment

can be used to determine the magnitude of the charge deformation and the shape of atomic nuclei. For such anomalies, there is no explanation within the shell models. The quadrupole moments of nuclei with one or several nucleons followed by the magic numbers are well predicted by the shell model of the nucleus. The nuclear quadruple moment values, which are far from the magic ones, sometimes exceed calculations by an order of magnitude. The periodic isotope system allows explaining structural causes of these anomalies.

In fig. 5, the quadrupole moment distribution for the periods 7 and 8 is shown. The anomaly of 150-190 is related to the filling of the f_n-nuclear orbital. This orbital is the most massive and consists of 60 nucleons. The previous d_n-orbital is completed with a pair of stable isotopes ^{148}Sm, ^{148}Nd. The isotopes have a minimum negative moment, which corresponds to the nuclear shape close to spherical. The following is the isotope ^{149}Sm with one nucleon in the new f_n-orbital (the +1 configuration) and the minimum negative quadrupole moment Q=-0.075. After the first pair is formed in the orbital, the values are increased dramatically reaching the maximum for the nucleus ^{176}Lu, Q=4.92 (fig. 4). As the f_n-orbital and the period as a whole are completed in the region 189-208, the values of the quadrupole moment smoothly approach 0, which is expected for the completing nuclear shell. The nucleus gradually returns to the spherical shape of ^{205}Pb-^{208}Pb.

The second clearly defined anomaly of the quadrupole moment values arises at the transition of the p_n and d_n-orbitals of the period 8 for the nuclei with A>220. After A=220, together with the formation of the dn-orbital for the period 8, the quadrupole moment values are sharply increased ^{221}Ra(1,9), ^{233}U(3,66), ^{235}U(4,9), ^{241}Pu(6) exceeding the values in the initial s_n and p_n-orbitals of the period by an order of magnitude. As can be seen from the graph, both anomalies for the quadrupole moment of nuclei, as well as their deformation, clearly correspond to the boundaries of the orbitals in the periodic system of isotopes. The order of nuclear structure completion with nucleons and the quantitative characteristics of the internal force moments are determined by the periods and nuclear orbitals of the isotope system. It should be noted that within the interval of mass numbers $208 \leq A \leq 232$, there are no stable nuclei for the s_n, p_n orbitals and the beginning of the dn-orbital, except for ^{209}Bi, which also represents the +1 configuration of the nucleons. It should be assumed that the significant radius for the center of the nucleus, as well as the distance of the shell for the period 8 from the center, do not allow nuclear forces to come into engagement at the small number of nucleons at the beginning of the period and to form the closed shell up to the isotope ^{232}Th, which is the first advantageous nucleon configuration of the nucleon 24 in the period 8.

Near A=188, the quadrupole moment in the graph drops to less than 1, and the tent-like shape of Q distribution is changed to asymptotic. This change is characterized by the fact that a stable configuration of 40 nucleons, which is equal to the sum of mass numbers for the previous orbitals of the period s_n, p_n, d_n (40=2+10+28), is formed for the nucleus ^{188}Os in the outer f_n-orbital. This can be explained as a special case of secondary cyclicity within the period, when the orbitals are combined. This is known as the cases of *sp* or *spd*-hybridization of electrons. By filling the f_n-orbital, the nucleons form a configuration that is close to elliptical, and then, towards the end of the shell, the nucleus takes the form of a sphere with a stable orbital configuration — 60 nucleons (^{208}Pb).

At filling the f_n-nuclear orbital of the period 7 and the d_n-orbital of the period 8, there are 2 anomalous minima of the quadrupole moment observed for the nuclei ^{169}Tm (-1.2) and ^{231}Pa (-1.7). At the same time, it is observed that the nuclei arranged immediately after the filled orbitals or periods and having a +1 nucleon in the new shell, also have negative Q values: ^{149}Sm (-0,075), ^{209}Bi (-0,37), ^{221}Rn (-0,38). As the mass of +2, +3, etc. is increased, Q changes its sign and goes sharply upwards. In a series of stable isotopes for the period 6, when the mass number crosses the boundary of the p_n-orbital (A=120), the sign of Q moment is also changed from positive to negative (^{113}In (0,8); ^{115}In (0,81); ^{121}Sb (-0,4)). The values fluctuate within a small limit around 0 up to the end of the d_n-orbital. Within the d_n-orbital, weak deformations of the nucleus are observed. The isotope ^{121}Sb (-0.4) follows the filled pn-orbital (A=120) and is also the +1 configuration. The nuclei ^{169}Tm (-1,2) and ^{231}Pa (-1,7) can also be related to the +1 configuration of nucleons (^{169}Tm – 60+1 within the period; ^{231}Pa – 10+1 within the orbital). For the mass number A=168, there are 60 nucleons from the beginning of the period. This coincides with the number of nucleons for the f_n-orbital being a stable configuration with Q=0. For A=230, there are 22 nucleons from the beginning of the period and 10 nucleons from the beginning of the dn-orbital with the number of nucleons in the p_n-nuclear orbital (10), also with Q=0. Thus, the nuclei, whose number of nucleons from the beginning of the period or massive orbital is equal to the number of nucleons for one of the smaller orbital or period (A=168, 188, 230), demonstrate the properties of closed shells. This can be related to the cases of nucleon hybridization for the orbitals in the shell of the period.

The quadrupole moment anomalies and deformations fit into the periodic structure of the nucleus: the f_n-orbital of the period 7 and the d_n-orbital of the period 8 as a result of nuclear structural factors.

High positive values for the quadrupole moment of nuclei, in comparison with the negative ones, show the prevailing deformation of atomic nuclei along the z axis and the flattening of atomic nuclei in the XY plane within the quadrupole moment anomalies (fig. 6). This observation fits into the rotational model of non-spherical nuclei by J. Rainwater (1950). The model combines rotation of the entire nucleus as a whole and motion of individual nucleons in a non-spherical potential field, but does not explain the origin of rotational spectrum itself. Proof on the existence of deformed nuclei is the spectra of their excited states forming the system of rotational bands. Due to the generalized model of the nucleus (O. Bohr and B. Mottelson, 1952), large quadrupole moments of some nuclei were explained by the fact that the external nucleons of such nuclei deform the core (internal filled structures of the shell model) and it becomes prolate or oblate. In the nuclear gamma spectra, there are many levels that cannot be explained within the single-particle shell model (SSM is a quantum-mechanical continuation of the shell model). The studies have shown that in the nucleus there are excitations of collective type, during which the motion of large groups of nucleons is correlated. Within the liquid-drop model, the calculations were carried out to prove that the nucleus in the lowest excited states has the moment of inertia lower than 50% of the moment of inertia for a solid rotator with the same mass. Some part of nucleons is not involved in the rotational motion [10]. In general, it should be assumed that at the beginning and in the middle of massive shells for the f_n-orbital of the period 7 and the d_n-orbital of the period 8, the nucleus can be simulated as a disk-shaped vortex.

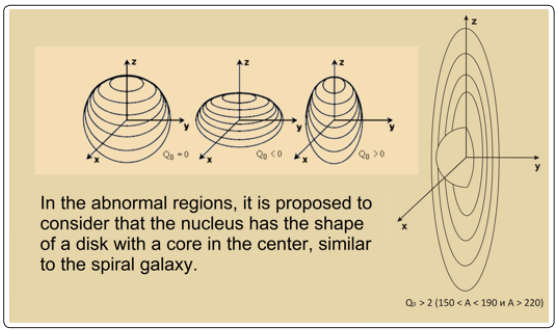

Figure 6: Nuclear shape in the abnormal areas

Natural Abundance of Isotopes and Periodic Structure of the Nucleus

In modern times, it is understood that all the constituent and surrounding matters are ejected from the depths of the stars as a result of supernova explosions and other stellar transformations. In geochemistry, extensive materials on the abundance of elements are presented. These materials are based on two main data sources: the measurement of matter composition available for analysis (the earth's crust, meteorites, comets, crust of terrestrial planets, atmosphere of giant planets, stellar photosphere) and results of hypothetical modeling for the composition of internal or inaccessible layers of the same objects. For 120 years of research, a great work has been done and a general picture on the abundance of elements has been revealed quite clearly. This primarily refers to the most common elements of O, Si, Al, Fe, Ca, Na, K, Mg and Ti, that is about 99.48%, almost the entire earth's crust. The remaining 80 elements are less than 1% and they are recognized as rare. The percentage abundance of most elements does not exceed 0.01-0,0001%. In the paper, a detailed analysis on the natural abundance of isotopes (in accordance with the data on the continental lithosphere; the solar system), as well as on the nuclear periodic structure, is presented [11, 12].

In modern geochemistry, the composition of rare elements in the earth's crust is determined by their correlation with more abundant elements. For example, if the content of sulfur in the earth's crust and the average content of sulfur, selenium and tellurium in sulfides are known, the ratio of selenium to sulfur as well as of tellurium to sulfur in sulfides can be calculated. Then, using the obtained coefficients and percentage of sulfur in the earth's crust, selenium and tellurium clarkes can be calculated. The clarks of these elements cannot be calculated directly, since their content in the earth's crust is lower than the minimum number of these elements determined by chemical analysis [13].

It is important to note that constitution of the nucleus and planet mantles, as well as of the inner layers of stars, is very hypothetical. It should be recognized that, perhaps, the common features of constitution for these spheres are determined correctly, but many important details are not yet available. When constructing the spectrum of element distribution, the data on 90% are not available for direct analysis, and in case of isotopes, this percentage is higher due to the inevitable insufficiency of data on the nuclear reactions in stars.

Determination of rare elements by correlation with the elements of one subgroup in the Mendeleev's periodic system inevitably leads to errors. The matter is synthesized in stars under the conditions of ultrahigh temperatures and complete or almost complete ionization. As is known, the electron shells, which determine the similarity of elements in the periodic system, practically do not participate in the processes of nuclear transformations. Only the external thermodynamic conditions and the internal structure of the nucleus can influence the synthesis process. For this and other reasons, for example, the abnormally low clarks of the elements: N, Se, Te, Mo, Ru, Rh, Pd, Re, Os, Ir, etc. may be reconsidered to a different extent. The periodic system of isotopes will be useful for more detailed definition of clarke numbers.

In general, the existence of periodic isotope abundance in both planetary and stellar systems is shown as a result of analysis. However, it should be recognized that a sufficiently large amount of geochemical data is obtained hypothetically or indirectly, and a large number of inaccuracies should be expected. Therefore, further study on the influence of nuclear structure in the realm of nature, along with the abundance of isotopes, requires introduction of additional data on the course of stellar evolution processes into the range of data analyzed.

Periodicity of Isotopes and Stellar Evolution

From the utilitarian point of view, the following questions may arise: "Why does a nuclear physicist need astrophysics"? "Why has this to do with stars"? Meanwhile, it is astrophysicists who know a lot of data that can give the understanding of periodicity, course and planning of nuclear reactions.

At the present stage, several processes of stellar nucleosynthesis are known:

- a large explosion, which results in the formation of a large amount of He – about 23% by mass;
- equilibrium stellar nucleosynthesis – is the formation of isotopes from ^{1}H to isotopes of the iron peak A≤68 as a result of sequential nucleosynthesis in the process of stellar evolution from the stars of the main sequence, such as the Sun, to the blue and red giants of about 100 M_{solar};
- the s-process or slow process of neutron capture – is the formation of heavier nuclei from lighter ones by successive neutron capture. The characteristic flow time of s-processes is much longer than that of the β-decay period. Therefore, s-processes include either stable nuclei or β-radioactive nuclei with long half-lives. The source element in the s-process is the iron isotope ^{56}Fe.

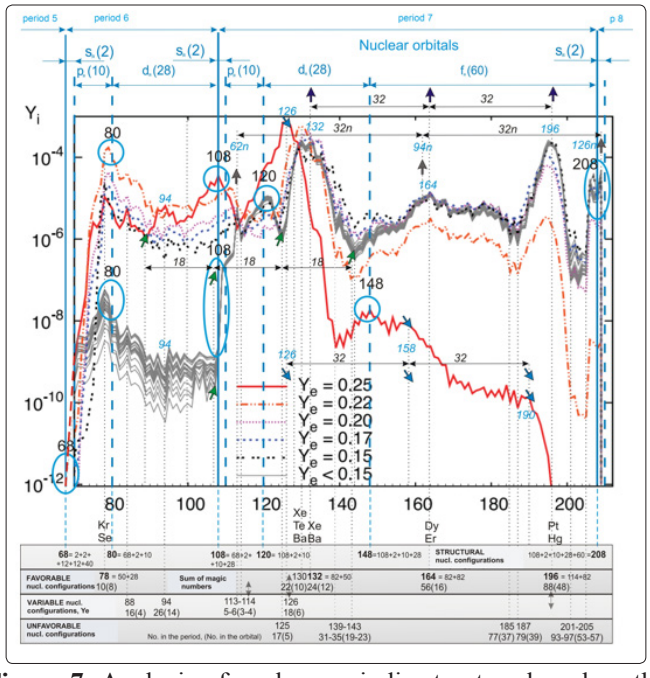

Figure 7: Analysis of nuclear periodic structure based on the abundance of heavy elements formed by the r-process as a result

of the observation over 23 binary systems (black hole – neutron star). Calculation of the abundances depending on the electron concentration in the core of the neutron star Ye is shown with color [3].

- the r-process or rapid neutron-capture process – is the formation of heavier nuclei from lighter ones by successive neutron capture. The neutron-capture process proceeds until the neutron-capture rate is higher than the isotope decay rate. Then the atom undergoes β-decay, and the neutron-capture process proceeds. The main source of nucleation r-processes is the supernova explosions.

In addition to the abovementioned, the proton-capture processes are also highlited: the p-process, rp-process and νp-process will be described throughout the paper. The processes of stellar nucleosynthesis, along with the analysis on the periodic structure of the nucleus, will be considered.

Simulation of the r-process was repeatedly performed depending on astrophysical conditions and ideas on the nuclear structure. In the paper of O. Korobkina et al., the ejection of matter from the compact binary systems consisting of the neutron star and black hole, which are considred to be the main source of heavy isotope abundance in the universe, is studied [3]. It is striking that the r-process shows extreme stability, and all the 23 binary systems being studied show almost identical abundance characteristics. Abundance is completely determined by nuclear properties rather than by astrophysical ones [3]. It is known that the pressure of matter in the outer crust of the neutron star is mainly determined by the electrons formed as a result of β-decays.

The final abundance was calculated using the equation of state (EOS) of nuclear matter for different concentrations of the electron component for the neutron star Y_e. In fig. 7, the calculation for the final abundance formation depending on Y_e is shown. The conclusion made by the authors of this paper that "the abundance is completely determined by nuclear properties rather than by astrophysical ones" is also confirmed by the analysis of the nuclear structure described by other authors using the principle of multilevel periodicity (later in the text) [14, 15]. The boundaries of nuclear structures for the periods or orbitals correspond to the extremum points of the graph (marked with ovals, fig. 7). The boundaries of the periods are clearly marked (A=68, 108, 208) at low electron concentration (Y_e<0.15). For these conditions, the abundance of isotopes is increased abruptly by 2–4 orders of magnitude as the new periods 6 and 7 appear, and is decreased abruptly to 0 as the period 8 appears. The boundaries of pn and dn-orbitals for A=80 and 120 are clearly shown with peaks. The boundaries of orbitals (A=80, 148) and periods (A=68, 108) are shown in the form of abundance peaks at high concentration of electrons (Y_e=0.25). Favorable nucleon configurations in the form of singular points with A=132, 164, 196 are described in the next section and are related to the "magic" numbers and continuous charge periodicity.

Stellar equilibrium nucleosynthesis is the process of sequential formation of nuclei heavier than ^{1}H by fusion at high temperatures up to 10^{10} K and overpressures as a result of natural stellar evolution. The mass of synthesized isotopes directly depends on the mass of a star: the larger the star, the heavier isotopes can be synthesized. The process of nucleosynthesis is multistage and periodic. A multistage nature is shown via the formation of nuclei which have the mass $A_1=A_0+4$ and which are the most abundant – the α-process. The α-process is reflected in the principle of multilevel periodicity. The column 1 in fig. 1-a corresponds to the group of particles with a rank lower than the orbital group and shows the tendency to the pair (2) dislocation of electrons and nucleons, as well as to the tetrad dislocation of nucleons (4). As the shell of the period is increased, the tetrad particles remain fixed. This is shown by the principle of multilevel periodicity and is reflected in the α-process. The tetrad group is the case of continuous mass periodicity for the nuclei with A from 1 to 40 (the boundary of the α-process). It should be assumed that there is a continuous periodicity of isotopes and elements, which is multiple to other shells and where the upper limit by mass or charge is shifted depending on the size of the corresponding orbital or period. It should also be assumed that there is a tetrad group of electrons, which is shown more clearly within the shell of two periods: 4 (2+2); 16 (8+8); 36 (18+18); 64 (32+32), where the total number of particles is multiple of 4, and the number of tetrads is proportional to the square of the natural numbers 1, 4, 9, 16.

Equilibrium nucleosynthesis can be divided into 2 stages in accordance with the structure of the nucleus, types of stellar processes and size of stars. The boundary between the first and second stages is found between the p_n and d_n-orbitals of the period 5 (Table 1). A sharp change in the abundance of adjucent even isotopes with A=40 and 42 (by 2–4 orders of magnitude) is observed on the boundary of nuclear structures [16].

Table No.1 Two stages of equilibrium nucleosynthesis depending on the nuclear structure

Characteristics of the stage 1 (^{1}H – ^{40}Ca)	Characteristics of the stage 2 (^{42}Ca – ^{68}Zn)
- as a result of equilibrium nucleosynthesis for the long-lived stars, the β-stable nuclei are synthesized (^{12}C, ^{16}O, ^{20}Ne, ^{24}Mg, ^{28}Si, ^{32}S, ^{36}Ar, ^{40}Ca), every 4th isotope is abundant;	- as a result of nucleosynthesis for the short-lived giant stars or supernova explosions, the β-unstable nuclei of the "iron" peak, which undergo β-decay, are formed (^{44}Ti→^{44}Ca, ^{48}Cr→^{48}Ti, ^{52}Fe→^{52}Cr, ^{56}Ni→^{56}Fe, ^{60}Zn→^{60}Ni, ^{64}Ge→^{64}Zn, ^{68}Se→^{68}Zn);
- the periodic nature of stellar evolution is shown within the short s_n and p_n-orbitals of the periods 1-5 (2, 12 isotopes), in the subgroups 1-12;	- the periodic nature of synthesis is shown within a more dimentional d_n-orbital of the period 5 (28 isotopes). It should be expected that nuclear reactions occur faster due to the size of the orbitals;
- within the short s_n and p_n-orbitals with several abundance peaks.	- within the orbital or the period with the d_n-orbital, one peak of the abudance is shown in the center (the "iron peak", figs.4a, 10 and 12).

It is noticed that the periodic course of stellar evolution (the first stage) is determined by the nuclear structure reflected in the system of isotopes. Using the data on the periodic structure of the nucleus and the types of stellar objects, 4 main stages of stellar evolution can be distinguished: mass formation, periodic nucleosynthesis, supernova stage, evolved object stage. For the stages of stellar evolution, the general visual scheme corresponding to many scenarios and collisions of stellar life can be presented:

1. Mass Formation

Stars of a certain mass correspond to each period. At this stage, the type of star is predetermined. Also, it is determined to what stage nucleosynthesis lasts and what period it corresponds to (brown dwarf – period 1, red dwarf – period 2, solar-type star –

period 3, supergiant – period 4, hypergiant – period 5). Heavy stars with the synthesis of up to ^{16}O, ^{28}Si, ^{40}Ca undergo the stages of nucleosynthesis for all the previous periods.

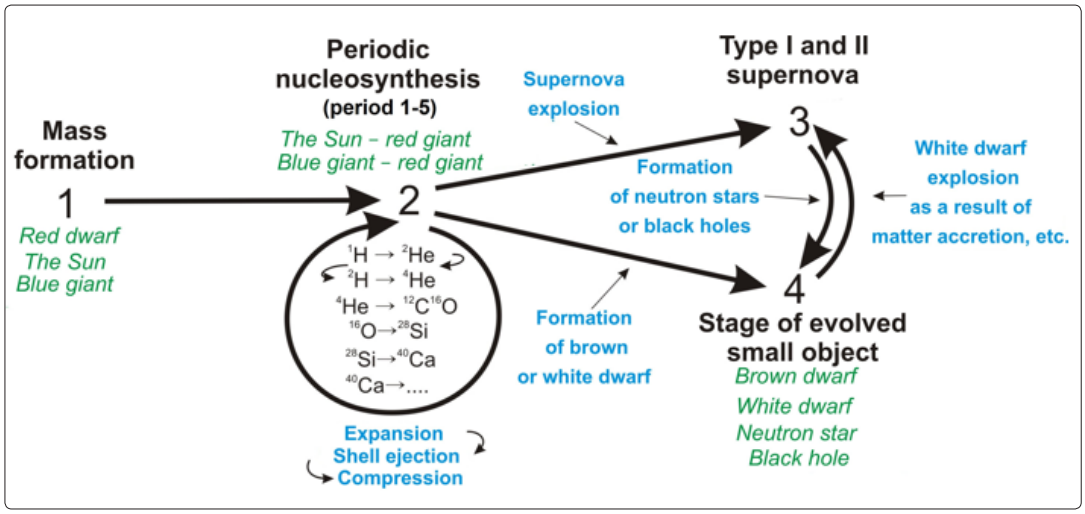

Figure 8: Periodic nucleosynthesis in stars.

stars with the synthesis of up to ^{16}O, ^{28}Si, ^{40}Ca undergo the stages of nucleosynthesis for all the previous periods.

2. Periodic Nucleosynthesis. Expansion – shell Ejection – Compression

Burning of "isotopes" for each period corresponds to the periodic stages of expansion and compression. Isotopes are arranged at the end of each period, and the further course of reactions is determined by their "ignition" (^4He, ^{12}C-^{16}O, ^{28}Si). The processes of expansion – shell ejection – compression are repeated again.

Period 2. Reaction: $^1H \rightarrow {}^4He$; red dwarf (expansion) – shell ejection (H) – He-white dwarf (compression).
Period 3. Reactions: $3\,^4He \rightarrow {}^{12}C$; $^{12}C \rightarrow {}^{16}O$; solar-type star – red giant (He burning, expansion) – C-O-white dwarf (compression).

In the periods 4 and 5, the stages of expansion – shell ejection – compression can be repeated several times per period in the process of cycling of the blue-red giant stages. This indicates the beginning of synthesis for new, heavier isotopes inside the star. The evolutionary tracks of giant stars on the Hertzsprung-Russell diagram correspond to this process. At the end of each period, depending on stellar mass, one of the 3 variants of scenario is selected: ignition of isotopes for the end of the period and transition to isotope synthesis for the next period, repeated stage 2; the end of synthesis and transition to stage 4 – formation of a small object (dwarfs); supernova explosion (stage 3) and repeated stage 4 – formation of a neutron star or a black hole. The periodic approach allows developing simple and universal scheme of stellar evolution (fig. 8).

3. Explosion Stage

Nucleosithesis of isotopes for each period, starting from the third one, corresponds to different types of supernova explosions. The period 3: thermonuclear explosion – scattering; the period 4: collapse – explosion – neutron star; the period 5: collapse – explosion – black hole.

4. Stage of Small Long-Lived Objects (Brown Dwarf, White Dwarf, Neutron Star, Black Hole)

If stellar nucleosynthesis stops, then the evolved long-lived small object corresponds to the end of each period. Small objects of the same type – white dwarfs (2 – He; 3 – CO; 4 – O-Ne-Mg) – correspond to the end of the periods 2, 3 and 4. A neutron star or a black hole left after supernova explosion corresponds to the end of the periods 4 and 5. Under the influence of external factors for interaction with other stars (accretion), the small object stage can turn into the explosion stage. The stages 3 (explosion) and 4 (small object stage) are similar to the processes of shell ejection and compression. This stage can be called the "new aggregation state", in which stellar plasma changes its aggregation state not only by temperature, but also by density and pressure (brown dwarf – gas, solid; white dwarf – degenerated electron gas; neutron star – nuclear matter, black hole – black hole matter (superdensity).

The periodic stellar evolution is described in Table 2 in more detail together with the system of isotopes (periods 1-5). The main process of periodic stellar nucleosynthesis is the α-process (^4He attachement), during which the periodic maximum of reaction energy yield is observed for the isotopes of the end of the period (fig. 8). It is assumed that in the interior of massive stars with $M>30M_{solar}$, equilibrium nucleosynthesis ends in the "iron peak" isotopes, i.e. at the end of the period 5. As a result of observations, the supermassive stars with the mass of 100-300 M_{solar} are discovered in the universe. There is an assumption that such stars could have a greater abundance at the early stages of the universe development. This provides balance for the presence of heavy isotopes at the modern stage of evolution. It should be assumed that equilibrium nucleosynthesis proceeds in the interior of such stars with the involvement of isotopes for the period 6 – A=69-108.

Table 2: Periodicity of stellar evolution in accordance with the periodic system of isotopes

Period	Stellarmass	Subgroups 1-12/Periodicity of stages 1-4.											
		1	2	3	4	5	6	7	8	9	10	11	12
													
1	0,077-0,3	^{1}H	^{2}H	Hydrogen "burning" (the proton-proton cycle) $^{1}H \rightarrow {}^{2}H$ (D)									
		$^{1}H \rightarrow {}^{2}H$											
		1. Red dwarf with the synthesis of H →D											
		2. Shell ejection. Compression. → 4. H-D – brown dwarf of up to 0,3 M_{solar}											
													
2	0,5-2,25	^{3}He	^{4}He	Hydrogen "burning" (the proton-proton cycle) $^{3}He \rightarrow {}^{4}He$									
		$^{3}H \rightarrow {}^{4}He$											
		1. Red dwarf with the synthesis of $^{1}H \rightarrow {}^{4}He$											
		2. Shell ejection. Compression. → 4. He-white dwarf of up to 0,5 M_{solar}											
		3. Supernova explosion does not occur due to low mass. 2. Mass > 2.25 M_{solar} → helium "ignition".											
		5	6Li	7Li	8	9Be	10B	11B	12C	13C	14N	15N	16O
													
3	2,25-8	Helium "burning" (3α-process) $^{4}He \rightarrow {}^{12}C$							CNO-cycle $^{12}C \rightarrow \ldots {}^{16}O \rightarrow {}^{4}He$				
									C detonation → type Ia supernova				
									C "burning"				O
		Main sequence star ($^{1}H \rightarrow {}^{4}He$) → 2. He "ignition", red giant with 12C synthesis and CNO cycle. Shell ejection. Compression. → 4. CO-white dwarf of 0.6-0.7 M_{solar}, planetary nebula.											
		17O	18O	19F	20Ne	21Ne	22Ne	23Na	24Mg	25Mg	26Mg	27Al	28Si
4	8-12												
		α-process → ^{20}Ne				α-process → ^{24}Mg				α-process → ^{28}Si			
		Carbon "burning" stops due to O-Ne-Mg degeneration, shell ejection occurs									α-process → ^{28}Si		
	12-30	Oxygen "burning" $^{16}O \rightarrow {}^{28}Si, {}^{32}S$											
		$^{16}O \leftarrow$ neon "burning" $^{20}Ne \rightarrow 24Mg$									α-process → 28Si		
		1. Blue supergiant. → 2. Alternation of supergiant and red-blue supergiant stages. Shell ejection – compression.											
	8-12	4. O-Ne-Mg-white dwarf with a mass similar to the Chandrasekhar limit (1.44 M_{solar}).											
	12-30	3. Gravitational collapse. Type II supernova flare → 4. Neutron star											
		2. Neon "ignition" 2. Silicone "ignition" →											Si
5	>30	29Si	30Si	31P	32S	33S	34S	35Cl	36Ar	37Cl	38Ar	39K	40Ca→
		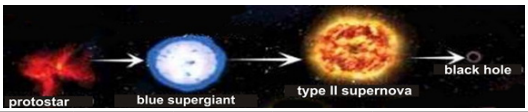											
		α-process 32S					α-process → ^{36}Ar				α-process → $^{40}Ca \rightarrow$		
		Oxygen "burning" $^{16}O \rightarrow {}^{32}S$					α-process → ^{36}Ar				α-process → $^{40}Ca \rightarrow$		

		Silicon "burning" $^{28}Si \rightarrow {}^{32}S, {}^{36}Ar$	α-process → $^{40}Ca\rightarrow$
		The processes are unclear. Prediction: 1. Blue supergiant. → 2. Even more frequent alternation of the red-blue supergiant stages. Shell ejection	
		3. Gravitational collapse. Type II supernova flare → 4.Black hole	
		2. Supergiants with the mass of about >100 M_{solar} (prediction), degeneration of the nucleus does not occur and nucleosynthesis (α-process+capture e) proceeds until the end of the period 5, formation of the "iron peak" isotopes A≤68 (Fe, Co, Ni, Cu, Zn, Ga, Ge, As, Se) → 3. Supernova flare → 4. Black hole.	

The second stage of stellar equilibrium nucleosynthesis includes the formation of isotopes for the "iron" peak and has several qualitative differences from the first stage:

1. The abundance of isotopes synthesized by the Sun drops sharply by 2.5 orders of magnitude at the boundary of the p_n- and d_n-orbitals (isotopes ^{40}Ca – ^{42}Ca, this shows the change in the structural levels of the nucleus and the change in the nature of synthesis processes [16]. On the whole, the "iron peak" is well defined within the dn-orbital. After ^{68}Zn, the abundance A=68/70 drops by an order of magnitude, and the inclined region A=56-68 is replaced by the horizontal region A=70-88 (fig. 11).

2. The synthesis of isotopes within the dn-orbital of the period 5 occurs at the sharp increase in the proportion of β-unstable isotopes with the excess of protons (p-nuclei). The most abundant are the nuclei which undergo pair capture of protons +2p, similar to pair distribution of electrons in the electron shells. The property of pairing shows the tendency of the atom to form the equilibrium motion of nucleons in the orbital towards the center. +2p nuclei eventually undergo (2β+)-decay ($^{44}Ti\rightarrow{}^{44}Ca$, $^{48}Cr\rightarrow{}^{48}Ti$, $^{52}Fe\rightarrow{}^{52}Cr$, $^{56}Ni\rightarrow{}^{56}Fe$, $^{60}Zn\rightarrow{}^{60}Ni$, $^{64}Ge\rightarrow{}^{64}Zn$, $^{68}Se\rightarrow{}^{68}Zn$). This feature is easy to explain with the help of the periodic system. Within the dn-orbital of the period 5, inhomogeneous distribution of electric charge is observed. Due to such distribution, the conditions for easier proton capture are created. ^{40}Ca is the last stable isotope with equal number of protons and neutrons: 20p + 20n. ^{40}Ca has the filled s_n- and p_n-orbitals in the period 5 with the same number of n and p: 6p+6n. As the synthesis proceeds within the d_n-orbital, the positive proton charge undergoes repulsion from the previous orbital, and the balance shifts towards the excess of neutrons through 2β+decay. For ^{68}Zn (30p+38n), the composition of d_n-orbital is 10p+18n. Thus, the nonuniform charge distribution is formed inside the nucleus — the positive nuclear charge is concentrated closer to the central part; the neutral or relative negative charge in the form of neutrons is concentrated closer to the periphery of the nucleus. This feature of nuclear structure is confirmed by the fact that the nuclei with N=Z, including in particular ^{68}Se, have the waiting point of proton capture until β-decay occurs. Therefore, the unstable ^{68}Se nucleus with 14n+14p at the d_n-orbital ejects the excess positive charge, and then continues to absorb protons. The data are calculated and confirmed by the results of astrophysical observations [17, 18, 19]. It should be in view that the waiting point is related not only to the equality of n and p, but also to the complete filling of dn-orbitals and the period 5 as a whole, when the nuclei with A=68 show similar inertness in reactivity observed for inert gases in chemistry (He, Ne, Ar ...). Inhomogenity of charge distribution, as well as a large size of d_n-orbitals, in comparison with p_n-orbitals (28 and 10 nucleons), reduces the magnitude of the Coulomb barrier for proton repulsion at the capture by the isotopes of the "iron" peak. Due to this, under high pressures and temperatures of stellar core, the conditions for easier capture of protons or positrons, as well as for the synthesis of β+ active nuclei, are created.

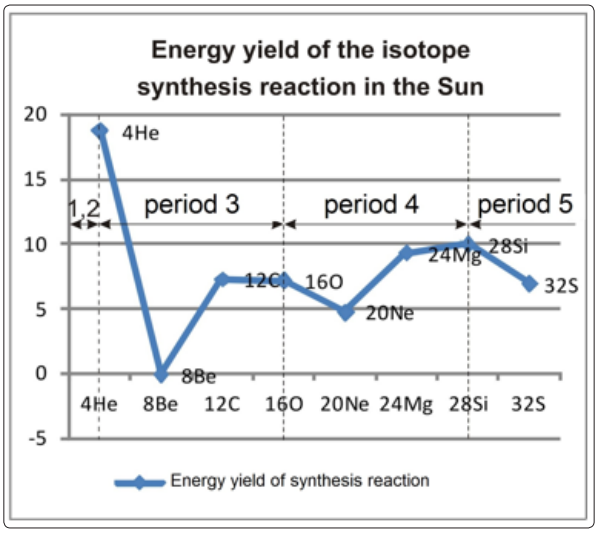

Figure 9: Energy yield of the isotope synthesis reaction with A=^{4}He+4. The diagrams are presented in [20].

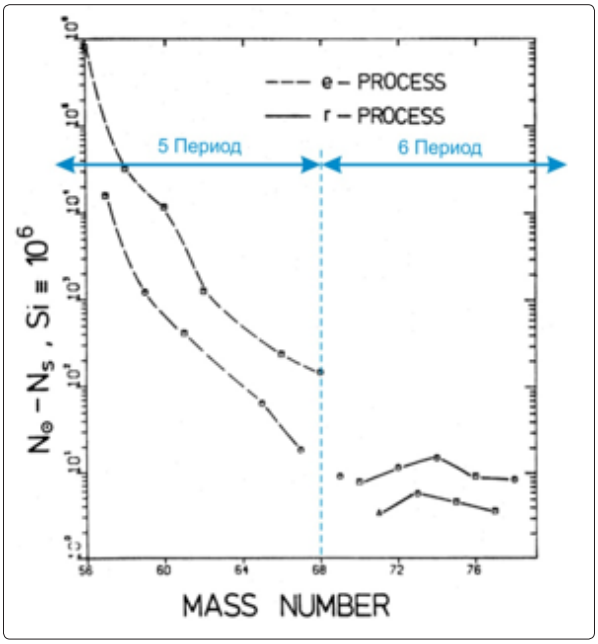

Figure 10: Abundance of isotopes in the Sun (Cameron 1981) [15]. The end of the "iron peak" – the boundary of the periods 5 and 6.

3. Since the synthesis of isotopes for the "iron peak" is possible only in the interior of massive stars, the proportion of isotopes synthesized at the explosive processes of supernovae with the involvement of the rp and vp-processes is increased dramatically for the dn-orbital.

The rp-process is the process of capturing fast protons by the atomic nucleus. It is one of the processes of nucleosynthesis responsible for the formation of many elements heavier than iron. Unlike the s-and r-processes, the nuclei rich in protons are formed as a result of the rp-process.

The νp-process is the process of ejecting matter enriched with protons from the interior of collapsing supernova. The *ν*p-process occurs under the action of strong neutrino fluxes. This process has been discovered recently. The ejected matter is heated to the temperatures more than 10^9 K and is completely dissociated into protons and neutrons. Then the matter is captured by other nuclei as a result of supernova blast wave. The presence of proton-rich medium is indicated by the synthesis of p-nuclei at the second stage of stellar equilibrium nucleosynthesis. It should be expected that at the stage of synthesis before the explosion in stellar core, the proportion of rp-reactions is increased gradually. Some of the isotopes "dissociate" into nucleons and immediately form new and heavier ones. As a result, the star begins to pulsate and gradually overcomes the barrier of destruction or collapse.

As a result of calculations, it is predicted in that the rp-process in neutron stars cannot proceed further than ^{105}Te due to the inhibition by α-decay. In fig. 11, the diagram of the rp-process is shown [21]. The diagram is constructed as a result of comparing the data from 6 different mass spectrometers with the Penning trap, where the upper limit is ^{107}Te. The stadial flow of the rp-process is shown with the bold line. It is easy to see that the upper limit of the rp-process (^{107}Te) is above the "magic" line with n=50, z=50, and is limited by the end of the period 6 (A=108). To confirm the last conclusion, the results of measurements are given, where the dome-shaped distribution of the abundance within the period 6 is shown for the isotopes with A=68-108. In fig. 11, the results (2003 and 2008) of direct measurements for the isotope abundance in supernova remnants (M=15 M_{solar}) are compared for the nuclei arranged behind the "iron peak" and formed as a result of the νp and rp-processes.

Such a distribution is similar to the boundaries of the "iron" peak in the period 5 (A=41-68) and is caused by the structural division of the nucleus into periods (fig. 4-a). Using the periodic system of isotopes, it can be established that the filled d_n-orbitals of the periods 5-7 include unequal number of protons and neutrons: the period 5 – (10p+18n); the period 6 – (14p+14n); the period 7 – (10p+18n); the period 8 – (10p+18n). The d_n-orbital of the period 6 includes (14n+14p) the excess amount of protons – 14 out of 28 (p-nuclei).

Further course of the rp-process is limited by several factors: the start of α-decay in proton-rich p-nuclei (^{107}Te), energy barrier for the formation of a new nuclear shell (period 7), increased Coulomb barrier of the dn-orbital for the period 6 (14n+14p). The d_n-orbital of the period 6, in comparison with the dn-orbital of the period 5 (10p+18n), does not have the excess amount of neutrons reducing the barrier. This explains the reduced distribution of isotopes for the d_n-orbital of the period 6 (Mo, Tc, Ru, Rh, Pd). α-decay in p-nuclei becomes possible at the end of the period 6, when the d_n-orbital gains mass and is arranged at the sufficient distance from the center of the nucleus and has the excess positive charge of protons. It is interesting to note that the maximum α-decay cross-section for stable 147Sm nuclei is arranged symmetrically to ^{107}Te in the system of isotopes (the subgroup 39) at the end of the d_n-orbital for the period 7 (fig. 27). Due to the distance from the center of the nucleus, it becomes possible for the isotopes of the period 8 to eject the nuclear fragment (which is even larger than the α-particle) with A=14-34 – cluster radioactivity, which represents the shell ejection of the period 8, similar to the massive star (fig. 23. Section 12. Lifetime of isotopes, radioactivity and periodic structure of the nucleus).

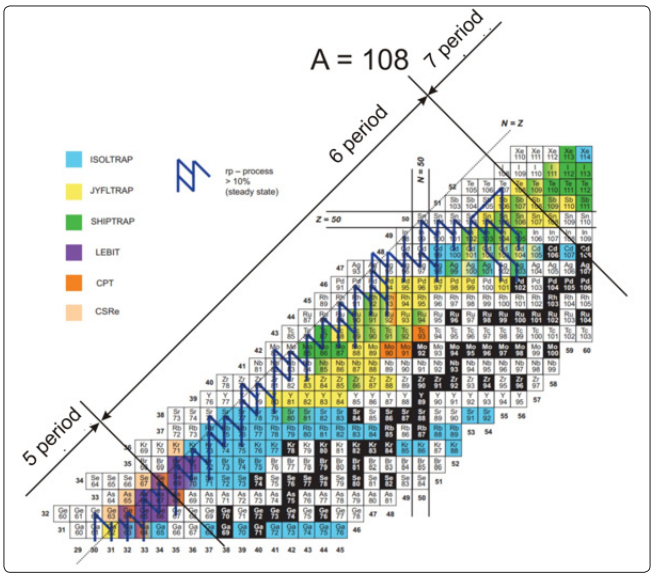

Figure 11: Upper boundary of the rp-process together with the boundary of the periods 6 and 7 for A=108. The diagram fragment shows the mass measurements of nuclei corresponding to the rp-process in the Penning trap accumulators [22]. Stable isotopes are shown with black cells. The rp-process is shown with a bold line, N = Z nucleus is shown with a dotted line.

In accordance with the abovementioned measurement data and analysis, the abundance of a particular isotope is determined by a more periodic structure of the nucleus, rather than by astrophysical properties. In accordance with the nuclear structure and mass, the evolutionary processes of the main-sequence stars are of a periodic nature (Table 2). Stellar processes are determined by the type of nuclear reaction. In the diagrams, it is shown that the boundary of the periods 5 and 6 for A=68 is the lower boundary for the r-process (fig. 10), (fig. 7) and the νp-process (fig. 12) [15, 4, 14]. In accordance with the same data and diagram in fig. 12, the end of the period 6 for A=108 is the upper boundary for the νp and rp-processes and is the structural barrier for the r-process (fig. 12) [22]. Also, the periodic structure of the nucleus is fully confirmed. A multistage development of the r- and rp-processes in time at supernova explosion in accordance with the periodic structure, in which the synthesis of proton-rich nuclei abruptly changes into a new period or orbital, should be expected. As a result of the analysis on stellar processes and isotope abundance, it can be stated with a high degree of confidence that the boundary length and the nature of nucleus formation correspond to the nuclear periodic structure. Analysis of data on the duration of nucleosynthesis and the nuclear periodic structure makes it possible to form the model of stellar process duration (fig. 13).

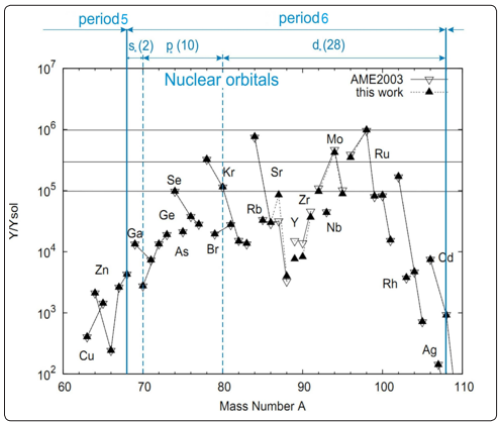

Figure 12: The vp and rp-process, peak of isotope abundance (A=60-110) in supernova remnants (15 M_{solar}) and boundaries of the period 6. The data on stable nuclei (after β+ decay) normalized by the solar abundance Y/Y_{solar} are shown [14].

In addition to the periodic structure of nucleons, a significant contribution to the process of synthesis, as well as to the values of isotope abundance, is made by the electronic component Y_e (fig. 7) [4]. Due to the electronic component Y_e, there occur additional structural transitions (A=132, 164, 196) in the massive shell – the f_n-orbital of the period 7. It should be assumed that their occurrence is related to the occurrence of continuous charge cycles in the nucleus for the periods up to 32 etc. (fig. 16. Section 10. Origin of "magic" numbers).

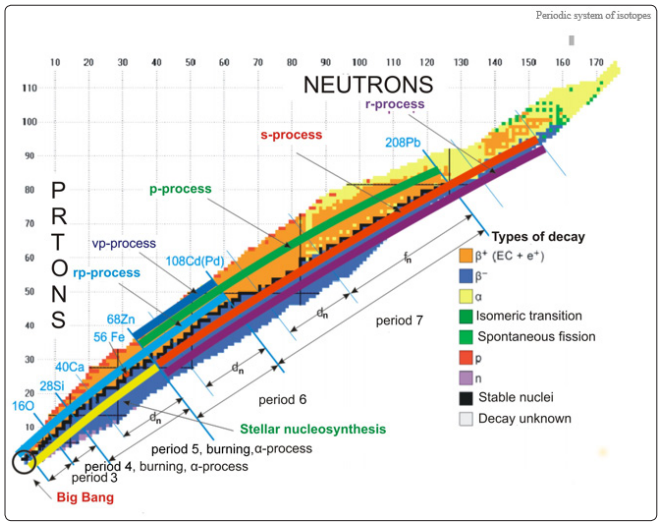

Figure 13: Duration of stellar processes in accordance with the periodic structure of the nucleus

Ore Formation and Periodic Structure of Isotopes

Formation of minerals in nature can be divided into two categories in accordance with two types of forming processes: nuclear and chemical. All matter of the Earth and planets is formed in the interior of stars. In accordance with modern concepts, the main source of isotopes heavier than Fe-Zn are supernova explosions. It is convenient to study the course of nuclear processes of ore formation on the example of polymetallic ores. A distinctive feature of ore formation due to nuclear processes is the joint concentration of minerals, in which the isotopes of the main element have the same arrangement in the periodic system.

Polymetallic ores are complex ores containing a number of chemical elements, among which the most important are lead and zinc. In addition, polymetallic ores may contain copper, gold, silver, cadmium, sometimes bismuth, tin, indium and gallium. Ubiquitous dual high concentration of zinc and lead can in no way be caused only by the chemical processes occurring in the body of the planet or at the stage of protoplanetary disk. The main isotopes of zinc: ^{64}Zn (48, 63%), ^{66}Zn (27,902%), ^{67}Zn (4,101%), ^{68}Zn (18,755%) and lead: ^{206}Pb (24, 1%) ^{207}Pb (22,1%) ^{208}Pb(52,4%) are arranged in the table at the end of the periods (Table 3 and 4). The isotopes ^{68}Zn (18,755%) and ^{208}Pb (52, 4%) complete the period 5 and 7, respectively. The isotopes of the elements included in the impurities of lead-zinc and other types of polymetallic ores are arranged in the adjacent subgroups of the isotope periodic system. Analysis on the composition of ores for the non-basic elements (Cu, Ni, Ag, Cd, Pd, Hg) included in polymetallic ores is presented below:

- one of the most important sources of silver mining are deposits of lead-zinc ores;
- cadmium does not form independent deposits, but it is included in the composition of ores for deposits of other metals; it is always found in zinc minerals and partially in copper-pyrite deposits;
- palladium is mainly obtained by processing sulphide ores of nickel, silver and copper;
- the most common copper ores are copper pyrite and vitreous copper, containing 1-2% copper. In accordance with mineral composition, pyrite ores are subdivided into copper and copper-zinc, polymetallic and sulfur ores. In sulfur-pyrite ores, sulfur is of primary importance; copper, lead and zinc are of subordinate importance;
- nickel is concentrated in copper-nickel sulphide, nickel silicate and cobalt-nickel silicate deposits;
- complex mercury ores contain antimony, copper, lead, zinc, gold and silver.

Table 3: End of the periods 5 and 6, subgroups 32-40

	32		33	34		35	36		37	38		39	40	
period 5	**^{60}Ni**	**^{60}Fe**	**^{61}Ni**	**^{62}Ni**		**^{63}Cu**	**^{64}Ni**	**^{64}Zn**	**^{65}Cu**	**^{66}Zn**		**^{67}Zn**		**^{68}Zn**
% in mixture	26,2		1,14	3,63		69,2	0,93	48,6	30,8	27,9		4,1		18,8
period 6	$^{100}_{Ru}$	$^{100}_{Mo}$	$^{101}_{Ru}$	$^{102}_{Ru}$	$^{102}_{Pd}$	$^{103}_{Rh}$	$^{104}_{Ru}$	$^{104}_{Pd}$	$^{105}_{Pd}$	$^{106}_{Pd}$	$^{106}_{Cd}$	$^{107}_{Ag}$	$^{108}_{Pd}$	$^{108}_{Cd}$
% in mixture	12,6	9,63	17,1	31,6	1,02	100	18,7	11,1	22,3	27,3	1,25	51,8	26,5	0,89

Table 4: End of the period 7, subgroups 92-100

	92	93	94	95	96		97		98	99	100
period 7	$^{200}_{Hg}$	$^{201}_{Hg}$	$^{202}_{Hg}$	$^{203}_{Tl}$	$^{204}_{Hg}$	$^{204}_{Pb}$	$^{205}_{Tl}$	$^{205}_{Pb}$	$^{206}_{Pb}$	$^{207}_{Pb}$	$^{208}_{Pb}$
% in mixture	23,1	13,2	29,9	29,5	6,87	1,997	70,5		24,1	22,1	52,4

Modern localization of the planetary material can be defined as a result of the action of 3 types of processes: ejection of matter as a result of stellar explosion; concentrations at the stage of protoplanetary disk, chemical and mechanical processes in the body of the planet. It should be assumed that the main proportions of concentration and localization are obtained by the planetary material during synthesis and ejection of stellar matter. As the analysis shows, the complex of polymetallic ores consists of isotopes from the last subgroups of the periods 5, 6 and 7 (the period 5: Ni, Cu, Zn; the period 6: Pd, Ag, Cd; the period 7: Au, Hg, Tl, Pb) with a small inclusion (~ 1-2%) of isotopes for the elements at the beginning of the periods (Cd, Zn, Ga, In, Sn, Bi) (see Tables 3 and 4). Such a joint concentration of elements and isotopes, which differ greatly by mass and atomic number (Zn (30), Cd (48), Pb (82), etc.), indicates that they are formed as a result of nuclear processes of the same type under the conditions of excess nucleons, when the free nuclear shells are filled completely. Such conditions are possible as a result of fast explosive processes of supernovae (the r-, rp- or νp-processes). As already noted, the scenarios of isotope formation are determined on the basis of the internal nuclear structure. Since the isotopes are arranged at the end of the periods and massive orbitals, they have similar formation characteristics. This explains the composition of the main isotopes for the elements of polymetallic ores. In the language of a chemist, they have the same "nuclear valence" and similar reactivity. It should be assumed that the isotopes arranged in the last subgroups of the periods have the high-energy proton and neutron-capture cross-section of the same order. The shock wave of free nucleons forms the layer of ejected matter with the isotopes arranged at the end of the periods 5-7 in the isotope periodic system. Due to the excess energy and nucleon concentration during explosion, a proportion of isotopes from the beginning of the periods is formed. These isotopes are included in the impurity composition in the form of Ga, In, Sn, Bi isotopes. Thus, it should be assumed that the nuclear periodic structure is one of the main causes of the initial mineral concentration for the planetary material.

Magnetic Moment of the Nucleus and Isotope Periodicity

To evaluate the contribution of the nucleon anomalous magnetic moments to the total nuclear magnetic moment, general quantitative and theoretical analysis of data should be performed. Magnetic moment is observed for the nuclei with the odd number of protons Z or neutrons N. The nuclei with even numbers Z or N have zero magnetic moment. This means that nucleons, like electrons, tend to form pairs. It is empirically observed that for two nucleons in the orbit, it is energetically advantageous to form the pair with the total moment μ=0 [23]. The property to form pairs is determined by the first row of the Pascal's triangle (fig. 1-a).

All the macro and micro systems in nature experience movement, and the nucleons are of no exception. The periods and orbitals of the isotope system have a fixed number of nucleons and, in the final form, create shells shaped like a sphere. From this it follows that at the point moment in time, they can be considered as evenly distributed in space over the sphere. Odd Z nuclei have the positive magnetic moment within the range of 0.3–2.5 for the proton magnetic moment $\mu p=2.79\mu_n$ (where μn is a nuclear magnetron). Most nuclei with odd N have the magnetic moment ranging from $-1.91<\mu N<+1$, where 1.91 is the magnetic moment of the neutron $\mu_n=-1.9131\mu$. Magnetic moments of the nuclei with odd Z and N have values of the same order as μ_p and μ_n. This means that the main contribution to μn is made by the magnetic moment of the unpaired proton and neutron or by the superposition of several unpaired moments for the odd-odd nuclei (^{40}K, ^{50}V, ^{176}Lu, ^{180m}Ta).

In general, it can be determined that the contribution to the nuclear magnetic moment is made by the following two main components: the magnetic moments of the unpaired nucleons μ_{bound_nucl} and the magnetic moment components related to the structure of the outer nuclear shell μ_{str}.

$$\mu_{nucleus} = \mu_{bound\_nucl} + \mu_{str}, \quad (2)$$

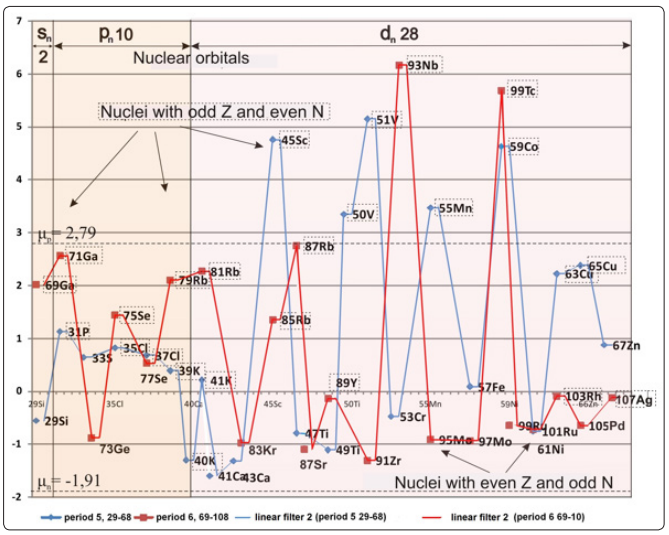

Figure 14: Magnetic moment of stable nuclei, the periods 5 and 6

Quantitative analysis shows that the main contribution to the value of the magnetic moment is made by the unpaired nucleon. The contribution of the remaining additive components related to the nuclear structure μstr can be preliminary estimated using the example of light isotopes with a relatively simple internal structure: ^{3}He (2p; 1n; μ_{3He}=-2,12762$_{\mu n}$) and ^{3}H (1p; 2n; μ_{3H}=2,97896μn). For this, it is necessary to subtract the magnetic moment of the free nucleon from the total magnetic moment of the isotope: μстрHe3=μ3He - μn= -0,21447 (10,08% of μn) – for the unpaired neutron or μstr3He=μ_{3He}-μp=-4,918 (231% of μp) in case of the unpaired proton; μstr3H=μ3H–μp=0,18611 (6,25% of μ_p). The contribution of the magnetic moment related to the nuclear structure for the isotopes of the periods 1 and 2 is within the range of 6-10% or 231%. It should be determined which of the estimates is correct. It can be assumed that the contribution of the nuclear structure μstr depends on the nuclear periodic structure.

The nuclei having the magnetic moment can be divided into 3 categories: 1 – the nuclei with an unpaired proton p, 2 – the nuclei with an unpaired neutron n, 3 – the nuclei with an unpaired p and n. In figs. 14 and 15, the periodic distribution of magnetic moments for stable isotopes in the massive periods 5, 6 (40 nucleons) and 7 (100 nucleons) is shown. Within the periods 5 and 6 (fig. 14), the nuclei with an unpaired proton have the increased magnetic moment within the massive dn-orbitals (the period 5: ^{45}Sc, ^{50}V, ^{51}V,^{55}Mn, ^{59}Co; the period 6: ^{87}Rb, ^{93}Nb, ^{99}Tc). When the dn-orbitals are filled in the last subgroups of the period, the magnetic moment values for the nuclei with an unpaired proton are sharply decreased (the period 5: ^{63}Cu, ^{65}Cu; the period 6: ^{103}Rh, ^{107}Ag) and the distribution similar to the dome-shaped one is formed within the orbital. Such a distribution corresponds to the nuclear shell structure obtained in accordance with the principle of multilevel atomic periodicity. The moment values at the end of the period 6 are especially contrastive, when the nuclei with a free proton have a negative magnetic moment, which is anomalous. However, if the periodic structure is taken into account, it becomes clear that these isotopes are arranged in the almost filled d_n-orbital, the shape of which tends to be elliptical. Due to the larger size of the shell, the magnetic moment values are on average by 100-300% larger for the d_n-orbital (28 nucleons) in comparison with the p_n-orbital (10 nucleons) (fig. 14).

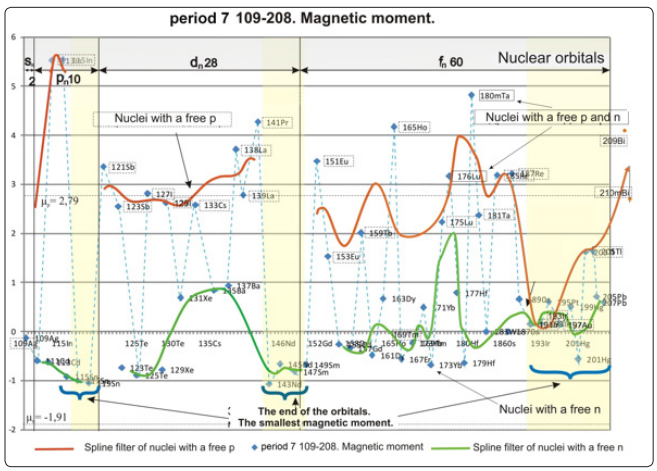

Figure 15: Distribution of magnetic moments for stable nuclei of the period 7

Within the massive period 7, the magnetic moment values (fig. 15) also correspond to the nuclear periodic structure. The magnetic moment has large values at the beginning and in the middle of p_n, d_n and f_n-orbitals and drops to negative values at the end of the orbitals. Such a distribution is related to the fact that within the large orbitals (d_n-orbitals of the periods 5 and 6; p_n, d_n, f_n are the orbitals of the period 7), a free proton is far from the central shells of the core providing the increased centrifugal moment. At the end of the orbitals, the shapes of the shells approach spherical ones and, despite the presence of a free proton, the magnetic moment is decreased (^{191}Ir, ^{193}Ir, ^{203}Tl, ^{205}Tl). Contribution of nuclear structure to the value of the magnetic moment for the isotopes with a free proton for the massive shells: dn-orbitals of the periods 5 and 6 and p_n, d_n, f_n-orbitals of the periods 7 and 8 is +20-100%.

Among the isotopes with an unpaired proton arranged in the middle of the massive d_n and f_n-orbitals, there are two abnormally low values of the magnetic moment for ^{89}Y (μ89Y = -0,13742) and ^{169}Tm (μ169Tm = -0,232). These two isotopes have similar features related to the presence of the factor for nuclear geometric structure. As mentioned in Section 5 (Quadrupole moment), the nuclei arranged immediately after the filled shells having a +1 nucleon in the new orbital or period (the +1 configuration) show the values of the quadrupole moment Q at the level of the isotopes arranged at the end of the previous shells: ^{149}Sm (-0,075), ^{209}Bi (-0,37), ^{221}Rn (-0,38) (fig. 5). Further, as the mass is increased by +2, +3 nucleons etc., the Q values change their sign and sharply go up by adding from 300 to 1000%.

The isotope ^{169}Tm (69p, 100n) refers to the +1-configuration, 61 nucleons are arranged in the shell of the period and 21 nucleons are arranged in the f_n-orbital; ^{89}Y (39p, 50n) includes: 21 nucleons in the period and 9 nucleons in the orbital. Both isotopes have the number of neutrons equal to the number of nucleons in the largest period of the isotope system — 100, and in the half of the period — 50. It is necessary to determine which of the factors is the most important for such a low and negative value of μ: the configuration of 21 nucleons in the shell or the number of neutrons multiple of the period. Radioactive isotopes with a free proton and 21 nucleons in the shell of the period or f_n-orbital: ^{89}Rb (37p, 52n), the subgroup 21, period 6, as well as ^{89}Y; however, ^{89}Rb has μ = +2.304; ^{89}Nb (41p, 48n) μ = +6.216; ^{129}I (53p, 76n) – the subgroup 21, period 7 μ = +2.621; ^{169}Lu(71p, 98n) μ = +2.30. Radioactive isotopes with a free proton having 50 or 100 neutrons: ^{87}Rb (37p, 50n) – the subgroup 19, period 5 – μ = +2.7512; ^{171}Lu (71p, 100n) – the subgroup 63, period 7, 23 nucleons in the fn-orbital – μ = +2.30. As a result of quantitative analysis, it is obvious that the values of μ for each of the factors separately have positive values of 2.30–6.216 μn. It should be assumed that the abnormally low values of μ are determined by the coincidence of the sum of both factors: the number of neutrons multiple of 50 and the presence of 21 nucleons in the shell. Both isotopes ^{89}Y and ^{169}Tm, as well as 21 nucleons in the outer shell, are divided into 12 neutrons and 9 protons, where 12 nucleons correspond to the number of nucleons in the periods 3 and 4. Thus, there is a double coincidence in the number of nucleons in the periods, both as common and in the outer shell. It can be assumed that in a dense spherical nucleus, the factor of geometric structure acquires particular importance, as shown by the fixed number of nucleons multiple to the "magic" number 50 and the number of nucleons of the same type coinciding in periods 100 and 12. This allows suggesting that the factor of geometric structure becomes particularly important in a dense spherical nucleus. Nucleons of the same type contribute to the geometric factor. This conclusion is also confirmed by the fact that the nuclear isomers of one isotope, for example, ^{90m}Y (39p, 51n) and ^{90}Y (39p, 51n) have a huge variation in the values of μ, 5.1 and -1.630, respectively. Thus, the following explanation can be put forward: the isotopes with a free proton ^{89}Y and ^{169}Tm represent a unique case, where the total number of neutrons is 50

or 100, and the number of neutrons in the outer shell of the period or orbital is equal to the number of nucleons in the period – 12, the nucleus forms a dense shell similar to the completed shell of the period and binds the free proton as a +1 configuration. At the same time, the nucleus is reduced in size, close to the spherical shape, and the values of the magnetic and quadrupole moments are much lower than those of the adjacent ones in the orbitals. This phenomenon can be defined as the case of intershell hybridization of nucleons of the same type. The geometric factor and the origin of "magic" numbers are discussed in more detail in the following sections (see Section 10 "Origin of magic numbers" and Section 11 "Models of filled nuclear orbitals"). No measured values of the quadrupole moment Q_{89Y} are found in the literature. It should be assumed that the nucleus 89Y has the quadrupole moment of the same sign and order as 169Tm. As the nucleus is less massive, the value of Q_{89Y} can be predicted at the level of 50-70% of Q_{169Tm} = -1.2, i.e. Q_{89Y} = -0.6: - 0.84.

It should be assumed that when the pair is formed, the nucleons tend to form groups in accordance with their type of charge. Taking into account this assumption, it is accepted for ^{3}He that two protons form a pair or a complete shell of the s_n-orbital, and the value of the isotope magnetic moment is formed due to the anomalous magnetic moment of the neutron. For the nuclear structure contribution, it is necessary to choose the estimation with a free neutron ($\mu_{strHe3} = \mu_{3He} - \mu_n = б$ -0, 21447 (10, 08%).

Among the values of the magnetic moment, the isotope ^{109}Ag, which has one proton in the shell of the period 7 and the anomalously low μ_{109Ag} = - 0.232, belongs to the + 1 configuration. As the number of nucleons is increased for the isotopes with a free proton ^{113}In (μ_{113In} = 5,529), the values of ^{115}In (μ_{115In} = 5,541) change the sign and increase by more than 20 times in the absolute value and then decrease again to the negative sign by the end of the p_n-orbital, where the nuclei with free n are arranged in the column of stable isotopes.

In formula (2), the magnetic spin moment of the nucleus is not identified. There are several reasons for this:
- in electromagnetic interactions, the isotopic spin conservation law is violated;
- the isotopic spin values are in complete inconsistency with the magnitude of the nuclear magnetic moment;
- the magnetic moments of the proton and neutron are of a spin nature; they are also called the anomalous magnetic moments, because contrary to the theoretical predictions (about $1\mu_n$), the measurements show 2.79 μ_n and -1.91 μ_n for the proton and neutron respectively. The intrinsic magnetic moments of the proton and neutron are caused by the charge motion inside of them, and the use of additional virtual moment in this case is not required.

Most authors also agree that "the spin nature of hadrons has not yet been revealed." There were attempts to understand it taking into account the internal structure of hadrons consisting of partons. However, this approach has not yet led to the solution of the hadron spin issue [24]. Nucleons have their own magnetic moments. This can be explained by the charge motion inside of them and shows that nucleons have a complex structure. It should be assumed that during further studying of the nucleon internal structure, the spin nature of nucleons will appear in a different form than that of electrons.

In the massive dn- and fn-orbitals, the nuclei with an unpaired neutron have the magnetic moment of $-1 < \mu_n < +1$, i.e. greater than -1.91 μ_n. Although the neutron has the negative magnetic moment of 1.91 μ_n, the positive μ_n values are observed in the form of peaks in the middle of the orbitals for the period 7. The presence of stable isotopes with a free neutron, which have positive magnetic moment values, varies depending on the period number. They are absent in the periods with even numbers and are present in the periods with odd numbers. In addition, the number of such isotopes is increased together with the shell size: in the period 1 -1 (^{2}H); in the period 3 -1 (^{13}C); in the period 5 there are 3 isotopes (^{33}S, ^{57}Fe, ^{67}Zn), in the period 7 there are 11 isotopes (the dn-orbital: ^{131}Xe, ^{135}Ba, ^{137}Ba; the fn-orbital: ^{163}Dy, ^{171}Yb,^{177}Hf, ^{189}Os, ^{195}Pt, ^{199}Hg, ^{205}Pb, ^{207}Pb). The value and sign of the magnetic moment vector for the isotope depends on the period number μ_{per}. The free-neutron nuclei have a small dispersion of the negative magnetic moment (within 50% of -1.91μ_n) in contrast to the nuclei with an unpaired proton (within 200% of 2.79μ_n).

The odd-odd isotopes (^{6}Li, ^{10}B, ^{14}N, ^{40}K, ^{50}V, ^{176}Lu, ^{180}mTa) have positive magnetic moment values. The exception is ^{40}K, which is completed by the p_n-orbital of the period 5 and has a significant negative magnetic moment μ_{40K}=-1,2981. The odd-odd isotopes are also arranged only in the odd periods. The isotopes ^{50}V, ^{176}Lu, ^{180m}Ta are located in the middle of large d_n and f_n-orbitals and have significant positive magnetic moments $>\mu_p$=2.79μ.

Within the small periods (1-4, 2-12 nucleons), the characteristics of magnetic moment periodicity appear to a lesser extent. It should be assumed that the interaction between the nucleons (μ_m) is of greater importance. As the shell is much smaller, the nuclei are closer to a spherical shape and have no deformation; the nucleons move closer to the previous shell.

The magnetic moment values of the d_n- and f_n-orbitals for the period 7 are at the same level. At the same time, the quadrupole moment values for the isotopes of the f_n-orbital are much greater. Such a discrepancy becomes resolvable if it is taken into account that the speed of the proton can be lower in the massive orbital of 60 nucleons, and the magnetic moment can be correspondingly lower. In this case, it is necessary to take into account the nuclear component structure related to the size of the orbital – μ_{orb}. This explanation is confirmed by the fact that with the beginning of the fn-orbital, the thermal neutron capture cross-section is increased (fig. 25-a). This strongly depends on the nucleon energy, i.e. the smaller the kinetic energy of nucleons in the outer shell is, the "easier" the thermal neutron enters the nucleus, the lower the speed of nucleons and the current strength of their charges are and the smaller the magnetic moment is.

Thus, in accordance with the magnetic moment values, the isotopes show correspondence to the periodic structure of the nucleus (figs. 14 and 15). The most contrastive values are observed within the massive d_n- and f_n-orbitals of 28 and 60 nucleons respectively. For the periods 5 and 6, the values of μ are maximal in the middle of the d_n-orbital. By the end of the orbital and the period as a whole, μ is decreased, which is expected for the filling shell. At the end of the period 6, the proton-rich nuclei with a free proton ^{103}Rh (μ=-0.09) and ^{107}Ag (μ=-0.11) are concentrated. For these nuclei, a significant positive magnetic moment determined by $\mu_p = 2.79\mu$ is expected. However, the determining factor is the nuclear structure component related to the completion of the d_n-orbital. In the period 7, nuclei with a free neutron having a small negative magnetic moment are concentrated at the ends of the orbitals. The odd-odd isotopes are also arranged only in the odd periods 3, 5, and 7. The presence of stable isotopes with a free neutron, which have positive magnetic moment values, also varies depending on the period number. In the periods with even numbers, they are absent;

in the periods with odd numbers, they are present. In addition, the number of such isotopes is increased together with the shell size. The free-neutron nuclei have a small negative amplitude of the magnetic moment of less than 50% of -1.91μ_n, in comparison with the unpaired-proton nuclei (within 200% of 2.79μ_n). When deriving the magnetic moment expressions, it is important to take into account the factors related to the internal structure: the spin μ_{sp}, free nucleon motion μ_{free_nucl}, charge motion μ_{charge}, magnetic moment of the period μ_{per}, interactions of nucleons in the shell μ_{mutual}, orbital size μ_{orb}:

$$\mu_{str} = \mu_{sp} + \mu_{free\_nucl} + \mu_{charge} + \mu_{per} + \mu_{mutual} + \mu_{orb} \quad (3)$$

Origin of "Magic" Numbers

Table 5. The mutual inclusion property for the orbitals and periods of electrons and nucleons.

Electron orbitals	2	6	10	14
Electron periods	2	8	18	32
Nucleon orbitals	2	10	28	60
Nucleon periods	2	12	40	100

In the Pascal's triangle, there is an algebraic regularity between the number of elements in the periods and nuclear orbitals. Just as the value of the period for the system of elements makes up the sum of electron orbitals, the sum of periods amounts to the number of nucleons in the nuclear orbitals: 2 = 2; 10 = 2 + 8; 28 = 2 + 8 + 18; 60 = 2 + 8 + 18 + 32. The sum of nuclear orbitals amounts to nuclear periods. The mutual inclusion property "all in all" is active from the electron pairs and orbitals to the nuclear periods (Table 5).

It is noticed that the "magic" numbers for protons and neutrons (2, 8, 20, 28, 50, 82, 114) are random combinations of the sums of charge periods, the system of elements (2, 8, 18, 32, 50): 2, 8, 20=2+18; 28=2+8+18; 50 or 50=32+18, 82=32+50 or 82=32+32+18; for neutrons: 114 = 50 + 32 + 32. Such a dependence suggests that the regularities typical for the electron shells are maintained by the charge of protons and neutrons. Mass periodicity of the orbitals for the system of isotopes is formed by a strictly consistent sum of charge periods: 2=2; 10=8+2; 28=2+8+18; 60=2+8+18+32. This is the main difference between the "magic" numbers and the orbitals and periods of the nucleons obtained using the principle of multilevel periodicity. In the periodic system of isotopes, there is a sequence of orbital summation: s_n, p_n, d_n, fn of the charge shells. The "magic" numbers are formed from random combinations of the sums of charge periods and represent the secondary quasi-periodic structures inside the nucleus. The structure has some characteristics of nuclear orbitals and can be defined as suborbitals. The "magic" number 28 coincides with the number of isotopes in the dn-orbital and is a consecutive sum of 2+8+18 periods. Previously, the periods of charge inside the nucleus can be simulated as the systems of circuits and magnetic fluxes having the structure and force moments. The resulting moment of the suborbital for the "magic" number of the isotope is formed by the interaction of the moments for different circuits. Special stability of "magic" nuclei should be explained by the interaction of completed charge cycles (periods) in the nucleus. The property of summation or mutual inclusion of atomic shells makes it necessary to take into account the action of charge cycles in the nucleus (periods) for the existing models.

The "magic" numbers outside isotope stability have been theoretically derived: 2, 8, 20, 50, 82, 114, 126, 164 – for protons; 2, 8, 20, 28, 50, 82, 126, 184, 196, 228, 272, 318 – for neutrons. The properties of isotopes with the "magic" numbers of more than 82 protons and 126 neutrons cannot be verified experimentally. Taking into account the requlrities considered above, these numbers have two perculiarities:

1. If these numbers are presented without any reference to the nucleon type (p or n), but as the mass numbers, it is easy to see that the isotopes, where A is equal to the magic number 114, 126, 164, 196, are the advantageous nucleon combinations having the increased cosmic abundance (fig. 16).
2. The mass numbers of heavy isotopes with the increased cosmic abundance (114, 164, 196) also consist of the combinations of period numbers or smaller "magic" numbers (114=50+32+32; 164=82+82=50+50+32+32=4*32+2*18; 196=114+82=5*32+2*18).

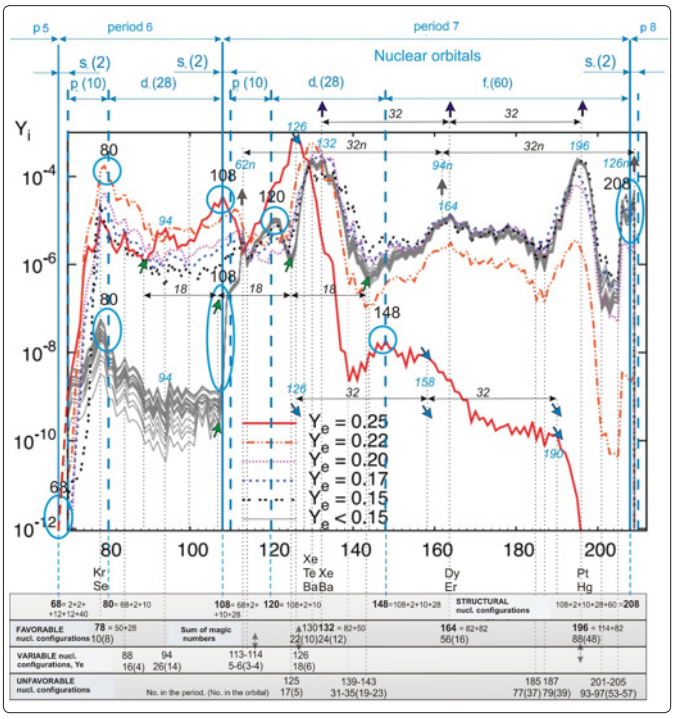

Figure 16: Analysis of the nuclear periodic structure based on the abundance of heavy elements formed by the r-process as a result of the observation over 23 binary systems (black hole – neutron star). Calculation of the abundances depending on the electron concentration in the core of the neutron star Y_e is shown with color [4].

In fig. 16, the maximum peaks for the abundance of isotopes contained in the emissions of matter from the compact binary systems are shown: neutron star – black hole [4]. In accordance with the authors of the study, the extremes on the abundance graph are determined by the internal structure of the nucleus [4]. In addition to the structural transitions between the periods and orbitals, the isotope abundance peaks are formed. These

peaks are beneficial or variable nucleon configurations consisting of "nonmagic" numbers: 78=50+28; 132=82+50; 164=82+82; 196=114+82. In this case, the advantageous nucleon configurations are a combination of 3–4 filled charge structures inside the nucleus. The number 78 is not “magical”, but it fits into the summation rule. Moreover, the isotope with the given mass number forms a stable abundance peak in the considered binary systems. The mass number 126 is considered to be “magic” for neutrons and is represented by the isotope $^{208}Pb^{82}126$, which is “magic” twice (82 protons, 126 neutrons). Position of the isotope $^{208}Pb^{82}126$ coincides with the end of the period 7 and is the transitional structural configuration of the nucleus. The number 126 does not meet the summation rule for magic numbers. This fact shows that the number 126 may be identified as a magic number as a result of two coincidences. The close number 128=32+32+32+32 corresponds to the summation rule. Nevertheless, if the number 126 is considered as a mass one without any reference only to neutrons, then it is noticed that the abundance peak is formed at A=126 (fig. 16). For this configuration, the isotope synthesis with A = 126 depends on the concentration of electrons in the interior of the star. It should be assumed that the electron component contributes to the increased concentration of neutrons at the ejection of matter and provides the synthesis of "magic" nuclei for neutrons.

The mass numbers of heavy isotopes on the abundance peaks can also be decomposed into the number of periods for the elements: 164=50+50+32+32; 196=50+50+32+32+32. Such an algebraic regularity suggests that there exists a continuous periodicity formed by the charge cycles of one duration (fig. 16). Characteristics of such periodicity are observed in the system of elements, for example:

- boiling temperatues of Al, Si → 8 → Sc, Ti have clearly defined peaks through 8 elements despite the fact that the period of 18 elements has already begun for Sc and Ti, and there are no vertical connections in the subgroups. It is interesting to note that both pairs of the elements are first and second in their orbital: Al and Si in the p-orbital, and Sc and Ti in the d-orbital;
- Tc, Pm and At are the elements which are absent on Earth and are the fifth in the orbital for the system of elements: Tc is the fifth element in the d-orbital of the period 5, Pm is the fifth element in the f-orbital of the period 6 and At is the fifth element in the p-orbital of the period 6. Such a coincidence is hardly accidental and suggests the existence of advantageous/disadvantageous charge configurations for the number in the period and orbital both of the nucleus and the electron cloud;
- the increased abundance of every sixth element at the beginning of the sequence of H, N, Al, K and He, O, Si, Ca, Fe may be the consequence of continuous periodicity of 18 elements, which extends over the periods of 8 and 2 elements;
- the specific magnetic susceptibility of iron is the highest among all the elements, while there is an anomalously high magnetic susceptibility of the element spaced by 18 atomic numbers; oxygen – (by 5 orders of magnitude in comparison with the adjacent elements in the period: B, C, N, F(?), Ne) spaced by 8 atomic numbers. The paradox is enhanced by the fact that iron is a solid, and oxygen is a gas;
- the increased electrical and thermal conductivity of aluminum Al and copper Cu is well-known. There are 8+8 atomic numbers between these elements, although Al is in the period of 8 elements and Cu is in the priod of 18 elements, and there are no vertical connections between them.

Table 6. Mass numbers of the filled orbitals and periods for fig. 17.

Period\orbital	sя	pя	dя	fя
1	2			
2	4			
3	6	16		
4	18	28		
5	30	40	68	
6	70	80	108	
7	110	120	148	208
8	210	220	248	308

In the mineral metabolism of living matter, there often occur chemical processes which are more diverse and subtle than the chemistry of laboratory experiments. When considering the properties of chemical elements in the periodic system, it is observed that the analogy of the properties for the chemical elements in the subgroups is far from perfect. For example, lithium properties are more similar to those of magnesium than to sodium or potassium; boron is more similar to carbon or phosphorus than to aluminum, etc. It makes necessary to search for additional forms and similarity algorithms for the properties of chemical elements. The periodic system both of elements and isotopes is a flat table in which there are only horizontal and vertical connections. In this regard, the logical questions arise: “Why there are only two directions? Can there be three-dimensional or other connections?”, “How does the nuclear periodic structure affect the properties of the elements?”. Due to the analysis of both structures — nuclear and electronic — as well as of a wider range of chemical processes, the similarity algorithms for chemical elements which can be useful and applicable in materials science or biology were found. As a result, the search for new materials can be carried out faster. The similarity algorithms can not be described partially or without proof. This topic is under development and will be presented separately.

Continuous periodicity can also be observed in the system of isotopes. For example, periodicity of the orbital 60 is observed in the increased abundance of isotopes: ^{28}Si ^{88}Sr ^{148}Nd; ^{208} or ^{16}O,^{76}Se, ^{136}Ba, ^{196}Pt; periodicity of the orbital 28: ^{28}Si, ^{56}Fe, ^{84}Kr, ^{112}Cd, ^{140}Ce, ^{168}Er, ^{196}Pt, etc. Continuous periodicity can be simulated as diverging harmonics from the basic cycle of the orbital or period. The property of summation for the charge cycles, as well as the features of continuous periodicity, suggests that there are transitions of the negative electric charge in the nucleus of the neutron-proton-neutron system. The electron-hole model of internal currents applied in semiconductor physics can also be useful for the nucleus.

This idea should be developed together with a complex nuclear model showing the spatial orientation of shell moments for the periodic structure, magic numbers, charge cycles and divergent harmonics of continuous periodicity. For such a model, the periodic structure, property of mutual inclusion for the shells and property of summation for the charge shells, which show the difference between the "magic" and periodic structural transitions, etc., should be taken into account. The generalized Bohr-Mottelson nuclear model differs from the single-core shell model mainly by introducing static deformation of the average nuclear field. Due to the static deformation, the rotational degrees of freedom occur. In more advanced versions of the generalized model, the collective degrees of freedom related to the vibrations of nuclear

surface around the equilibrium deformed form are also taken into account. In the generalized model, the discovered regularities in the form of the periodic structure, properties of mutual inclusion for the shells and summation properties for the charge shells are not taken into account. However, the generalized model does not exclude the presence of these regularities. Due to this, the regularities can be combined with the model, additional degrees of freedom can be found and classified.

In view of the obtained numerical regularities, in addition to the well-known "magic" combinations, there are other combinations for the sums of periods. This implies that there are missing "magic" numbers: 8+2 = 10; 8+18 = 26; 32+8 = 40; 32+2 = 34. This fact requires verification. In the classical paper of M. Goeppert-Mayer, I.G.D. Jensen, "The elementary theory of nuclear shells", several criteria for the "magicalness" of nuclei are given:

Table 7. The criteria of "magicalness" in accordance with M. Heppert-Mayer, I.G.D. Jensen "The elementary theory of nuclear shells" [2].

1.	A sharply predominant abundance of one isotope in the natural mixture of a heavy even nucleus is found only for the magic numbers.
2.	Among the isotopes of this element, the isotope with the magic number of neutrons has anomalous abundance.
3.	The absolute cosmic abundance of nuclei with the magic number of neutrons or protons is greater than the normal abundance of nuclei in the corresponding mass range.
4.	There are more stable nuclei for the "magic" numbers of neutrons and protons than for the ordinary numbers.
5.	Nuclei with the "magic" number of neutrons have an unusually small neutron absorption cross-section.
6.	Nuclei with the "magic" numbers have the increased resistance to different kinds of decay; they should be interpreted as the "closed shells", similar to the closed shells of noble gas atoms.

In Table 8, the criteria for known and missing "magic" numbers are analyzed. The stability of isotopes is estimated on the basis of the most common type of decay related to the mass transfer – the thermal neutron capture.

Table 8. Analysis of known and missing "magic" numbers

"Magic" number	Sum of periods (2, 8, 18, 32, 50).	Number of isotopes	Isotopes (% in natural mixture).	Number of "magic" atoms in the solar system (in relation to 106 of Si atoms) [8], 2010.	Thermal neutron capture cross-section for isotopes with the largest abundance (barn).
2p	2	2	^{4}He (99,999863); ^{3}He (0,000137)	2,51E+09	^{4}He – 0 ^{3}He – 5333
2n		2	^{2}H (0,015); ^{3}He (0,000137)	1,53E+06	^{2}H - 0,00510
8p	8	3	^{16}O (99,7571); ^{17}O (0,0380); ^{18}O (0,2051)	1,57E+07	^{16}O – 0,0001 ^{18}O – 0,00018
8n		2	^{15}N (0,368); ^{16}O (99,7571)	1,57E+07	^{15}N – 0,00004
20p	2+18	6	^{40}Ca (96,9411); ^{42}Ca (0,6472); ^{43}Ca (0,135); ^{44}Ca (2,0861); ^{46}Ca (0,004); ^{48}Ca (0,1872)	60151	^{40}Ca – 0,41 ^{42}Ca – 068 ^{44}Ca – 0,88
20n		4	^{40}Ca (96,94115); ^{36}S (0,02); ^{37}Cl (24,22); ^{38}Ar (0,0632)	74720	^{37}Cl - 0,43 ^{38}Ar - 8
28p	2+8+18	5	^{58}Ni (68,07698); ^{60}Ni (26,22317); ^{61}Ni (1,1399); ^{62}Ni (3,634); ^{64}Ni (0,925)	49093	^{58}Ni – 4,64 ^{60}Ni – 2,9 ^{62}Ni – 14,5
28n		5	^{48}Ca (0,1872); ^{50}Ti (5,18); ^{51}V (99,75); ^{52}Cr (83,7891); ^{54}Fe(5,8453)	61226	^{48}Ca – 0,88; ^{50}Ti 0,179 ^{51}V – 4,94; ^{52}Cr – 0,76 ^{54}Fe – 2,25
50p	50 or 32+18	10	^{112}Sn (0,97); ^{114}Sn (28,734); ^{115}Sn (0,34); ^{116}Sn (14,54); 117Sn (7,68); ^{119}Sn (8,59); ^{120}Sn (32,59); ^{122}Sn (4,63); ^{124}Sn (5,79)	3,61	^{114}Sn – 0,336 ^{116}Sn – 0,075 ^{120}Sn – 0,141
50n		6	^{86}Kr (17,302); ^{87}Rb (27,83); ^{88}Sr (82,58); ^{89}Y (100); ^{90}Zr (51,45); ^{92}Mo (14,843)	42,86	^{88}Sr – 0,058;^{87}Rb – 0,1; ^{90}Zr – 0,0771;^{89}Y –1,28

82p	32+50	4	^{204}Pb (1,997) ^{206}Pb (24,1) ^{207}Pb (22,1) ^{208}Pb (52,4)	3,31	^{208}Pb – 0,0049 ^{206}Pb – 0,03; ^{204}Pb – 0,4
82n		7	^{136}Xe (8,871); ^{138}Ba (71,6984); ^{139}La (99,91); ^{140}Ce (88,48); ^{141}Pr (100); ^{142}Nd (27,131); ^{144}Sm (3,1)	5,74	^{138}Ba – 0,41;^{141}Pr – 4 ^{140}Ce – 0,58; ^{139}La – 9,2
Missing “magic” numbers					
10p	2+8	3	^{20}Ne (90,48); ^{21}Ne (0,27); ^{22}Ne (9,25)	3,29E+06	^{20}Ne – 0,036;^{21}Ne – 0,67 ^{22}Ne – 0,046
10n		3	^{18}O (0,2051); ^{19}F (100,0); ^{20}Ne (90,48)	3,07E+06	^{18}O – 0,00018; ^{19}F – 0,0096
26p	8+18	4	^{54}Fe (5,8453); ^{56}Fe (91,7543); ^{57}Fe (2,119); ^{58}Fe (0,2819)	827600	^{54}Fe – 2,56;^{56}Fe – 2,59; ^{57}Fe – 2,48; ^{58}Fe – 1,28
26n		2	^{48}Ti (73,72); ^{50}Cr (4,3451)	1948	^{48}Ti - 7,84;^{50}Cr – 15,8
40p	32+8	4	^{90}Zr (51,45); ^{91}Zr (11,22); ^{92}Zr (17,15); ^{94}Zr (17,382)	10,78	^{94}Zr – 0,011;^{91}Zr – 1,17 ^{92}Zr – 0,22;^{94}Zr – 0,05
40n		4	^{70}Zn (0,62); ^{71}Ga (39,892); ^{72}Ge (27,543); ^{74}Se (0,89)	54,3	^{71}Ga – 3,61 ^{72}Ge -0,8
34p	32+2	5	^{74}Se (0,89); ^{76}Se (9,372); ^{78}Se (23,772); ^{80}Se (49,614); ^{82}Se (8,732)	100,12	^{74}Se – 50;^{76}Se - 85; ^{78}Se – 0,43; ^{80}Se - 0,61;^{82}Se – 0,61
34n		3	^{62}Ni (3,634); ^{63}Cu (69,17); ^{64}Zn (48,63)	73,73	^{63}Cu – 4,5; ^{62}Ni – 14,5 ^{64}Zn – 0,93
58p	32+ 18+8	4	^{136}Ce(0.19); ^{138}Ce(0.25); ^{140}Ce(88.48); ^{142}Ce(11.08)	1.18	^{136}Ce – 1; ^{138}Ce - 0.018 ^{140}Ce - 0.58;^{142}Ce -0.97
58n		5	^{100}Mo(9.63); ^{102}Ru(31.573); ^{103}Rh(100); ^{104}Pd(11.14); ^{106}Cd(1.25)	1.68	^{100}Mo; ^{102}Ru – 1.2; ^{103}Rh – 144.9; ^{104}Pd -0,65; ^{106}Cd - 1.004

Characteristics for the missing magic numbers, which are similar to or greater than those for the magic numbers, are presented in the table and marked in italics. The missing “magic” number 10=8+2 is fixed for the nuclei ^{20}Ne; ^{21}Ne; ^{22}Ne – for protons and ^{18}O; ^{19}F; ^{20}Ne – for neutrons. Neon nuclei together with helium, carbon and oxygen are the stage of nuclear fusion in the α-process. At the end of their evolution, massive stars of 8-12 M_{solar} form a whole class called neon dwarfs. In fact, all these nuclei meet the criteria for magicalness and have a high relative abundance (^{20}Ne, ^{21}Ne, ^{22}Ne – 3,29E+06) within one order of magnitude, similar to oxygen nuclei (smaller by 80%), and an order-of-magnitude higher abundance than that of calcium. There are 5 stable nuclei with the “nonmagic” number 10, 4 stable nuclei with the “magic” number 8, 4 and 5 stable nuclei with the “nonmagical" numbers 6 and 12. The number of stable isotopes in even nuclei with small values of A is not a contrastive criterion of "magicalness". Isotopes with the number 10 have a high relative stability. The thermal neutron capture cross-section for ^{20}Ne (0.036) etc. is in the middle range between the magic nuclei ^{16}O (0,0001) – ^{40}Ca(0,41). From the abovementioned criteria, high cosmic abundance is the most reliable. It plays an important role in stellar processes in combination with a relatively low neutron capture cross-section.

The missing “magic” number 26=8+18 is expressed in 4 nuclei for protons and 2 nuclei for neutrons (^{54}Fe (5,8453); ^{56}Fe (91,7543); ^{57}Fe (2,119); ^{58}Fe (0,2819); ^{48}Ti (73,72); 50Cr (4,3451)). For comparison, nuclei with 28p – 10 isotopes. However, iron nuclei (26p) have a high relative cosmic abundance (827600), that is an order of magnitude higher than that of nuclei with 28p (49093) at the same order of stability. The thermal neutron capture cross-section – for ^{56}Fe (2.59) at ^{58}Ni (4.6) (Table 8). In addition, iron atoms have the highest bonding energy of the nucleus among the atoms of all the elements. In general, nuclei with the number of protons 26 meet the classical criteria for "magic" numbers in Table 7.

Stable isotopes with 26 neutrons are represented by two nuclei: ^{48}Ti (73, 72%) and ^{50}Cr (4, 35%). ^{48}Ti^{22}26 has a high relative abundance in the rocks of the Earth's mantle and on the Moon, as well as the contrasive value of 73.72% in the natural mixture. However, the thermal neutron capture cross-section is relatively high for such a light isotope (7.84). The isotope 26n has an even higher value – ^{50}Cr^{24}26 (15, 8). The number 26 for neutrons has implicit characteristics of "magicalness". The number 40 in paper [p. 758] is often referred to as “magic” or “semi-magic” and is singled out into a separate shell [2]. Nuclei with 34 protons have a low relative abundance in the solar system and an extremely high abundance in the ejection of matter for the compact binary systems at A=78, ^{78}Se, ^{78}Kr (fig. 17). Selenium isotopes show a sharp decrease in the thermal neutron capture cross-section when reaching A = 78 (50 + 28): ^{74}Se – 50;^{76}Se - 85;^{78}Se – 0,43;^{80}Se – 0,61;^{82}Se – 0,61 barn, which meets the criteria of "magicalness". In general, nuclei with 34 protons also have partial characteristics of "magicalness" in the aspects of cosmic abundance and stability. At that, the depth of analysis on the missing magic nuclei should be reduced for the reasons outlined below.

Fig. 16. The single-particle levels for harmonic oscillator (on the left) and infinite rectangular well (right); interpolation between them (in the center). The total number of underlying states, including the missing magic numbers 132, 58, 40, 34, is shown in square brackets.

The reasons mentioned above allow expanding a series of "magic" numbers to 4, 8, 10, 20, 26, 28, 34, 40 ..., but at the same time it is shown that the multiple nuclei with even number of protons or neutrons can more or less correspond to the accepted criteria for magic numbers. For example, ^{12}C, ^{24}Mg, ^{28}Si, etc., with 6, 12, and 14 protons and neutrons, respectively, will also meet the criteria of "magicalness". Therefore, the concept of "magic" numbers is quite vague. Calculations for the nuclear energy levels almost always depend on the accepted theory or model. In fig. 17, the single-particle levels for harmonic oscillator (on the left) and infinite rectangular well (right), as well as interpolation between them (in the center), are shown.

The total number of underlying states is shown in square brackets, including the variety of structural transitions: the “magic” numbers 2, 8, 20; the missing “magic” numbers 132, 58, 40, 34; the nucleon configurations with A=18, 68, 92, 106, 138. In this situation, clearer criteria should be developed and structural transitions in the nucleus should be classified, taking into account the principle of multilevel periodicity and summation regularities of charge periods for "magic" numbers.

It is reasonable to leave the theoretical definition of “magic” number in the form of correspondence to the principle of charge period summation. To do this, it is necessary to clearly distinguish the concepts of nuclear orbitals and magic numbers. Experimental confirmation should be found in cosmic abundance and other properties showing energetically favorable configurations of nuclear fusion and revealing internal structural formations. “Magic” numbers should be considered not only by the type of nucleon, but also as a mass number A.

Nuclear orbitals are the nuclear shells which include the number of nucleons determined by a strictly consecutive sum of numbers for charge periods – 2, 8, 18, 32: the sn – orbital: 2=2; the pn – orbital: 10=2+8; the dn – orbital: 28=2+8+18; the f_n – orbital: 60=2+8+18+32. Within the orbital, the properties of nuclei are changed gradually, and with the change of the orbital – more rapidly. The sum of 1-4 orbitals in ascending order is a period.

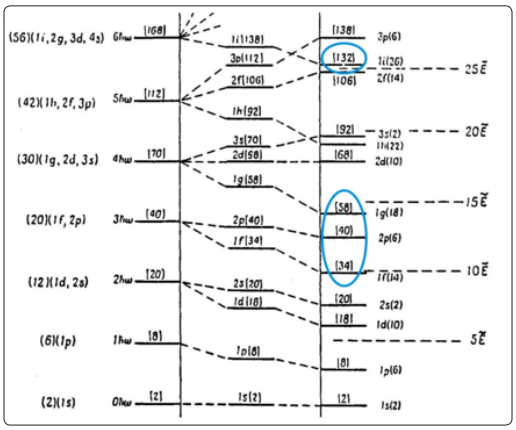

Figure 16: The single-particle levels for harmonic oscillator (on the left) and infinite rectangular well (right); interpolation between them (in the center). The total number of underlying states, including the missing magic numbers 132, 58, 40, 34, is shown in square brackets

Magic number of nucleons is a mass number, which is a random sum of charge periods 2, 8, 18, 32. The fewer numbers there are in the total amount, the more rigorously "magic" criteria are expressed (Table 8). Structurally, magic numbers represent a set of charge shells inside the nucleus.

Magic numbers consist of combinations of the sum of charge periods. Taking into account the missing magic numbers, they can be divided into two categories: charge numbers of protons and neutrons (2, 4, 8, 10, 20, 26, 28, 34, 40, 50, 82) and magic numbers of nucleons (78, 114, 132, 164, 196, are equal to the mass number of the isotope). The numbers for nucleons are the number of positive charge concentrated in protons and neutrons. These numbers are equal to the mass number A. Magic numbers of nucleons are advantageous nucleon configurations with increased cosmic abundance. The nucleon configurations consist of the sum of magic numbers or the consecutive sum of charge periods: 78=50+28; 114=82+32; 126(?); 132=82+50; 164=82+82; 196=114+82.

Before proceeding to the next section, it is useful to summarize the coincidences and differences in the nuclear shell model and periodic system of isotopes. Isotopes corresponding to the “magic” numbers 20, 50 and 82 – $^{40}_{20}$Ca, $^{120}_{50}$Sn and $^{208}_{82}$Pb are arranged on the boundary of the orbitals and periods and, from the point of view of both theories, have filled outer shells. For the nuclear shell model, the filled shells of protons are 20, 50, 82, and of neutrons are 20 and 126. In the context of the periodic system, the isotope $^{40}_{20}$Ca is the latest in filling the pn-orbital of the period 5 and subgroup 12 with nucleons. The “magic” isotope ^{120}Sn^{50}70 completing the pn-orbital of the period 7 is symmetrically arranged in the same subgroup. The “magic” nucleus ^{208}Pb^{82} completes the fn-orbital and the period 7 as a whole. In the description of "magic" nuclei [p. 755], the main examples of energy stability for the shells are related to these nuclei [2]. The shell model shows a disproportionate number of nucleons in the nuclear shells (in brackets) when moving away from the center and when the inner shell is larger than the outer one: 4 – (4) – 8 – (16) – 20 – (8) – 28 – (22) – 50 – (32) – 82. Even at parallel filling with protons and neutrons, such a sequence cannot correspond to a uniform spherical shape. This shows a discrepancy according to which the internucleon interaction forces should have different properties for different shells. In the periodic system of isotopes, the change in the properties of periods and the similarity of properties for isotopes in subgroups are shown, the sequence of filling periods and orbitals is determined, the total mass of protons and neutrons is taken into consideration. The periodic system defines several nuclei, which are the filled orbitals and periods: ^{2}H, ^{4}He,^{16}O, ^{18}O, ^{28}Si, ^{30}Si, ^{40}Ca (K, Ar), ^{68}Zn, ^{80}Se (Kr), ^{108}Pd(Cd), ^{110}Pd(Cd), ^{120}Sn(Te), ^{148}Sm(Nd), ^{208}Pb, ^{210}Po, ^{220}Rn. These nuclei are extrems for such parameters and processes as quadrupole moment, magnetic moment, scattering length and neutron capture cross-section, α-particle yield, cluster decay (see Sections 12-14), cosmic abundance, stellar evolution, etc. At the same time, “magic” numbers show special points of stability and abundance for the isotopes of the orbitals and periods. The properties of mutual inclusion and summation of charge periods show that these singular points are determined not due to the mass, but due to the charge occupancy of nuclear shells.

In this regard, the concept of “charge period – nuclear orbital” requires development. Taking into consideration the property of mutual inclusion, this allows revealing the interaction mechanisms in the system “electronic orbital – period – nuclear orbital – nuclear period” more clearly. Just as the views on magnetic

properties of matter were expanded by the spin-orbit interaction, the mechanisms of many other properties of simple matter can be explained by the interactions between the periodic structures of electrons and protons. It should be assumed that the mystery of mass formation should be solved by identifying the arrangement, shape and interaction of electric and magnetic fluxes in the nucleus.

As a result of the analysis, the origin of magic numbers, which are a random sum of charge periods 2, 8, 18, 32, is determined. The fewer numbers there are in the total amount, the more rigorously "magic" criteria are expressed. Structurally, magic numbers are a set of charge shells inside the nucleus with some characteristics of nuclear orbitals, while nuclear orbitals are the nuclear shells which include a number of nucleons determined by a strictly consecutive sum of numbers for charge periods – 2, 8, 18, 32; the s_n-orbital: 2=2; the p_n-orbital: 10=2+8; the d_n-orbital: 28=2+8+18; 60=2+8+18+32; the f_n-orbital: 60=2+8+18+32.

Models of Filled Nuclear Orbitals

Direct methods for measuring nuclear shape are almost not available yet, so indirect methods should be involved. It is noticed that the most common configurations of carbon clusters (fullerenes) have the same number of atoms, similar to the number of nucleons in the orbitals of isotopes (28 – the d_n-orbital, 60 – the f_n-orbital) and in the periods of elements (32, 50) (fig. 18). The data on the magnetic and quadrupole moments of nuclei show that the nucleons do not form any static fixed configurations and, at the same time, the isotopes with completed nucleon orbitals have the shape similar to spherical (^{16}O, ^{40}Ca, ^{68}Zn, ^{120}Sn, ^{148}Ce, ^{208}Pb, etc.). It is logical to assume that the filled shells follow successively in the form of spherical layers; i.e. it can be assumed that at the point moment of time, the nucleons of the filled outer orbital occupy dislocations with a uniform distribution over the sphere.

The fullerenes C_{28} and C_{60} have a hollow inner part. Therefore, they can be used as nuclear orbital models containing the inner filled shells of the core. Such a coincidence in the number of fullerene atoms and nucleons of nuclear shells suggests that structural representation of the most probable arrangement of nucleons in the sphere of the outer filled nuclear orbital, at the point moment of time, can be obtained on the basis of stereometry principles. For this, it is necessary to pay attention to the structure of carbon cluster molecules.

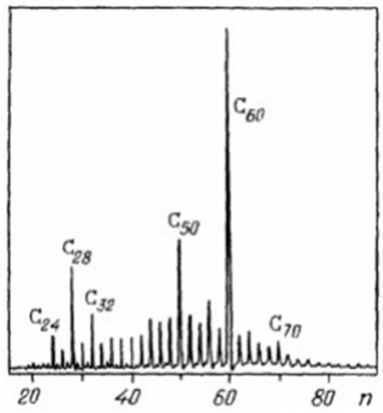

a) The typical spectrum of thermal evaporation for carbon atoms [25, p.178].

b) Adamantane 10 ($C_{10}H_{16}$) is the analogue of the pn-nuclear orbital.

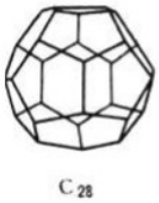

c) Fullerene 28 is the analogue of the dn-nuclear orbital.

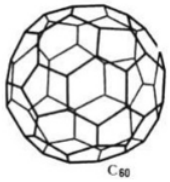

d) Fullerene 60 is the analogue of the fn-nuclear orbital.

Fig. 18. The models of filled nuclear orbitals. Development at the level of atomic clusters

The flow of carbon fragments formed as a result of thermal evaporation from the surface of graphite contains the most common stable configurations with 28, 32, 50, and 60 atoms (fig. 18-a). The shape of fullerene molecules and other carbon compounds allows obtaining static visual representation for the shape of filled nuclear orbitals.

Adamantane molecule, a substance with many physical properties similar to diamond, corresponds to the symmetric form of 10 carbon atoms (fig. 18-b). Analysis on chemical properties of compounds with 10, 28, 60 shows their similarity. Adamantane and fullerenes C_{28} and C_{60} have the same basic valence – 4, similar to that of a single carbon atom. Fullerene C_{28}, as well as admantan, forms a stable crystal with a diamond structure – hyperdiamond, and the material with a hardness greater than the diamond with a similar structure is synthesized from C_{60} molecules. The similarity of physical and chemical properties is determined by the similarity of fullerene forms. Adamantane faces and the largest faces of C_{28} — the hexagons – coincide with the faces of a commensurate tetrahedron (fig. 18-b and 18-c). The model of the most common cluster configuration of 4 nucleons – the α-particles – has the same shape.

In addition to the forms with 10, 28, and 60 atoms, carbon can form pair configurations, similar to atomic electrons and nucleons. At different types of carbon polymolecule breaking, both in case of monomolecular decomposition and in case of photodissociation, the main decay channel of molecules with even n is related to the breaking of C_2 fragment. This fact is surprising, since the binding energy of C2 fragment is smaller than the corresponding value for C3. Due to this, a situation that contributes to the persistence of clusters with even *n* is created, and the proportion of clusters with odd *n* does not exceed 1% [25, p.180]. The same situation is observed for the isotopes – even numbers are the most common.

The increased abundance of each fourth isotope in stellar nucleosynthesis: ^{4}He, ^{12}C, ^{16}O, ^{20}Ne, ^{24}Mg, ^{28}Si, ^{32}S, etc. is a result of similarity of the tetrahedral form [12]. This feature is reflected in the principle of multilevel periodicity; the tetrad group property for the shell with a rank lower than that of the orbital is shown by the first slanted row of the Pascal's triangle (fig. 1-a). This observation is also confirmed by the absence of the isotope with the number A = 5 and the increased thermal neutron capture cross-section for each fifth isotope of the general sequence and subgroups (see Section 13, "Review of nuclear reactions for the thermal neutron capture (n, γ) and α-particle yield (n, α)"). The structure of C_{10}, C_{28} molecules, as well as the valence of fullerene C_{60} (-4), is also similar to a terahedron (fig. 18-b and 18-c).

Formation of clusters with the number of atoms fewer than 24 is energetically unfavorable because of the stress of σ-bonds between the carbon atoms at the formation of 3D figures inscribed in the sphere (fig. 18-a). Radioactive isotopes have a cluster radioactivity phenomenon, when the nucleus ejects the nucleon cluster – the shell of the period 8 (figs. 2-a, 2-b, Section 12). The most probable configurations are the clusters of ^{14}C, ^{24}Ne. The cluster of 24 nucleons is the smallest threshold step; after 24 nucleons are formed, large clusters from the nucleon remnant of the period 8 are formed gradually with A = 24, 26, 28, 30, 32, 34, etc. (Section 12). In the subgroup 24 of the periodic system of isotopes, the long-lived natural isotope ^{232}Th (1.40×10^{10} years) being the first in the period 8 is found. There are no long-lived isotopes in the previous subgroups 2-23. Similar to carbon clusters, in both cases of atoms and nucleons, the configuration 24 is the smallest advantageous nucleon configuration. Thus, it should be assumed that the principles of stereometry have significant influence on the distribution of nucleons in the shells, especially in the completed orbitals and periods. The following questions should also be clarified: "What is the determining factor in the formation of nucleon configurations — strong interaction properties and stereometric regularities and/or the properties of nuclear wave medium, due to which the configuration space is created and the nucleon motion and position in the shells are modulated?"

The similarity of structural forms of 4, 10, 28, 60, etc., which is also the similarity of properties for crystal lattices and valences of the corresponding fullerenes, suggests that there is a 3D type of periodic systems. In 3D view, not only the usual flat types of regularities can be presented – the periods and subgroups (horizontal and vertical symmetry), but also the symmetry of third dimesion. The similarity of isotope properties in the subgroups is a result of coincidence in the orbital shapes for different periods, similarity of their motion trajectories and vibrations. To build a 3D view for the periodic system, it is necessary to correctly place the elements into the structure nodes. There are many variants of placement. The placement algorithm, due to which a 3D view for the periodic system of elements will be defined and the new regularities (of third dimension) will be identified, still needs to be found. There may be several such algorithms.

Lifetime of Isotopes, Radioactivity and Periodic Structure of the Nucleus

The task of this section is to answer the question: "How does radioactivity depend on the nuclear structure?". The "stability valley" of isotopes comes to an end together with the period 7 of ^{208}Pb. Starting from the period 8 (A>208), all the isotopes show their radioactivity. Recently, it was discovered that the first isotope of the period 8 – ^{209}Bi, which is considered to be stable, is α-active with a half-life of about $1,8\text{-}2*10^{19}$ years. It should be noted that ^{209}Bi is the +1-configuration of nucleons. For +1-configurations, it is characteristic to retain the properties of the previous shell (see previous sections). The "stability valleys" of ^{232}Th, ^{234}U, ^{235}U, ^{238}U, which are abundant in nature, also show α-activity with a half-life of 10^{5}-10^{9} years. Starting from the period 8, a continuous series of stable isotopes is replaced by a radioactive sequence – this change occurs exactly at the end of the period 7 (A>208). This fact can hardly be related to an accident. It should be assumed that one of the reasons for rapid change of the stable isotope series to the radioactive sequence is that the shell of the period 8 is far from the core and is less associated with it in comparison with the previous periods.

For each chemical element there is a mass number of isotope A, where nucleons form the most stable nuclear configuration; the lifetime and abundance for given a are the greatest. To determine the tendency of how the lifetime of isotopes changes together with the increase in mass number, 3 isotopes with the longest lifetime T_1, T_2, T_3 are selected for each mass number in descending order (fig. 19). All the three sequences have a similar mass distribution and, on their basis, the shape of the line for the general lifetime distribution trend of the isotope for the period 8 is calculated:

$$T = \sqrt[\$]{T1 * T2 * T3} \qquad (4)$$

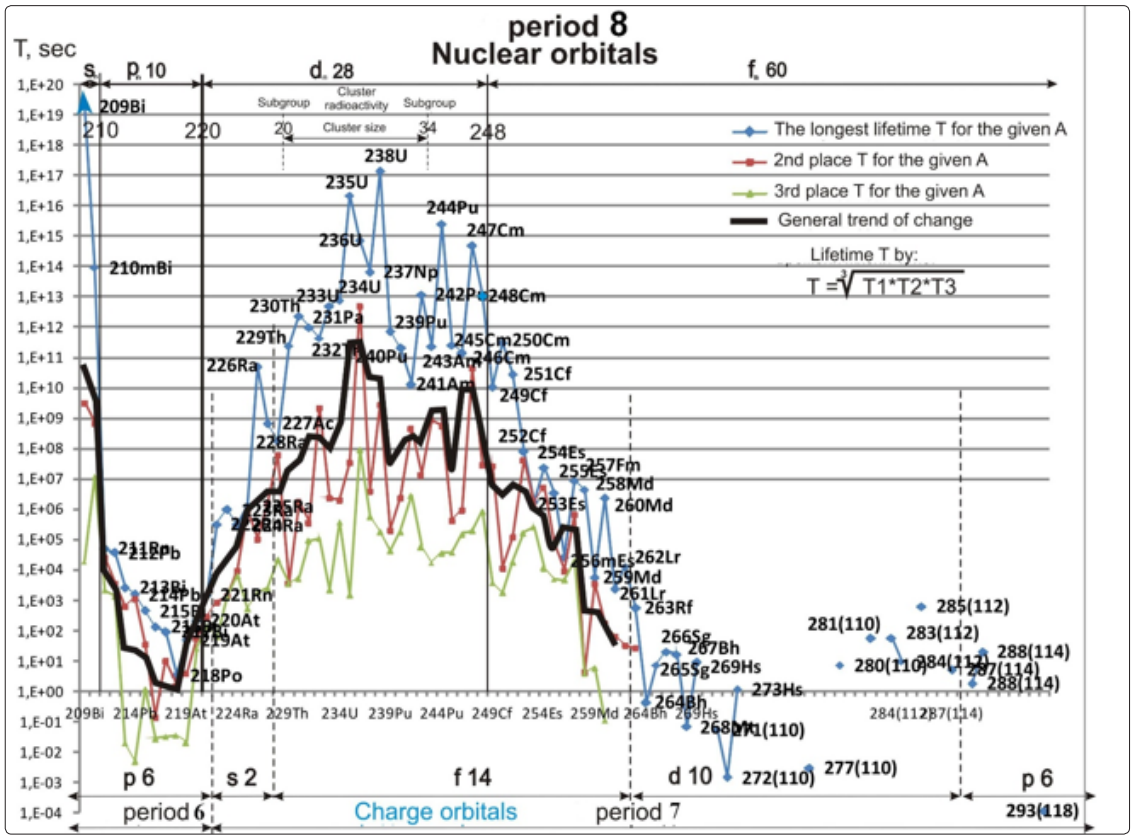

Figure 18: Lifetime of radioactive isotopes for the period 8

Among various types of decay for this isotope, the decay which occurs more often (dominates) is taken into account. For the orbitals s_n, p_n, d_n, as a rule, these are α, β decays or electron capture (EC). Other types of decay are: spontaneous fission (SF), cluster radioactivity – have important features; however, they occur 5–15 orders of magnitude less often and do not affect the shape of the curve. After A = 248, with the beginning of the fn-orbital, the proportion of spontaneous fission (SF) in the decay channels is sharply increased to 80–100%.

To answer the question of how the nuclear structure affects the lifetime, it is necessary to compare several features:
- the decrease in the lifetime trend starts at the boundary of the d_n and f_n nuclear orbitals (fig. 19 above) and approaches the boundary of charge orbitals for the elements of the f- and d-orbitals for the period 7 of the Mendeleev's Periodic System (figs. 19 and 22).
- the drop in the lifetime graph is clearly shown for the pn-orbital (fig. 19);
- the "stability islands" – isotopes: ^{232}Th, ^{234}U, ^{235}U, ^{238}U are arranged in the center of the dn-orbitals; in the subgroups 24, 26, 27 and 30 of the period 8 (Table 9);
- the most abundant and long-lived isotopes of the period 8 ^{235}U, ^{238}U are in the same subgroups as the isotopes of the "iron" peak for the period 5 (fig. 19). The largest peak on the trendline (235-236) is symmetric to the "iron" peak of 56Fe for the isotope abundance in the solar system (fig. 20, subgroup 28). In the subgroup 30, isotopes of the elements having the increased abundance (U, Ba, Mo, Ni) among the adjucent mass numbers, as well as the greatest abundance in the natural mixture of their element (table 9), are arranged symmetrically to ^{238}U.
- the shape of the trendline is similar to the peaks of the "double-humped barrier" for the mass distribution of isotopes at nuclear fission, especially to the "heavier" peak of the period 7, including the f_n-orbital (fig. 20).

Table 9: Isotopes of the subgroups 22-32 for the periods 5-8. Subgroups with the most advantageous nucleon configurations of the d_n-orbital (the most abundant and long-lived isotopes are shown in the cells) are marked with color

Subgroup	22	23	24	25	26	27	28	29	30	31	32
5 period	^{50}Ti	^{51}V	^{52}Cr	^{53}Cr	^{54}Fe	^{55}Mn	^{56}Fe	^{57}Fe	^{58}Ni	^{59}Co	^{60}Ni
%	5,18	99,75	83,789	9,501	5,845	100	91,754	2,119	68,077	100	26,223
6 period	^{90}Zr	^{91}Zr	^{92}Zr	^{93}Nb	^{94}Zr	^{95}Mo	^{96}Mo	^{97}Mo	^{98}Mo	^{99}Ru	^{100}Ru
%	51,45	11,22	17,15	100	17,382	15,92	16,68	9,55	24,133	12,74	12,601
7 period	^{130}Te	^{131}Xe	^{132}Ba	^{133}Cs	^{134}Ba	^{135}Ba	^{136}Ba	^{137}Ba	^{138}Ba	^{139}La	^{140}Ce
%	44,09	11,18	0,101	100	2,4171	6,59	7,854	11,23	71,698	99,91	88,48
8 period	^{230}Th	^{231}Pa	^{232}Th	^{233}U	^{234}U	^{235}U	^{236}U	^{237}Np	^{238}U	^{239}Pu	^{240}Pu
%			100		0,0055	0,72			99,2745		
T (years)	7,54e4	3.25e4	1.40e10	1,59e5	2,455e5	7,04e8	2,342e7	2,14e6	4,47e9	2,41e4	6,56e3

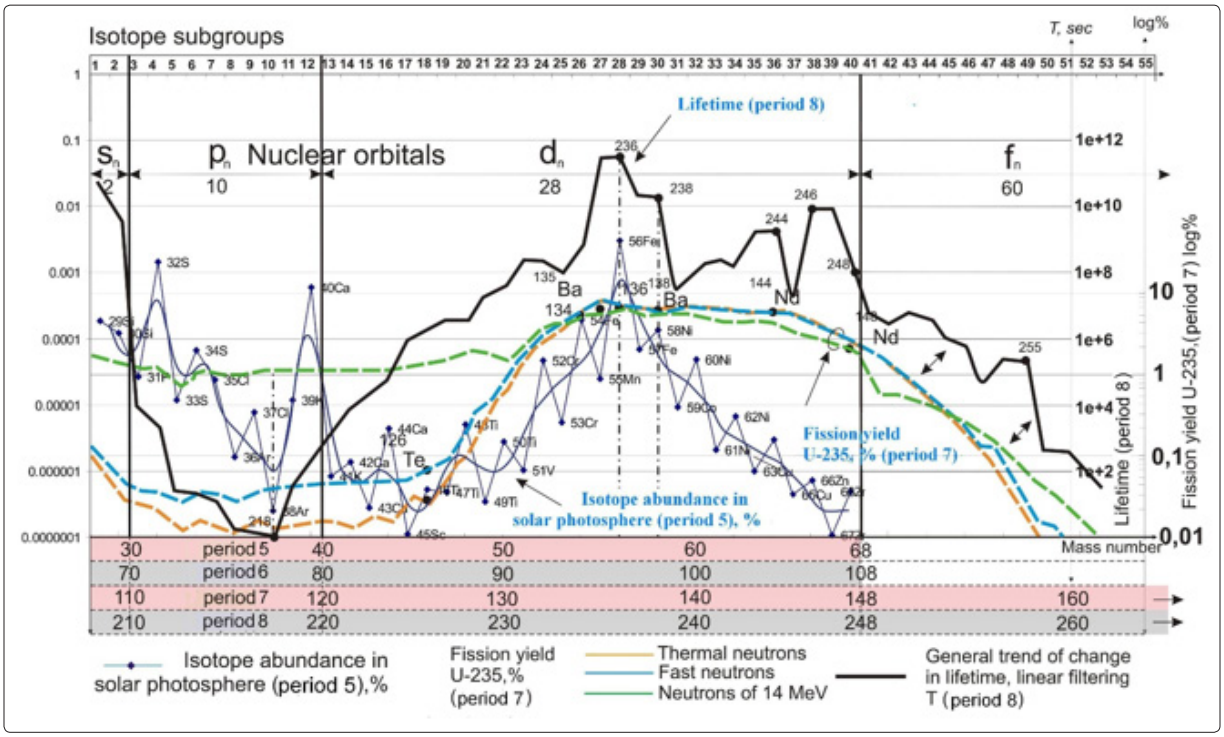

Figure 19: Symmetry of the graphs: distribution of the "iron peak", fission fragments and lifetime of isotopes for different periods in accordance with the periodic structure.

The arrangement of "stability islands" in the center of the dn-orbital, symmetry of subgroups with the "iron peak" isotopes, sharp development of radioactivity at the beginning of the period 8 allow concluding that the isotope position in the periodic system and the nuclear structure as a whole affect the isotope lifetime. The isotopes arranged in the center of the d_n-orbitals have the longest lifetime. The "drop" of the isotope lifetime in the pn-orbital of the period 8 can be explained by the fact that in the space of a small pn-orbital, it is impossible to form a stable closed shell of 10 nucleons around the massive core. As the central part of the nucleus (closed shell of the period 7) is quite large, the period 8 is far from the center of the nucleus and, consequently, nucleons are separated by centrifugal forces with α decay, etc. A stable shell within the whole period is formed only in the center of the d_n-orbital towards the subgroup 24 (^{232}Th).

Table 10. The probability of decay through spontaneous fission [26].

Nucleus	Half-life period, years	Probability of spontaneous fission
^{235}U	$7{,}04 \cdot 10^{8}$	$2{,}0 \cdot 10^{-9}$
^{238}U	$4{,}47 \cdot 10^{9}$	$5{,}4 \cdot 10^{-7}$
^{239}Pu	$2{,}41 \cdot 10^{4}$	$4{,}4 \cdot 10^{-12}$
^{240}Pu	6569	250Cm
^{250}Cm	8300	0,80
^{252}Cf	2,638	$3{,}09 \cdot 10^{-2}$

The trendline for the lifetime has fluctuations along the upper part of the peak from the subgroup 20 to the subgroup 40 and drops to a split second after A = 248 and when the f_n-orbital begins. The same distribution is demonstrated by the "heavy" part of the two-humped barrier at the distribution of fission fragments. The reason for this similarity is the same structure of the periods 7 and 8.

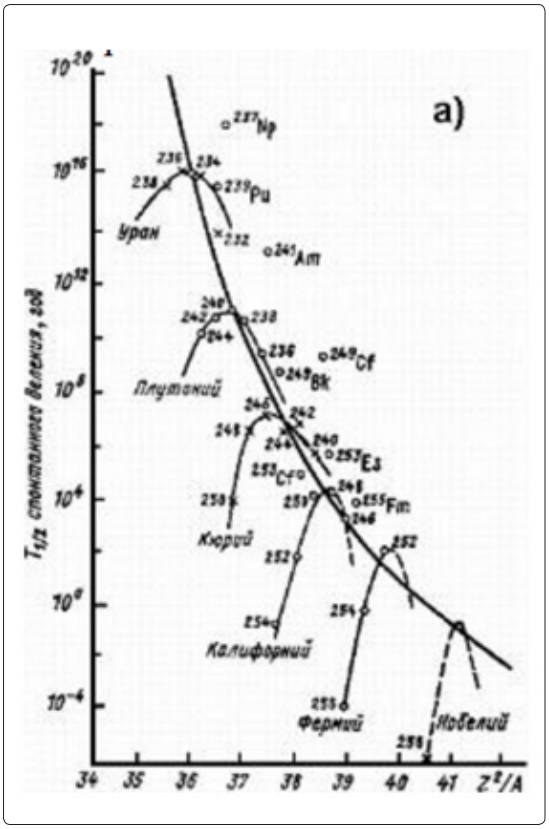

Figure 20-a: Dependence of the half-life period on Z^2/A [27].

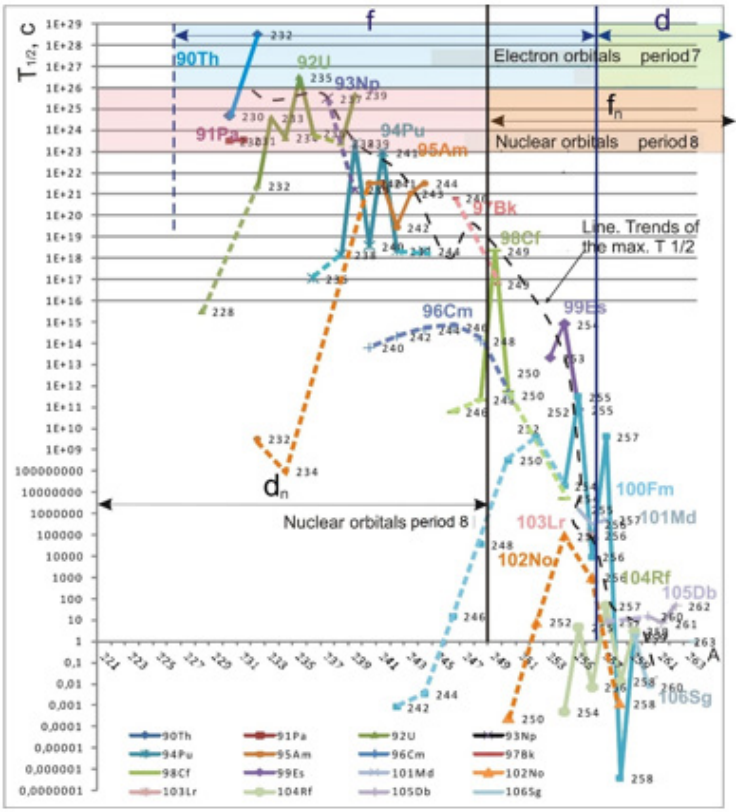

Figure 21: The half-life of isotopes only through spontaneous fission [28] and the periodic structure of the nucleus, the period 8 of isotopes, the period 7 of elements.

At the boundary of the dn-and fn-orbital at A> 248, spontaneous fission (SF) in the decay channels is sharply increased from 0-1% (at A, 230-248) to 85-99% for the isotopes: ^{250}Cm (SF-85,8%); ^{254}Cf (SF-99,7%); ^{256}Cf (SF>90%); ^{256}Fm (SF-91%); ^{258}Lr (SF>91%); ^{258}Md (SF>92,6%) [6] etc. (Table 10).

In fig. 21, the half-lives calculated only for spontaneous fission in the isotopes having this type of decay are shown. The estimated dependence on the parameter Z2/A is presented [27]. The trendline is defined graphically and has no extremes. In fig. 21, all the isotopes with spontaneous fission known at present time are selected [28]. The boundaries of nuclear and charge (electron) orbitals are shown. The trendline for each isotope is calculated by determining the midpoint of segments (dichotomy) between the maxima of the graphs. There are 3 characteristic bends on the line: horizontal section following the isotopes of thorium and uranium abundant in nature drops, subgroup 27 (^{235}U); minimum in front of the boundary for the d_n- and f_n-orbitals of isotopes, subgroup 36 (^{244}Cm); bend to the left upon completion of the f_n-orbital of charge at $^{254}_{103}$Lr.

It should be assumed that different directions of bending correspond to different types of structural transitions of the nucleus and interaction forces. At the end of the dn-orbital A>249 ($T_{1/2}$ – 10^{17} years), the trendline dramatically drops by 22 orders of magnitude at the mass range of A=10, asymptotically approaches the boundary of charge orbitals and croses it following the boundary for the f-orbital of charge at the half-life of $T_{1/2}$ – hours.

At the boundary of nuclear structures for the d_n- and f_n-orbitals of the period 7 (A=148), isotope lifetime is unstable. Natural samarium consists of four stable isotopes: ^{144}Sm (isotope abundance of 3.07%), ^{150}Sm (7,38 %), ^{152}Sm (26,75 %), ^{154}Sm (22,75 %), and of three weakly radioactive isotopes: ^{147}Sm (14.99%, the half-life is $1.06 \cdot 10^{11}$ years), ^{148}Sm (11,24 %; $7 \cdot 10^{15}$ years), ^{149}Sm (13,82 %; > $2 \cdot 10^{15}$ years, in some sources it is defined as stable). Such a development of radioactivity among the "stability valley" (A=147, 148, 149) is abnormal and symmetric to the considered boundary of the orbitals in the period 8 at A=248.

Thus, it is necessary to distinguish 3 structural causes of sharp drops in the lifetime of isotopes through spontaneous fission: favorable nucleon configurations for the subgroups 24, 27, 28, and 30, transition of the dn- and fn-orbitals for isotopes and transition of the f- and d- orbitals of charge. The local maximum of ^{249}Cf can be explained by the development of a +1-effect, when the +1-isotope with an unpaired nucleon, which follows the isotope completing the orbital or period, still retains the properties of the previous filled nuclear structure (the +1 configuration: ^{209}Bi – stability, ^{149}Sm – quadrupole moment, etc.). Knowledge on the nuclear periodic structure allows dividing the combined mass-charging index Z^2/A used for half-life estimation, as well as showing the change of boundaries separately.

Cluster radioactivity or cluster decay – is the phenomenon of spontaneous ejection of nuclear fragments (clusters) heavier than α-particle by nuclei. The resultant nuclei formed as a result of cluster decay, as well as the final products of their decay, are the nuclei of the end of the period 7 with A=204-208. The phenomenon of cluster decay (fig. 23, table 11) shows that depending on the isotope mass the escaping clusters represent the entire shell of the period 8. At the decay, the nucleus is released from the unstable shell and tends to preserve the previous stable layers of the period 7 (A=208).

The escaping clusters can be divided into two groups by mass: light clusters with A=12-14 and heavy clusters with A=20-34. Among heavy nuclear clusters, the most probable is the formation of nuclei with 24 (^{24}Ne) and 28 (^{28}Mg) nucleons. The cluster of 24 nucleons is the smallest threshold step; after 24 nucleons are formed, clusters from the nucleon residue of the period 8 are formed gradually with A=24, 26, 28, 30, 32, 34, etc. In the subgroup 24 of the period 8 for the periodic system of istopes, there is the first in the period long-lived natural isotope ^{232}Th (1.40x10^{10} years); in the previous subgroups 2-23, the long-lived isotopes are absent. Among the atomic carbon clusters, the configurations with 24 and 28 atoms are also most probable in the range from 2 to 32 atoms (fig. 18-a).

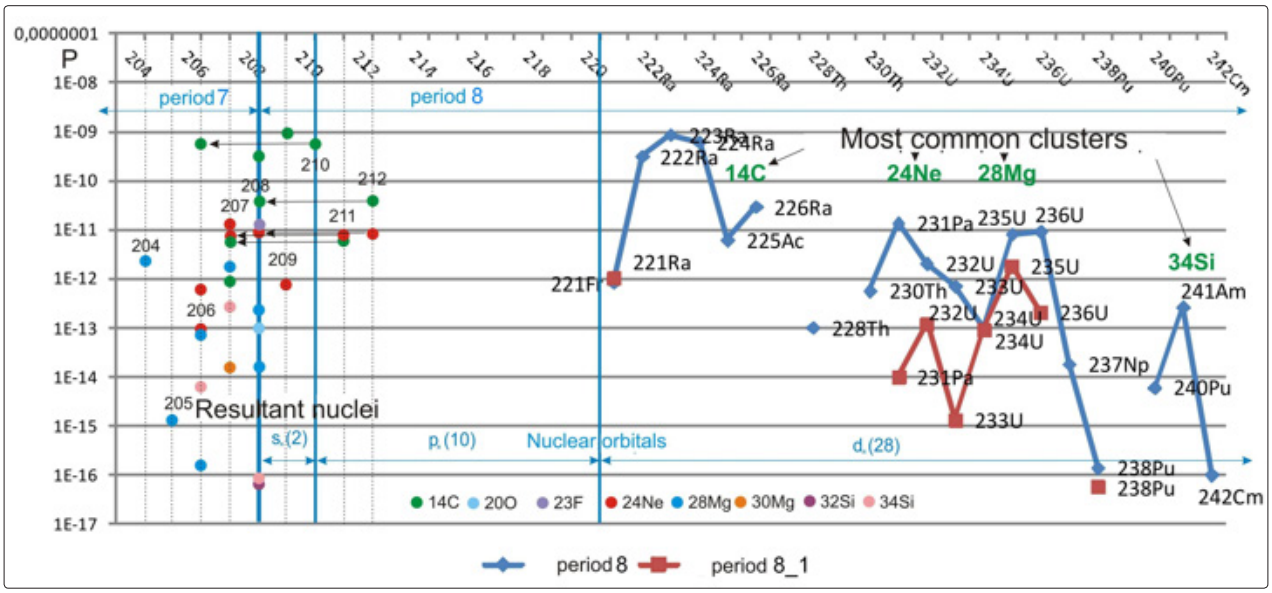

Figure 22: The probability of cluster yield for the nuclei of the period 8 and the resultant nuclei of decay through cluster radioactivity

As in case of carbon clusters, in both cases of atoms and nucleons, the configuration 24 is the smallest. This coincidence in the number of nucleons and atoms for the clusters of different levels shows that the number of nucleons for the smallest stable configuration in the period 8 may be the effect of form.

Therefore, during the shell formation for the period 8, the nucleus tends to form a geometrically closed shell, the first of which is 24 – for the nucleon. At the point moment of time, this shell can be simulated in the form of C_{24} fullerene. It should be assumed that, together with separation from the core, cluster nuclei undergo the internal transformation, in which the inner shells of the nucleus and β-decay are formed. The α-particle (^{4}He) consisting of 4 nucleons is often simulated by a tetrahedral cluster and is a complete shell for 2 periods of the isotope table and for the 1st period of the element table. It is interesting to note that the most common clusters of Ne and Mg are the elements with completely filled electron shells of the period for Ne ($1s^22s^22p^6$) and s-orbital for Mg ($1s^22s^22p^63s^2$). Among the light group of clusters in isotopes of the period 8, the cluster ^{14}C is formed among the nuclei with A=221-225. Resultant nuclei formed due to cluster decay have A=207–212. At the same time, the most probable (~10–10) are the resultant nuclei – 208–210. Among the carbon clusters, the C^{14} molecule is almost not formed (fig. 18-a); the lower quantitative limit of clusters is 24 carbon atoms. Probably, this discrepancy is related to a different elasticity of interatomic and nucleon cohesive forces.

Thus, cluster size is determined by shell size of the period 8 for the given isotope. The existence of stability islands for ^{232}Th, ^{234}U, ^{235}U, ^{238}U is determined by the geometric factor of the most favorable spherically-closed nucleon configurations and the arrangent islands in the central part of the dn-orbital. Clusters have the excess amount of neutrons, since they are formed from the outer shell of heavy isotopes. In the outer shell, the proton/neutron ratio is directed towards the neutrons, whereas for the isotopes of the same mass it is equal. In the process of transformations, the resultant nucleus tends to maintain the completed form for the periodic structure of the period 7 for A=208 (fig. 22).

Table 11: The known cluster decays and their probability with respect to the main mode of decay for the parent nucleus [42].

Parent nucleus	Ejected cluster	Resultant nucleus	Relative probability of decay	End product of decay
^{114}Ba	^{12}C	^{102}Sn	~3,0•10^{-5}	^{102}Pd
^{221}Fr	^{14}C	^{207}Tl	8,14•10^{-13}	^{207}Pb
^{221}Ra	^{14}C	^{207}Pb	1•10^{-12}	^{207}Pb
^{222}Ra	^{14}C	^{208}Pb	3,07•10^{-10}	^{208}Pb
^{223}Ra	^{14}C	^{209}Pb	8,5•10^{-10}	^{209}Bi
^{224}Ra	^{14}C	^{210}Pb	6,1•10^{-10}	^{206}Pb
^{226}Ra	^{14}C	^{212}Pb	2,9•10^{-11}	^{208}Pb
^{225}Ac	^{14}C	^{211}Bi	6•10^{-12}	^{207}Pb
^{228}Th	^{20}O	^{208}Pb	1•10^{-13}	^{208}Pb
	Ne		?	
^{230}Th	^{24}Ne	^{206}Hg	5,6•10^{-13}	^{206}Pb
^{231}Pa	^{23}F	^{208}Pb	9,97•10^{-15}	^{208}Pb
	^{24}Ne	^{207}Tl	1,34•10^{-11}	^{207}Pb
^{232}U	^{24}Ne	^{208}Pb	2•10^{-12}	^{208}Pb
	^{28}Mg	^{204}Hg	1,18•10^{-13}	^{204}Pb
^{233}U	^{24}Ne	^{209}Pb	7•10^{-13}	^{209}Bi
	^{25}Ne	^{208}Pb		^{208}Pb
	^{28}Mg	^{205}Hg	1,3•10^{-15}	^{205}Tl
^{234}U	^{28}Mg	^{206}Hg	1•10^{-13}	^{206}Pb
	^{24}Ne	^{210}Pb	9•10^{-14}	^{206}Pb
	^{26}Ne	^{208}Pb		^{208}Pb
^{235}U	^{24}Ne	^{211}Pb	8•10^{-12}	^{207}Pb
	^{25}Ne	^{210}Pb		^{206}Pb
	^{28}Mg	^{207}Hg	1,8•10^{-12}	^{207}Pb
	^{29}Mg	^{206}Hg		^{206}Pb
^{236}U	^{24}Ne	^{212}Pb	9•10^{-12}	^{208}Pb
	^{26}Ne	^{210}Pb		^{206}Pb
	^{28}Mg	^{208}Hg	2•10^{-13}	^{208}Pb
	^{30}Mg	^{206}Hg		^{206}Pb
^{236}Pu	^{28}Mg	^{208}Pb	2•10^{-14}	^{208}Pb
^{238}Pu	^{32}Si	^{206}Hg	1,38•10^{-16}	^{206}Pb
	^{28}Mg	^{210}Pb	5,62•10^{-17}	^{206}Pb
	^{30}Mg	^{208}Pb		^{208}Pb
^{240}Pu	^{34}Si	^{206}Hg	6•10^{-15}	^{206}Pb
^{237}Np	^{30}Mg	^{207}Tl	1,8•10^{-14}	^{207}Pb
^{241}Am	^{34}Si	^{207}Tl	2,6•10^{-13}	^{207}Pb
^{242}Cm	^{34}Si	^{208}Pb	1•10^{-16}	^{208}Pb

In the literature, many assumptions are devoted to the prediction of new "stability islands" in superheavy nuclei. In fig. 19, the increase in the lifetime of nuclei after A>281 within the range of 1-1000 seconds is shown. While drawing analogies with the isotope abundance among supernova remnants (fig. 7), it can be expected that the formation of isotopes with the longest lifetime in the given range with A=296 is symmetric to A=196 in the subgroup 88. There are no reasons to consider that the isotope with A=308, being the analogue of the ^{208}Pb isotope (the end of the period 7, as well as the end of all the decay chains), is the analog of the "stability island". For the "stability island", the lifetime of not more than tens of seconds should be expected. The period 9 (210 nucleons) is theoretically possible. For this period, it is logical to assume the existence of "stability island" symmetric to the "iron peak" and nuclei of ^{232}Th, $^{235\text{-}238}$U. The mass numbers of A=332-338 are arranged symmetrically in the subgroups; however, the period will be too massive and distant from the core, so the lifetime for this "island" is considered to be insignificant, at the level of the isotope with A=5 T½ ≈ 10^{-22} s.

The decay process for radioactive isotopes contains a paradoxical, unsolved mystery: decay occurs only for the part of isotopes of the same type corresponding to the decay rate which is individual for each isotope. One of the authors of the radioactive decay

law, Frederick Soddy, writes in his popular science book: "It should be noted that the transformation law is the same for all radio elements, the simplest and, at the same time, almost inexplicable. This law has a probabilistic nature. It can be represented as a spirit of destruction, which at any given moment randomly splits a certain number of existing atoms without selection of those that are close to the decay" [30]. Such a paradox requires development of a hypothesis on the decay mechanism".

Nuclear and atomic decay (life) as a whole should be considered as a result of the combined action of destructive and life forces. The life of atoms is ruled by some common force for all. It is possible that nuclei and atoms "float" in the ocean of this active force, which makes each of them to evolve and, in particular, dissociate in accordance with its structural features. To understand the nature of the force, the depths of the universe, nature of time, dark matter, dark energy, etc. should be studied. The image of this active force is common to all the atoms of this type and is determined by its internal structure. The joint fluctuations of this force and this type of atoms can have a certain statistical correlation. The atom of each type has its own range of wave parameters. Decay can be determined by the fluctuation phase ratio for the nucleus within a certain fluctuation cycle set by the force, etc. When coinciding with the external force phase, some of the nuclei dissociate and the next part dissociates into the next cycle of the external force. The ratio of dissociating nuclei and the remaining nuclei is proportional to the ratio of nuclear phases and the external force.

In accordance with the results of this section, the following conclusions can be made:
- nuclear structure directly affects the development of radioactivity. Starting from the period 8, the stability valley ends and there follow only radioactive isotopes. This change occurs exactly at the end of the period 7 (A> 208). Development of radioactivity for isotopes can be explained by a weaker bond between the shell of the period 8 and the core in comparison with other periods;
- the drop of the lifetime for the pn-orbital of the period 8 is observed. This can be explained by the fact that at the small number of nucleons in the period and massive core of the shell for the period 8, there are not enough nucleons to form the closed and advantageous configuration. The first such configuration in the period 8 is formed only up to the subgroup 24 (^{232}Th). As mentioned in Section 11, formation of the 24-nucleon closed shell should be related to the principles of stereometry. Absence of the elements Po and At in the composition of natural minerals is caused by the unstable structure of the core at the beginning of the period 8 – the drop in the lifetime for the pn-orbital;
- the "islands of stability": the isotopes ^{232}Th, ^{234}U, ^{235}U, ^{238}U are arranged in the center of the dn-orbital in the subgroups 24, 26, 27 and 30 for the period 8. Isotopes of these subgroups are the advantageous nucleon configurations. Isotopes of the subgroup 28 should also be referred to the advantageous nucleon configurations: ^{56}Fe (91,7543 %); ^{96}Mo (16,68%), ^{136}Ba (7,8542%); ^{236}U (2,342e7 years);
- cluster radioactivity is related to the ejection of shell for the period 8 by the nucleus. It should be assumed that the most probable nucleon configurations for ^{14}C, ^{24}Ne, ^{28}Mg clusters are formed in accordance with the stereometry laws, and the heavy group of nucleon clusters has a preferred distribution similar to C^{24} and C^{sss} carbon clusters – fullerenes (fig. 18-a). Presence of radioactivity with the increased probability of cluster ejection with A=32, 50 and 60 should be expected for the nuclei with A>240, 258 and 268.

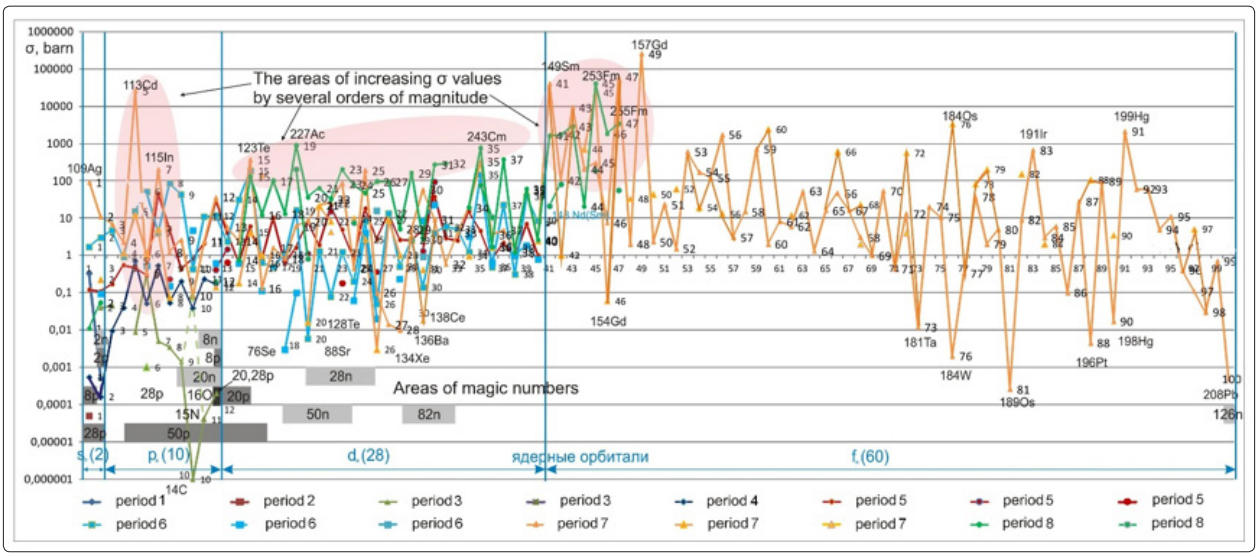

Figure 23: Thermal neutron radiation capture cross-sections and nuclear periodic structure [31].

For example, in accordance with the Nuclear Data Services or the ROSFOND encyclopedia of neutron data, the experimental values are mainly within the energy range of 102-107 eV and so far for no more than 25% of stable isotopes [32, 33]. Therefore, the 3D analysis covering the entire range of mass numbers will be less informative. Analysis of estimated data was carried out repeatedly [34, 35]. The most complete experimental data for neutron capture are accumulated for a point of neutron energy thermal region (T=20.4 C, E=0.0253 eV). Within the 2D analysis (δ (A) section/periodic structure) of thermal region, the periodic structure of nucleons is also shown and distinguished on a scale of several orders of magnitude (fig. 24). In fig. 25-a and 25-b, the symmetry of the periodic system is shown in more detail.

Structural transition at the boundary of d_n- and f_n-orbitals is expressed by a sharp increase in the cross-section values at A = 149 and 249 for the subgroup 40-41 in the periods 7 and 8. In fig. 35-b, a logarithmic scale is shown; at the completion of d_n-orbitals for both periods, the values of the capture cross-section are almost the same, which is expected in terms of the periodic structure of the

nucleus for the filling orbitals of the same type. When changing the orbital from d_n to f_n, the values of the absorption cross-section are increased by 3-4 orders of magnitude for both massive periods –7 and 8.

In fig. 25-a and 25-b, structural transition for d_n- and f_n-orbitals of the period 7 for different values of energy is shown. In the range of 10–5–10 eV, the change of orbitals is expressed by the increase of neutron capture values by 2–4 orders of magnitude; in the range of 10–107 eV, the capture cross-section values are significantly smaller; at the interaction of neutrons and nuclei, the scattering fraction is increased and the structural transition is not shown. A similar picture can be observed at ultrahigh pressures, where the periodic change in the properties of simple matter is bearly perceptible and the periodic law disappears.

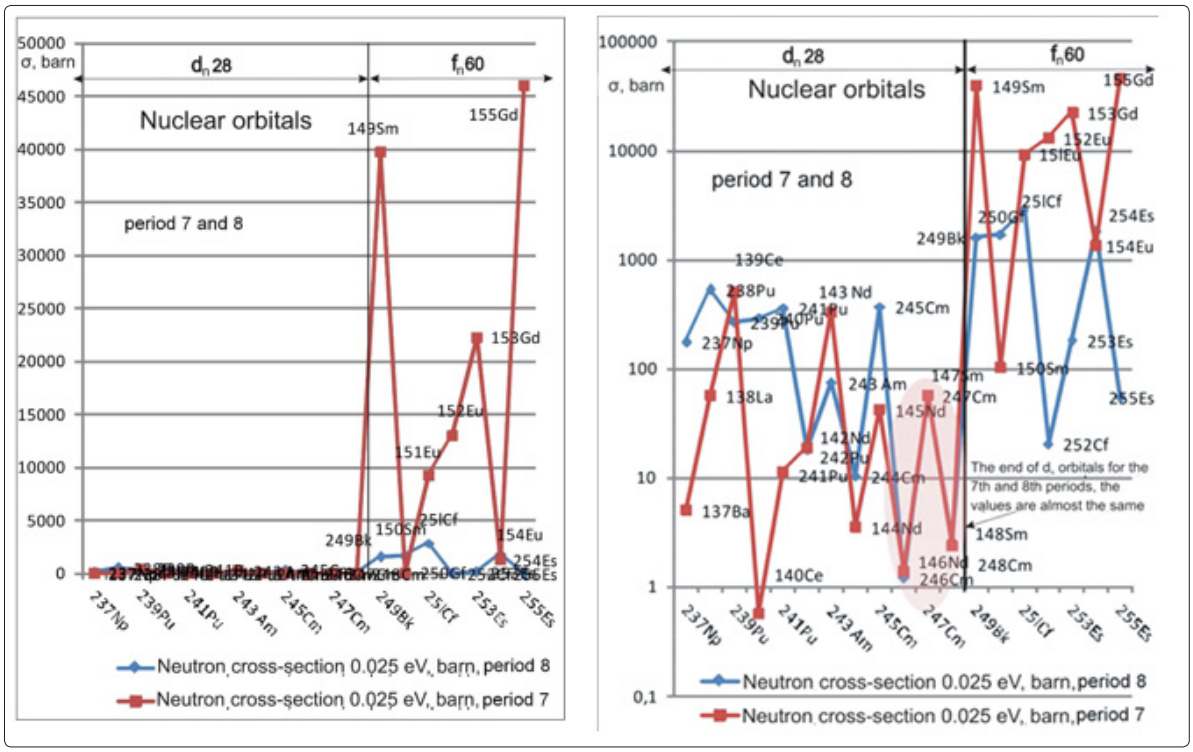

Figure 24-a: Symmetry of the subgroups for thermal neutron capture in the periodic system (normal scale). The boundary of dn- and fn-orbitals for the periods 7 and 8.

Figure 24-b: Symmetry of the subgroups for thermal neutron captrure in the periodic system (logrifmic scale). The end of dn-orbitals for the periods 7 and 8, the values are almost the same.

As the mass of the nucleus is increased, the values of the capture cross-section for thermal neutrons are also increased steadily. Quantitative data analysis allows identifying structural factors affecting the amplitude of the values for the thermal neutron capture cross-section (fig. 28). These factors should be considered when deriving expressions for the cross-sections of nuclear reactions.

There are several scale levels of the increased capture cross-sections for various structural shells of the nucleus. For the massive periods 7 and 8 (100 nucleons), the scale of δy values is greater in comparison with the previous period 6 (40 nucleons) by 2-5 times; in the period 6 (40) – by an order of magnitude; in the period 4 (12) – by 3-6 orders of magnitude; in the period 3 (12) – also by 3–6 orders of magnitude (fig. 32-a, the "*m*" factor – "*massive*"). The scale of factors for the increased cross-section values of δy depends on the shell size; when deriving the expression for δy, it is necessary to take into account its size and number.

1000-250000 barn – are giant cross-sections in the nuclei with massive shells of 100 nucleons for the periods 7 and 8; these cross-sections are related to the period-period and orbital-orbital structural transitions. Giant cross sections are observed for isotopes of the first 1–7 nucleons for the shell of the period or fn-orbital (^{113}Cd, ^{149}Sm-^{157}Gd, ^{249}Bk-^{151}Cf); (fig. 26, 27-a, the factor of *structural transition* "*str*"). Such exceptions as ^{3}He (5333, 7) and ^{10}B (3837) are the nuclei, in which the neutron capture is part of a whole complex of reactions, and δ_y values are not independent (see the text).

200-1000 barn is the next scale for the increased cross-section values; it is not related to the structural transitions and is shown only for the nuclei with the massive shells of 100 nucleons (the period 7 and 8, the "*m*" factor).

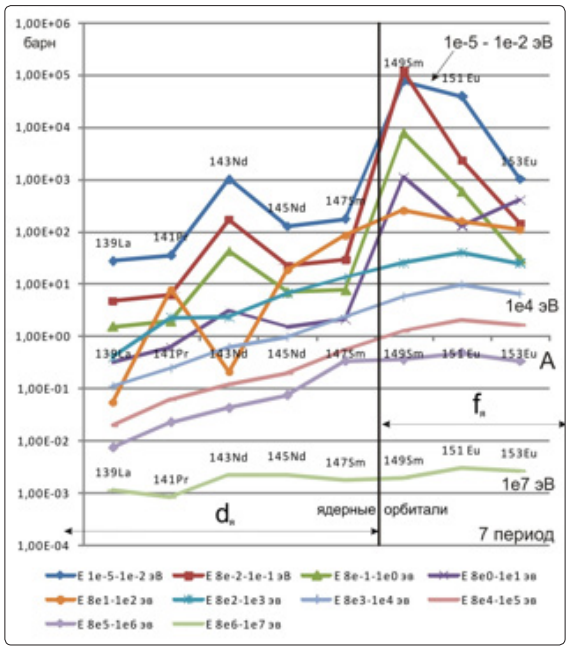

Figure 25: Radiative decay of the isotopes with A=139-153 for various values of energy 1e-5 -1e7 MeV. The boundary of dn- and fn-orbitals for the period 7.

The structure factor is also demonstrated at the end of the periods and orbitals, but to a much lesser extent, by 4-5 orders of magnitude weaker. If one nucleon is missing before the shell is completed, the radiation capture cross-section has the increased value of ^{67}Zn (6,9); ^{107}Ag(37,63); ^{147}Sm(56) (the "*str*" factor). A similar increase in the cross-section of the filling shells at the end of the periods and orbitals is also shown for the α-particle (n, α) yield reaction of the isotopes ^{67}Zn, ^{68}Zn, ^{147}Sm in the last subgroups of the dn-orbital for the periods 5 and 7 (fig. 27).

Often the value of the capture cross-section *n* for a particular isotope is determined by several structural factors (the scale of 0–200 barn):
- *Unpaired nucleon*. Due to the presence of an unpaired nucleon in the outer shell, the capture probability is increased. This property is demonstrated for all the periods and is expressed more clearly together with the increase in the number and size of the period.

- *Nucleus of inert gas without neutron excess – the "i" factor*. Increased cross-section values have the inert gas nuclei that are not overloaded with neutrons in comparison with the nuclei of other elements that are similar by mass: ^{3}He (5333); ^{21}Ne(0.7); ^{36}Ar(5); ^{80}Kr(11,5); ^{82}Kr(30,7); ^{83}Kr(183); ^{129}Xe(22); ^{131}Xe(85.05);^{133}Xe(190) (fig. 32-a, the "i" factor). For neutron-rich isotopes of inert gases, the n capture cross-sections is sharply decreased: ^{4}He (0), ^{22}Ne (0.051), ^{38}Ar(0.8), ^{40}Ar(0.64), ^{84}Kr(0.11), ^{86}Kr(0.003), ^{134}Xe (0.003), ^{136}Xe (0.26). Among the inert gas isotopes, the nuclei with odd number of neutrons have the greatest capture values: 83Kr (183); ^{129}Xe (22); ^{131}Xe (85.05);^{133}Xe (190). The nuclei of inert gases have complete charge structure for the protons of the nucleus, in which the proton magnetic moment is 0. This observation allows considering that the abnormal magnetic moment of the absorbed neutron and nuclear shell neutrons, as well as their interaction, play a significant role in the capture mechanism.

- *Multiplicity of 5 – the 5n and "5nα" factors*. Increased capture cross-sections have the nuclei arranged in the subgroups with the numbers multiple of 5: ^{43}Ca(6), ^{48}Ti(7.9), ^{53}Cr(18), ^{73}Ge(15), ^{83}Kr(183), ^{93}Nb(8.207), ^{103}Rh(144.9), ^{113}Cd(26000), ^{123}Te(370), ^{133}Xe(190), ^{143}Nd(330) ("the 5n factor"). In the isotopes of the periods 1-5 periods formed by the α-process, the increased values for two cases of multiplicity of 5 are observed: from the beginning of the mass series of isotopes ^{10}B(3837), ^{35}Cl(43.7), ^{40}K(30), ^{45}Sc(10), ^{50}V(21), ^{55}Mn(13.3) (the "5nα" factor) and in the subgroups of the period ^{43}Ca(6), ^{48}Ti(7.9), ^{53}Cr(18) (the "5n" factor). For the periods 1–5, the "5nα" factor is shown only in the odd periods — 3 and 5. Within the d_n-orbital of the period 5, the increase in δ_y values to the middle of the shell and the decrease from the shell end (similar to the iron peak) are observed. In the isotopes of the periods 6, 7, and 8, the increased δ_y values are distributed in the subgroups in accordance with the factors. This can be explained by the fact that the proton-rich nuclei formed by the explosive processes (r- processes) are concentrated in the d_n-orbitals 6, 7 and 8 (fig. 12), while the isotopes of the "iron" peak are also formed as a result of equilibrium nucleosynthesis of supermassive stars (α-process). In other words, with the beginning of the period 6 and the new process of nuclei formation (explosion), a new countdown of multiplicity of 5 begins only within the periods; the multiplicity of 5 from the beginning of the mass sequence "*5nα*" is interrupted. For the periods 1-5 (A<68), structural reasons for the increased δy cross-sections should be related to the α-process ($^{+4}$He), i.e. when the fifth nucleon is attached, the nucleus is deformed, becomes unstable, and the cross-section increases. The influence of geometric factor is not excluded. The α-particle consisting of 4 nucleons (^{4}He=1st+ 2nd periods) is often simulated as a tetrahedral form. Then the attachement of the fifth nucleon is not advantageous for symmetry reasons, and the nucleus acquiring a large moment of rotation for the first nucleon in the new shell is dissociated (the isotope with No. = 5-T½ ≈ 10-22 s). The influence of the central nuclear shell shape can be retained for subsequent shells. Increased values among the numbers multiple of 5 have all the nuclei with odd mass numbers. Multiplicity of 5

can be simulated using the fluctuations of current harmonics in electrical engineering, when odd harmonics have increased amplitude.

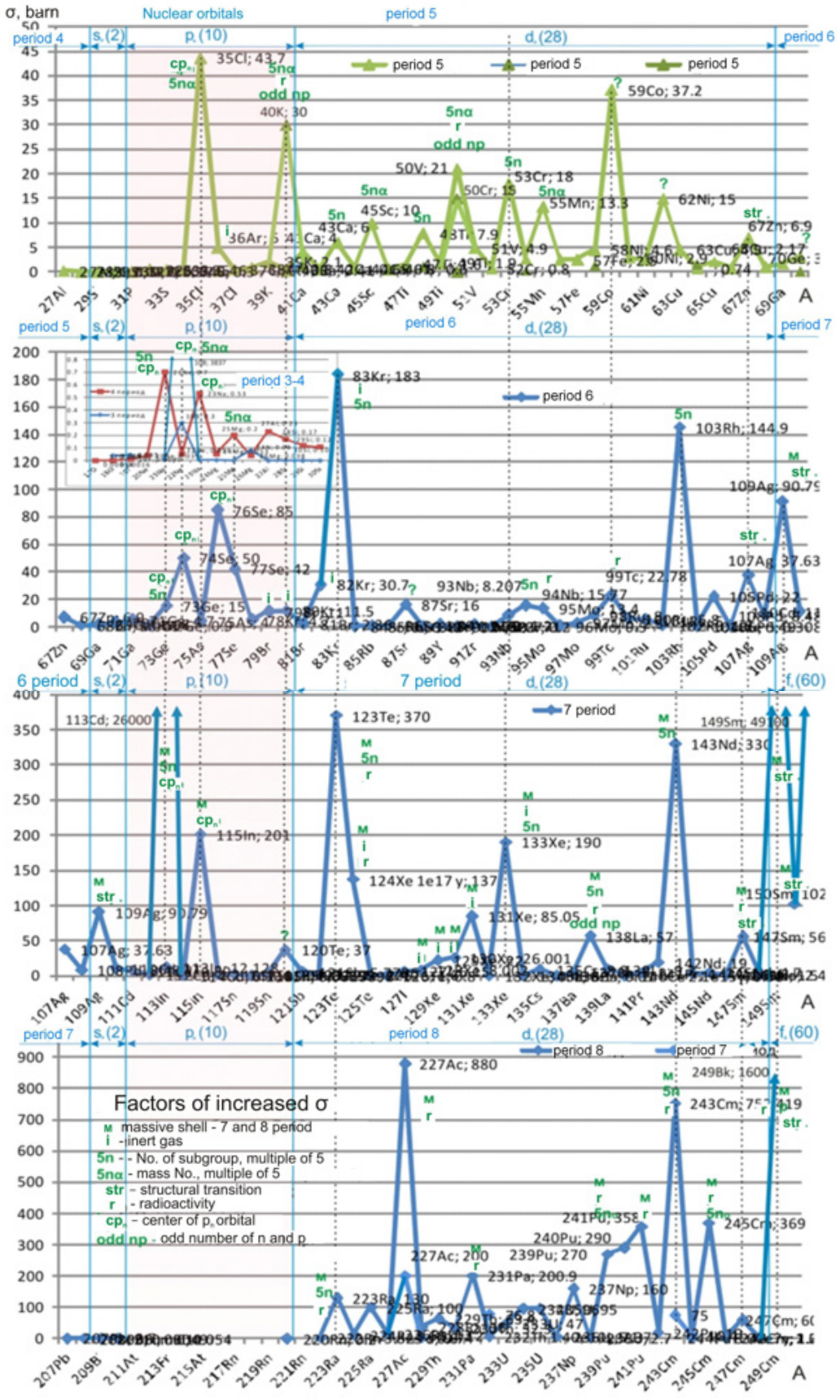

Figure 26-a: Analysis of factors for the increased values of the radiation neutron capture cross-section, the periods 3-8.

It should be expected that the vibration mode of the fifth nucleon has the influence on the nuclear shape both from the beginning of isotope series and within the shell. Among the even numbers of the isotopes with A multiple of 5, only the odd-odd nuclei of the odd periods have the increased δy values: ^{10}B (5n, 5p); ^{40}K (21n, 19p); ^{50}V (27n, 23p) (the "5nα" factor – the periods 3 and 5) and ^{138}La (91n, 57p) (57 barn, the "5n" factor – the period 7), the rest have minimum values and even number of protons. The nucleus 15N (0.00004) is odd with the low δ_y, but it has the excess and "magic" number of neutrons – 8n. In this case, it is important to remember the nuclear cluster model (J.A. Wheeler, 1937), in accordance with which the nucleus consists of A/4 number of α-particle clusters (due to the abnormal binding energy of 20 MeV) and the nucleon remnant. The effects of α-particle correlations appear systematically in the nuclei with A <40, i.e. until the end of small s_n and p_n-nuclear orbitals and α-process as a whole (the "5nα" factor).

- *Radioactivity – the "p" factor*. Radiation capture maxima are observed in radioactive isotopes: ^{41}Ca (4), T½ = 1.02x10^5 years; ^{93}Zr (4), 1.5x10^6 years; ^{94}Nb (15.77), 2.4x10^4 years; ^{99}Tc (22.78), 2.13x10^5 years; ^{129}I (22), 1.7x10^7 years; ^{135}Cs (8.9), 2.3x10^6 years. At the half-life period of T½ = 10^4-10^7 years, capture cross-sections are 4-23 barn. When two or more factors overlap, capture cross-sections are increased; thus, in radioactive isotopes with the odd number of protons and neutrons with a longer half-life of T½ = 10^9-10^{18}, the values δ_y = 20-60 barn: ^{40}K (30), 1.26x10^9 years; ^{50}V (21) >1.4x10^{17} years; ^{138}La (57), 1.06x10^{11} years, (the "*p*" and "*odd np*" factors). After this: ^{53}Mn (70), 3.7x10^6 years (the "*p*" and "*5n*" factors); ^{147}Sm (56), 1.06x10^{11} years (the "*p*" and "*str*" factors).

In the subgroup 10 multiple of 5, the abnormal minima of δ_y values are observed for the isotopes of the odd periods 3 and 7: ^{14}C (0.000001) 5715 years; ^{118}Sn (0.0823898). It should be expected that relatively small δy of ^{38}Ar (0,8) for the subgroup 5 of the period 5 is a consequence of the combined action of factors for the neutron-excess inert gas nucleus reducing δ_y and the multiplicity of 5 in the "5*n*" subgroup increasing δ_y.

- *pn-orbital center – the "cp$_n$" factor*. At the beginning of each period, the local maxima of δ_y values are observed in the center of the pn-orbital: ^{10}B(3837); ^{35}Cl(43.7); ^{73}Ge(15); ^{74}Se(50); ^{76}Se(85); ^{113}Cd(26000); ^{115}In(201) – the "*cpn*" factor. This factor is shown in the subgroups 4-9 of the periods 3-8, The factor can be related to the variety of structural "*str*" factors. The increase in the capture cross-section is related to the construction of nucleon configuration of 4 nucleons (α-particles) in the shell of the period and pn-orbital of the subgroups 4 and 6. As a result, the cross-section is increased (as for the isotope with A = 5). For ^{10}B(3837); ^{35}Cl(43.7); ^{73}Ge(15) and ^{113}Cd(26000), the sum of the factors "*cpn*", "*5n*", "*str*", "*m*" can be used (fig. 27-a). Giant section δ_y of the isotope ^{113}Cd(26000) should be explained by several factors: beginning of the massive period 7, large "capacity" of a new shell absorbing the nucleons – 100 nucleons of the subgroup 5, the first unpaired neutron after the ^{4}He configuration in the shell of the period. It should be assumed that there is a giant neutron capture cross-section for the isotope of the subgroup 5 of the massive period 8 with A = 213 and the odd number of neutrons, for example, ^{213}Po or ^{213}Rn.

^{10}B nucleus is a unique case: the isotope has a giant neutron capture cross-section of 3837 barn and is used as a neutron moderator, while the nuclei similar by mass have δy cross-sections by 5-9 orders of magnitude lower than 0.000001-0.04 barn (fig. 27-b). Discrepant data on 10B is often presented in literature: 0.3 or 3837 barn [p. 642] [36, 31]. The latter value is given in accordance with (n, α) reaction, which is about 99.9% of the reaction channel in thermal region at the energies of 10^{-11}-10^{-3} MeV. At the neutron capture, ^{10}B is dissociated into α-particle and ^{7}Li. The value of 0.3 barn is given for the capture reaction and transformation into ^{11}B without dissociation, just as for other isotopes, whereas for the value of 3837 barn, both reactions are taken into account. It is interesting to note that ^{10}B consists of 5 neutrons and 5 protons and is the case of a double multiplicity of 5. For the nucleus 3He (5333,7), which has a giant δy cross-sectional scale, there is also the sum of factors: radioactivity T½ = 1.37x10^{-4} years, "p", inert gas "i" and structure factor "p", in accordance with which the first odd composite nucleus tends to the simplest and most advantageous nucleon configuration of ^{4}He — the completed shell of the period 2 ("p", "i", "str" factors). ^{3}He is the only isotope in which the number of neutrons is lower than of protons, and which is abnormal for the nucleus and gives an additional factor of neutron affinity. Formation reaction of 4He: 2*^{3}He → ^{4}He + 2p is a part of the proton-proton cycle in astrophysics. Attachement of the neutron ^{3}He +n → ^{4}He requires immeasurably less energy and is more advantageous: the cross-section is increased.

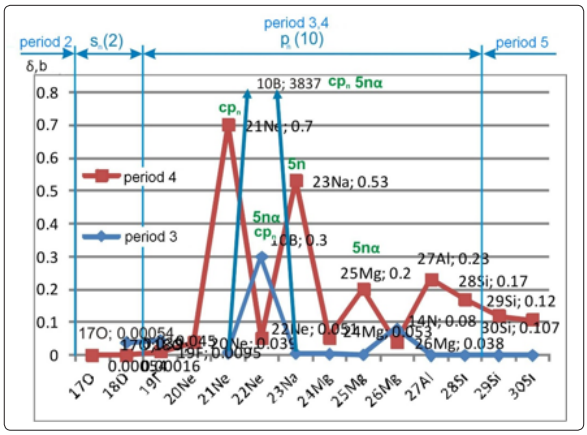

Figure 26-b: Analysis of factors for the increased values of radiation neutron capture cross-section, the periods 3–4.

Within the analysis, it is difficult to explain the increased nuclear cross-sections of halogens ^{35}Cl(43.7), ^{79}Br(11), ^{81}Br(2.36), ^{127}I(6.15). It is possible that the increased cross-section is caused by the fact that inert gases have similar charge values. It should be assumed that when deriving the expression for the nuclear reaction cross-sections, the element subgroup number should be taken into account. Within the change of shells, the symmetry of subgroups for the periodic system (A = 249, 149, 109, 69) suggests that there exists radioactive isotope with A = 69 and the capture cross-section of about 15-20 barn (for A =71,^{71}Ge (11,28 h; 13 barn); ^{71}As (65,28 h; 23 barn). For the p_n- and d_n-isotopes of ^{59}Co, ^{62}Ni, ^{87}Sr, ^{120}Te, it was not possible yet to describe the factors of increased δ_y.

When deriving the expression for the capture cross-section, several aspects of these cross-sections should be taken into account: the periodic structure of the nucleus, described factors of increased δ_y:
- "m" is the mass shell of 100 nucleons for the periods 7 and 8, the cross-section amplitude is increased as the period number is increased, and depends on the shell size;
- "i" is inert gas. The completed charge shell of protons for the nuclei with a neutron deficiency has increased δ_y;
- "5nα" is the isotope mass number multiple of 5, present for isotopes of the periods 1-5, only in the odd periods 3 and 5. The boundary of factor action coincides with the boundaries of

α-process (equilibrium nucleosynthesis of massive stars);
- "5n" is the number of subgroup in the period multiple of 5, present for isotopes of the periods 1-8. The boundary of factor action includes the isotopes formed by explosive processes;
- "str" is the structural transition of shells, present in the subgroups 1-7 for the new shell (of the period and orbitals) on a giant cross-section scale, as well as in the last subgroups of the period;
- "p" is radioactivity. The factor depends on the half-life of the isotope: the smaller $T_{1/2}$, the larger the cross-section;
- "cp_n" is the p_n-orbital center. The factor is shown for the subgroups 4–9 of the period 3-8 after the α-particle structure is repeated at the beginning of shells for the periods and p_n-orbitals;
- "odd np" is the odd number of *n* and *p*. It should be assumed that abnormal magnetic moments of a free neutron, nucleons of nuclear shells and their interaction play an important role in the capture mechanism;
- number of the period, subgroups and their parity.

In fig. 28, the data on the α-particle σ_α yield reaction cross-section under the action of neutrons (n, α) is presented [28]. At the beginning of all the periods having the dn-orbital – the periods 5, 6, 7 and 8, the values of the reaction cross-sections (n, α) are absent. This feature is noticed for the nuclei from the subgroups 15-24, which are symmetric for 4 periods with the dn-orbital. At the end of the dn-orbital for the odd periods 5 and 7, the probability of the α-particle yield is increased significantly, which is obvious for the shell densely occupied with nucleons (A region). It should be assumed that absorption or scattering is predominant for the filled dn-orbitals with a low density of nucleons. At the beginning of the dn-orbital, the values of σα reaction cross-section are observed for two isotopes: ^{41}Ca (0.19) and ^{123}Te (0.00005). ^{41}Ca is a +1 nucleon configuration for the pn-orbital of the period 5. As described above, +1 configurations retain the properties and values characteristic for the previous nuclear shells (the +1 configuration of the quadrupole moment Q: ^{149}Sm, ^{209}Bi, ^{221}Rn; the +1 configuration of the magnetic moment μ: ^{109}Ag, etc.).

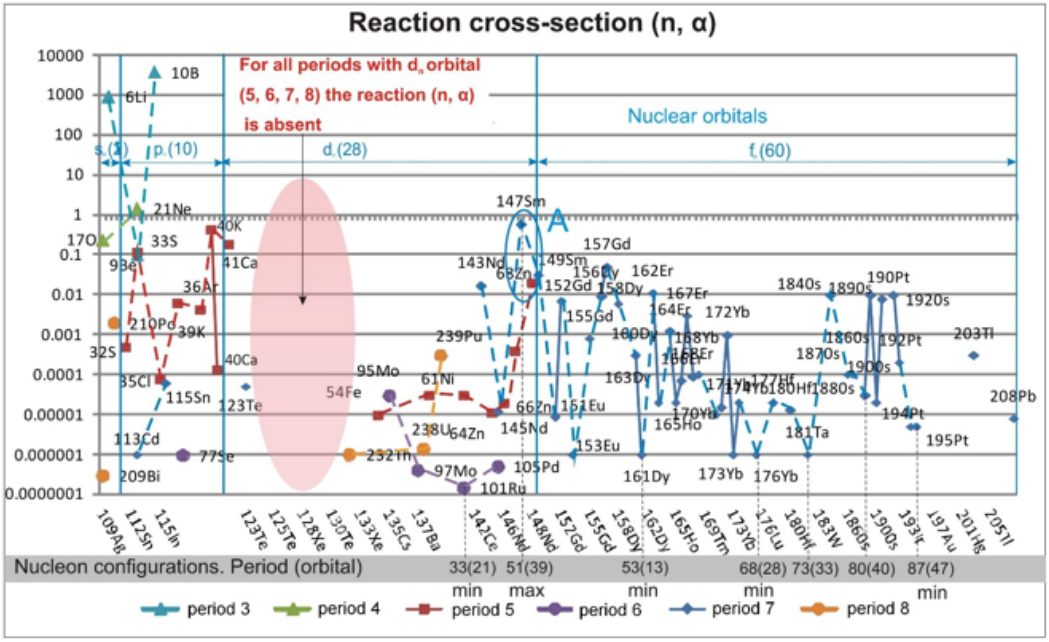

Figure 27: Reaction cross-section (n, α) depending on the nuclear periodic structure.

Large σα cross-section values for ^{41}Ca (at the level of ^{40}K (0.42)) should be explained by the properties of the +1 configuration. The ^{123}Te isotope has an abnormally large neutron capture cross-section (370 barn), which is by 3–4 orders of magnitude greater than for the isotopes of the adjacent subgroups, and is arranged in the subgroup 15 of the period 7 and in the subgroup 3 of the orbitals (fig. 27-a). As the neutron is attached to the dn-orbital of ^{123}Te, the nucleon configuration in the form of α-particle is created. The nucleon configuration can be detached from the parent nucleus due to sufficient distance from the previous nuclear shell (a large capture cross-section *n*). It should be assumed that there is (n, α) reaction for the isotope ^{83}Kr with σ_α cross-section at the level of 0.00001 barn. This isotope also has the abnormally large cross-section (183 barn) and is arranged in the subgroup 15 of the period 6.

In the initial subgroups 5 and 6 of the periodic system of isotopes, there are the isotopes for which the probability of α-particle yield under the action of neutrons is high. The isotope ^{9}Be is arranged in the subgroup 5 of the period 3. The total capture cross-section for the thermal region is 6–6.2 barn, which is by 6–7 orders of magnitude greater than the average over the period. The radiation capture cross-section for ^{9}Be (0.0088) is small in comparison with the total one due to a significant proportion of scattering with a subsequent decay up to 2 α-particles and *n*. For ^{33}S, as *n* is absorbed, the α-partial configuration is formed in the p_n-orbital of the odd period 5. A unique feature of the ^{33}S isotope (the subgroup 5) is that for this isotope, the reactions of proton yield (n, p) and α-particle yield (n, α) can occur under the action of neutrons at any energy values, which confirms the periodic nuclear structure [33]. Isotopes of the subgroup 5 for the periods 3, 4 and 5 demonstrate the numerically similar values of the reaction cross-section (n, α): ^{9}Be (0,1); ^{21}Ne(1,5); ^{33}S(0,12). It should be assumed that there are large cross-sections for the reactions (n, p) and (n, α) of other isotopes of the subgroup 5: ^{73}Ge, ^{113}Cd, ^{113}in. For the nucleus ^{113}Cd (0.000001), σ_α is by 5 orders of magnitude smaller due to the large capture reaction cross-section of 26000 barn. From the point of view of the periodic structure of the nucleus, large σ_α values for ^{6}Li (940) and

^{10}B (3840) are actually related to fission by the shell of the period 1-2 (^{4}He) and the nucleon remnant of the period 3. In case of 10B, one more nucleus of ^{4}He and second neutron is formed from the nucleon remnant of the period 3 through the decay chain; for this reason, the cross-section of α-particle yield and *n* absorption is greater than that of ^{6}Li.

For (n, α) reaction, as well as for other reactions, there is still a lack of data for a sufficiently large number of isotopes. So, it is unclear what cross-section there will be for the isotopes from the end of the dn-orbital for the even periods 6 and 8 (^{107}Ag, ^{247}Cm).

Due to the analysis of nuclear reactions (n, α) and (n, γ), several characteristcs of symmetry for the subgroups of the periodic system of isotopes are revealed: the absence of (n, α) reaction in the subgroups 15-24 for all the periods having the dn-orbital (5-8) ; the increase in the cross-sections (n, α), by the end of the dn-orbital, only for the odd periods 5 and 7 (fig. 28); the sharp increase in the cross-section (n, γ) at the boundary of the d_n- and f_n-orbitals for the massive periods 7 and 8 (fig. 25); the increase in the thermal neutron capture cross-section δ_y at the beginning of each period, the "*cpn*" factor – the center of the d_n-orbital; the increase in the δ_y cross-section for the isotopes of the subgroups multiple of 5 – the "5*n*" factor; the presence of the "5nα" factor for the isotopes formed in the course of α-process only in the odd periods 5 and 6 (fig. 27-a).

Both the electrons of the atom and the nucleons of the nucleus have the property of pair dislocations, but the nuclear forces are of a different nature than the electric ones. Due to compactness, short-range action and Coulomb repulsion, it is not typical for nuclear forces to form compounds from different nuclei and "extensive" nucleon clouds, as is typical for atomic electrons. For nuclei, the concept of "valence" is partially applicable in a sense that this is understood at the level of electrons (valency is the ability of atoms of chemical elements to form a certain number of chemical bonds). For nucleons, the numerical dependence of the mass number and subgroup number is clearly shown: the factors of multiplicity of 5, last nucleons in the d_n-orbital, "*str*" factor, etc. The attention should be paid to studying the phenomenon of sequential capture at the radiative neutron capture. In addition to the activation as a result of single neutron capture, in some cases, the activation as a result of double and multiple neutron capture is of vital importance. Moreover, the activation cross-sections for successive neutron capture are often quite large [37].

Neutron Scattering

In fig. 29, the change in the length of coherent neutron scattering at low energies depending on the periodic structure of the isotope system (at E=25.30 meV, k=3.494 A, wavelength h=1.798 A) is shown [38]. The neutron scattering length is calculated using complex numbers. The real part shows the actual length of neutron scattering for a specific nucleus, the imaginary part is responsible for absorption. In fig. 29, the values of the real part are shown; about 5% of isotopes have the imaginary part of the scattering length and are not shown in the graph.

It is noticed that, depending on the period number nper, the fluctuation range of the scattering length is changed. Within the odd periods, it has large values, and within the even periods – small (fig. 29 and 30).

Such a dependence shows that, as in case of magnetic moment neutron capture cross-section, the value of the neutron scattering length is affected by the oscillation phase of the nuclear period. Within the even periods, the scattering length is always positive. Within the odd periods, it can take negative values. The periods are repeated twice. If the periods of one duration are presented as a harmonic oscillation (2, -2; 12, -12; 40, -40; 100, -100), then during the first half-wave, the scattering length has a large range and values of both signs; during the second half-wave – a small range and only positive values. It should be assumed that during the second half-wave (the period 2 of the given duration), nucleon fluctuations of the first half-wave are compensated. From here it follows that there is a small amplitude for shell fluctuations. Due to this observation, it is shown that the shape of the wave function for nucleons within the nucleus is determined by the nuclear periodic structure. In the simplest case of the spinless particle scattering in a centrally symmetric field, the wave function at large distances from the center can be represented as follows:

$$\Psi(\vec{r}) \approx e^{ikz} + f(\theta)\frac{e^{ikr}}{r}, \qquad (5)$$

where k is the wave vector of a projectile $k = \sqrt{2mE}/\hbar$. Here m is the reduced mass of scattered particles; E is their energy in the system of mass center; $f(\theta)$ is the scattering amplitude or scattering length, which is expressed through the scattering phases of radial wave functions for the continuous spectrum.

$$f(\theta) = \frac{1}{2ik}\sum_{l=0}^{\infty}(2l+1)(e^{2i\delta_l}-1)P_l(\cos\theta). \quad (6)\ [39]$$

where $Pl\,(cos\theta)$ is the Legendre polynomial (the orthogonal system of polynomials in the interval [-1; 1], which is also used in electron orbital modeling), θ is the angle of particle deflection at scattering.

In the expression of the scattering length, the phase difference of the nucleus and projectile is dominant. To find the exact expression for the scattering length, as well as to create conditions for the controlled nuclear reaction, the nuclear fluctuation phase should be determined for different values of energy; the required phase and projectile energy should be specified.

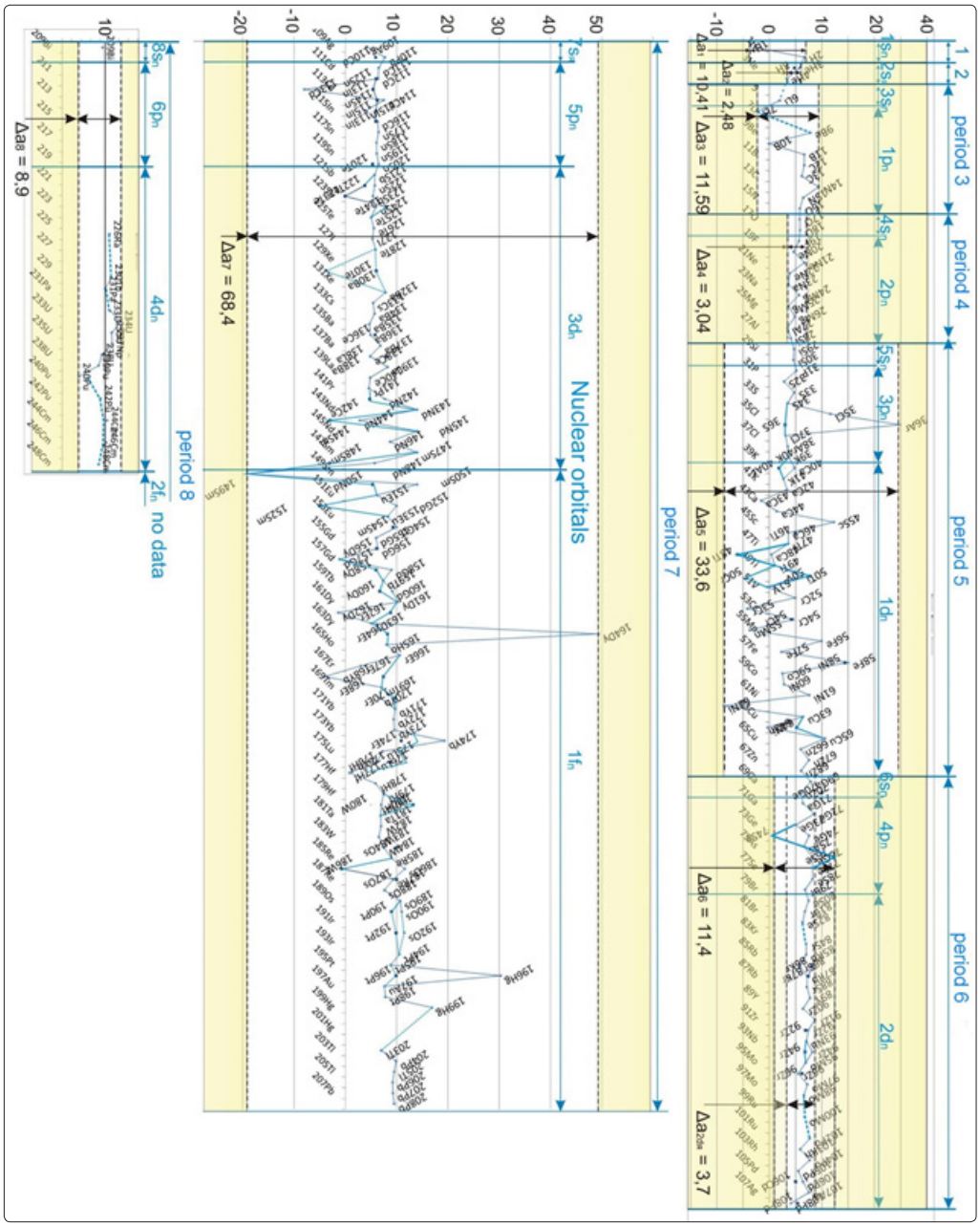

Figure 28: Analysis of the neutron scattering length at low energies (at E=25.30 meV) depending on the nuclear periodic structure.

In the classical case, the phase is also a complex quantity of δ=l±s, which is determined by the total moment of the particle j=l+s, where *l* is the orbital moment of the particle, and s is the spin. In the above mentioned expressieon, l is determined due to the nuclear shell model. Dependence of the scattering amplitude fluctuations on the period of the isotope system requires introducing additional variable of *nper*, which is the number of the isotope period, the analogue of the principal quantum number *n* for electrons. Taking into account the nuclear periodic structure within the accepted set of quantum numbers, the expression for the total angular moment of the nucleus takes the following form:

$$j = n_{per} + l_{orb} + s, \qquad (7)$$

where l_{orb} is the quantum orbital number, which is determined by the isotope periodic system, s is the nuclear spin (it should be assumed that the nuclear spin model should be specified, see Section 9. Nuclear magnetic moment and isotope periodicity).

It should be noted that within the periods or isotopes of one mass range, there are nuclei which form maxima peaks for the scattering length of ^{36}Ar, ^{45}Sc, ^{58}Fe, ^{164}Dy, ^{196}Hg (fig. 29). All these isotopes are special charge nucleon configurations consisting of filled shells. As noted in section 10, the numbers 164 and 196 are theoretical values of the "magic" numbers for *p* and *n*. It was also noted that when considering them as mass numbers, they have arithmetic decomposition as the sum of "magic" numbers: 164 = 82 + 82; 196 = 114 + 82. Magic numbers, in turn, are the sum of charge periods.

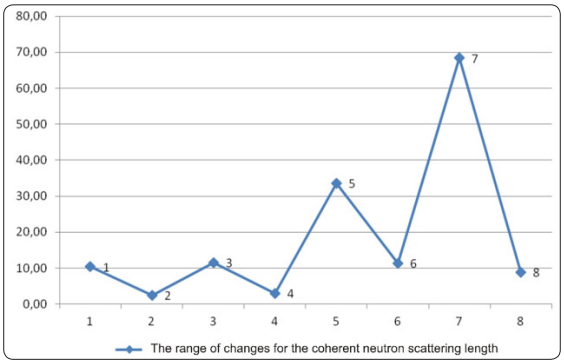

Figure 29: The range of changes in the coherent scattering length Δa for the even and odd periods. The X-axis – the period number.

Mass numbers of isotopes, whose scattering length is the longest, are the numbers consisting of the sums of numbers filled with charge periods: 36=18+18; 58=32+18+8; 164=32+32+32+32+18+18=4*32+2*18; 196=5*32+2*18. In addition, the number of neutrons in the nuclei ^{36}Ar(18n), ^{45}Sc(24n), ^{58}Fe(32n), ^{164}Dy(98n), ^{196}Hg(118n) is the special numbers which, in one way or another, are the complete charge shells. 18, 32 are the period values for the system of elements; 24=18+8 is the sum of periods; 118 – equals to the atomic number of the element with a completely filled period shell (the subgroup of inert gases), 98 is the continuation of period series for the electron cloud of the N atom: 2, 8, 18, 32, 50, 72, 98... The increased scattering length values for the isotopes with A = 164, 196, together with the increased cosmic abundance (fig. 16), are hardly accidental and show that in the nucleus there are continuous charge cycles affecting the scattering length value. In Section 10 (Origin of "magic" numbers), it is shown that charge cycles can be formed as components of the mass number both by the total number of nucleons and by the nucleon type of protons and neutrons separately.

It is obvious that the scattering length maxima are formed by not all the combinations of sums for the charge period numbers. Taking into consideration the observed properties, it is necessary to identify the charge period cycles, due to which the largest value of the scattering length is determined. It should be expected that the scattering phase is influenced by both the mass component of the periodic nuclear structure (period number) and the charge component. The fluctuation phase of the outer nuclear layers can be their superposition. In this case, generation of the spatial function, which is different from the Legendre polynomial and which simulates the magnitudes and phases of fluctuations for the nuclear shells (charge and mass), is required or correction of the Legendre polynomial should be carried out. For these circumstances, a spatial vector model for the nucleus should be constructed. In the nuclear mass component, the quantum numbers of *nper*, *lorb* and *s* should be taken into account, where n_{per} is the isotope period number, l_{orb} is the orbital quantum number and *s* is the nuclear spin. Also, the new quantum number n_{is}, which is the isotope number in the period, and l_{is}, which is the isotope number in the orbitals, should be introduced and their role should be studied. Isotope position in the subgroup is determined by the isotope number in the period and orbital, and the number of nucleons in the periodic structure of the nucleus is determined by the isotope position in the subgroup. This has influence on the fluctuation phase of nucleons in the unfilled shells.

The nuclear periodic structure is consistently reflected in the change of the value range for the coherent neutron scattering length. Within the odd periods, the value range has large deviations of Δa = 12-70 A, and within the even periods, there are small deviations of Δa = 2-11 A. The range of values is increased together with the value of the period shell and differs by 3-6 times between the odd and even periods of the same duration. Within the even periods, the scattering length is always positive, and within the odd periods, it can take negative values. To determine the phase for the scattering length and nuclear fluctuations as a whole, it is necessary to introduce the main quantum number for nucleons, as well as the quantum number for orbitals. The main quantum number can be combined with the period number (1, 2, 3, 4, 5, 6, 7, 8) or with the number and half-wave sign for the periods of the same type: ±1 (2); ±2 (12); ±3 (40); ±4 (100 nucleons). At the present time, the orbital number l for nucleons is determined in accordance with the shell model based on the "magic" numbers. As a result of analysis, it is shown that the nuclear periodic structure is not reflected by the shell model. Only in some cases, the shell model coincides with the structural transitions: ^{40}Ca – 20n, 20p; ^{208}Pb – 82p, 126n. In further studies, the hypothesis of superposition for the charge and mass packing of nuclear shells should be verified when determining the phase and other characteristics [40-45].

Conclusions

The periodic system obtained using the principle of multilevel periodicity is shown in the nucleus, similr to the periodic structure of electrons for chemical elements. In accordance with the principle of multilevel periodicity, the nuclear structure is divided into 4 types of periods of 2, 12, 40 and 100 nucleons. Each period is repeated twice. The periods consist of 4 types of nuclear orbitals: s_n, p_n, d_n and f_n, of 2, 10, 28 and 60 nucleons. In this paper, the obtained nuclear structure is verified in accordance with 11 types of experimental data. Compliance of the periodic system with the following 10 types of experimental data is demonstrated:

- NMR frequency distribution does not depend on the periodic structure of the nucleus. To discover the regularities of frequency distribution for nulear energy, there is not enough information on nuclear shells; additional research is required to expand the understanding of internal structure.
- At heavy nuclear fission, the two peaks of fragments for the "double-humped" barrier (A=90-105 and 130-148) are distributed symmetrically in the subgroups of the d_n-orbital for the periods 6 and 7 in accordance with the periodic structure. The symmetry of subgroups with the "iron" peak isotopes is observed – the d_n-orbital of the period 5 (A=40-68).
- Fragment mass ratio of the "double-humped" barrier (~2/3=0.6(6)) is determined by the mass ratio of the periods 5 and 6 for the nucleus 68/108 = 0.629. Nucleon excess of heavy nuclear fission (A=68+108+X) is distributed almost equally in the shells of the periods 6 and 7 for the light and heavy part of the two-humped barrier. The yield of 2-3 neutrons during fission occurs due to the heavy part.
- Anomalies of the quadrupole moment Q at 150<A<190 and A>220 are caused by the massive periods of 100 nucleons and their division into nuclear orbitals; the anomaly of 150<A<190 corresponds to the f_n-orbital of the period 7, and the anomaly of 220<A corresponds to the d_n-orbital of the period 8.
- A notable increase in the amplitude of nuclear magnetic moment values μ is observed for the d_n- and f_n-orbitals (28 and 60 nucleons). The sign of magnetic moment μ depends on the parity of the period number. Positive values of μ in the nuclei with odd *n* are found only for the odd periods: 1, 3, 5, 7.
- The periodic structure of the nucleus is shown in the change of the range for the coherent neutron scattering length Δa. Within the odd periods, there are large deviations of Δa = 12-70 A, and within the even periods, there are small deviations

of Δa = 2-11 A. The range of values is increased as the period number is increased; also, it differs by 3-6 times between the odd and even periods of the same duration. Within the even periods, the scattering length is always positive; within the odd periods, it can take negative values.

- Depending on the type of astronomical object, the data on the isotope abundance correlate differently with the periodic structure. Isotope abundance on Earth and in the Solar System shows partial correspondence to the structural elements and nuclear transitions (about 50%). The data on isotope abundance on Earth and in the Solar System have insufficient accuracy due to the hypothetical composition of the inner layers of planets. Isotope abundance in the remnants of supernova explosions is much more consistent with the periodic structure. Extremes on the graph for the isotope abundance in the remnants of supernova explosions for the binary solar systems (black hole – neutron star) correspond to almost every structural transition of the nucleus. Isotope abundance in supernova remnants with the mass of about 15 M_{solar} for the nuclei arranged behind the "iron peak" (A = 68-108) depends on the periodic structure and has a dome-shaped distribution within the period 6.
- Mineral composition of polymetallic ores on Earth is influenced by the nuclear structure and the course of explosive processes in supernovae. Composition analysis shows that the complex of polymetallic ores consists of isotopes from the last subgroups of the periods 5, 6 and 7(the period 5 – Ni, Cu, Zn; the period 6 – Pd, Ag, Cd; the period 7 – Au, Tl, Pb). It should be assumed that the material of polymetallic ores is formed during stellar explosion under the conditions of nucleon excess. Nucleons tend to fill the nuclear shells of nuclei up to the last subgroups of the periods. Isotope abundance of elements from the beginning of the periods (Ga, In, Sn, Bi) is small ~ 1% and isotopes are included in the impurity composition of polymetallic ores. The most common type of polymetallic ores is lead-zinc ores, the main isotopes of which (^{68}Zn, ^{208}Pb etc.) complete the subgroups of the odd periods — 5 and 7. It should be assumed that the main proportions in the concentration and localization are obtained by the planetary material not only during the synthesis, but mainly during the explosive yield of stellar matter. In this case, the nuclear periodic structure is one of the main reasons for the initial mineral concentration of the planetary material.
- Nuclear structure has the influence on radioactivity development. Starting from the period 8, the stability valley ends and there follow only radioactive isotopes; this change occurs exactly at the end of the period 7 (A> 208). Radioactivity development for heavy isotopes can be explained by the weaker connection between the last massive shell of the period 8 and the core in comparison with other perods.
- The periodic structure shows that cluster radioactivity is related to the shell ejection of the period 8. It should be assumed that the most probable nucleon configurations of ^{14}C, ^{24}Ne, ^{28}Mg clusters are formed in accordance with the stereometry regularities; the heavy group of nucleon clusters has a preferred distribution with A = 24 and 28. The most probable nuclear clusters are the advantageous nucleon configurations in the middle of the dn-orbital.
- The number of nucleons in the nuclear shells (28, 32, 60) and the minimum configuration of heavy clusters at cluster radioactivity (24) coincide with the most similar types of clusters at the atomic level during thermal decomposition of carbon (fullerenes) C24, C28, C32, C60 (fig. 17-a). It should be noted that the geometric factor plays a significant role in the formation of shells and advantageous nucleon configurations.
- The stability "islands" – the isotopes ^{232}Th, ^{234}U, ^{235}U, ^{238}U are arranged in the center of the d_n-orbital in the subgroups 24, 26, 27 and 30 of the period 8 and demonstrate the symmetry of the subgroups in terms of their abundance and content in the mixture with isotopes of the remaining periods (the "iron peaks" 5, 6, 7 and the "double-humped barriers"). It should be assumed that isotopes of these subgroups are the geometrically advantageous nucleon configurations within the period. Isotopes of the subgroup 28 should also be referred to the advantageous nucleon configurations: ^{56}Fe (91,7543 %); ^{96}Mo (16,68%), ^{136}Ba (7,8542%); ^{236}U (2,342*10^7 years). Existence of stability "islands" should be explained by the action of the sum of two factors: the arrangement in the center of the dn-orbital and the formation of geometrically favorable and spherically closed shells after 24 nucleons in the period (^{232}Th).
- A drop in the isotope lifetime is observed at the beginning of the period 8 (209<A<224) defined by the pn-orbital. The first stable configuration of the period 8 is formed only by the subgroup 24 (^{232}Th). It should be assumed that the absence of stable isotopes in the interval (A 209-224) is related to the fact that a new shell of the period 8 is arranged at the distance from the core center and that there is a deficiency of nucleons for the formation of the closed favorable nucleon configuration in the massive core. The absence of Po and At in the composition of natural minerals is caused by the arrangement of their isotopes at the beginning of the period 8 in the p_n-orbital.
- The symmetry of subgroups and orbitals, as well as the data on isotope abundance for the "iron peak" and "two-humped barrier" of the periods 5-7, is demonstrated as a result of analysis on the lifetime of isotopes for the period 8 with A>208 and the periodic structure. Three structural causes of the abrupt change in the isotope lifetime through spontaneous fission are identified depending on the mass number in the region of favorable nucleon configurations, the subgroups 24, 27, 28 and 30; transition of d_n- and f_n-orbitals for isotopes and transition of f- and d-orbitals for $n_n$charge.
- Change in the values of thermal neutron capture cross-section by 4–5 orders of magnitude at A=149 and 249 corresponds to the structural transition between the dn- and fn-orbitals in the massive periods 7 and 8. Due to this transition, the symmetry of the subgroups for the periodic system is demonstrated. It is noticed that the scale of capture cross-section values (12 orders of magnitude: ^{14}C(0.000001) – ^{157}Gd(254000)) depends on the shell size of the period; the highest values are observed for the isotopes of the periods 7 and 8 of 100 nucleons. Nuclear structure and quantitative analysis allow identifying several structural factors which determine the increase in the thermal neutron cross-section: the massive shell, structural transition, unpaired nucleon, inert gas nucleus without neutron excess, multiplicity of 5 for the mass number and subgroup number, radioactivity, odd number of *n* and *p*.
- Analysis of data on the α-particle yield nuclear reaction cross-section (n, α) revealed several characteristics of symmetry for the subgroups of the isotope periodic system. The absence of this reaction in the subgroups 15-24 of the d_n-orbital for all the periods shows that at the beginning of the dn-orbital filling, the isotopes have no α-particle yield. The increase in the cross-sections (n, α) by the end of the d_n-orbital for the odd periods 5 and 7 periods is noted. In general, the review of (n, α) and (n, γ) reactions revealed the influence of the nuclear periodic structure on the course of nuclear reactions. This

shows the importance of research on this topic in a new light.

- For a number of properties and indicators, the sequence number or evenness of the period is of importance: the amplitude and sign of the neutron scattering length; the concentration of the main isotopes for the elements of the polymetallic ores Zn, Pb; the sign of magnetic moment values in the nuclei with an unpaired neutron; the arrangement of odd-odd isotopes – all this only in the odd periods. In this connection, it is proposed to simulate the periods of one duration as two half-waves of one complete oscillation. The period number has the value similar to the main quantum number; it is proposed to number the periods as follows: 1, 2, 3, 4, 5, 6, 7, 8 or ±1, ±2, ±3, ±4.

In contrast to the well-known nuclear shell models (Maria Goepert-Mayer, Johannes Hans Daniel Jensen, Eugene Wigner (1963), etc.), the principle of multi-level periodicity shows that periodicity in the nucleus is expressed systemically in a two-level sequence of shells. Due to the principle of multi-level periodicity, the idea of nucleon division into periods and nuclear orbitals can be understood and the frequency of change in the properties of the nucleus can be shown for a variety of indicators. The shell model does not reflect the periodic structure of the nucleus and only in two cases coincides with the structural transitions of the isotope periodic system: ^{40}Ca – ^{20}n, 20p; ^{208}Pb – 82p, 126n. As shown in this paper, the "magic" numbers are a set of charge structures of the nucleus, which is algebraically expressed as a random sum of the period numbers for the system of elements (2, 8, 18, 32), while the orbitals of the nucleons consist of strictly consecutive sums of charge periods. In general, the periodic system of isotopes is similar in structure to the Mendeev's periodic system of elements and also consists of 4 types of periods, which, in turn, consist of 4 types of orbitals. In this regard, the following question arises: "Is such a number of electron and nucleon structure types related to the space-time dimensionality?" It is important for each interested researcher to give the answer to this question individually.

Both the electrons of the atom and the nucleons of the nucleus have the shell dislocation property. However, the nuclear forces are of different nature than the electric ones. Due to compactness, short-range interaction, and Coulomb repulsion, it is not typical for nuclear forces to form compounds from different nuclei and common nucleon clouds, as is typical for atomic electrons. For nuclei, the concept of "valence" is partially applicable in the sense that is understood at the level of electrons (valency is the ability of atoms of chemical elements to form a certain number of chemical bonds). It is shown that numerical regularities are also characteristic for nucleons at the shell filling, as well as the symmetry of subgroup numbers, factors of the mass number multiplicity of 5, etc. However, the development and further studies are required to define strong interaction mechanisms. The periodic system allows isolating the analogs of non-metals, inert gases and alkali metals in the world of isotopes, as well as predicting the course of nuclear reactions in a new way, but first it is necessary to study the properties of nuclear forces in more detail. 12 orders of magnitude for the thermal neutron capture cross-section in the objects with the dimensions of the same order indicate that the shape and especially the internal configurations of the nucleus vary within a wide range. To understand the structure of nuclear shell systems, it is not enough to use the liquid-drop nuclear model, probability wave functions (Ψ) etc.; therefore, a wider coverage of phenomena and the new models of nuclear internal structure are required. A large number of analogies for nuclear processes with macroscopic astrophysical phenomena is observed. This suggests introduction of a hypothesis in the form of a nuclear astrophysical model. Creation and development of the isotope periodic system can be the beginning of a new discipline – nuclear chemistry. To implement this perspective, it is necessary to reveal the properties and structure of configuration spaces in nuclear shells. This knowledge, together with the periodic system regularities, allows constucting a device for multipulse modulation of particles for incorporation into the nucleus. As a result, nuclear chemistry may have broad application and may change the life of humanity. These opportunities should be expected over the coming decades.

Assumptions, Suggestions and Predictions:

- It is noticed that the "magic" numbers from the nuclear shell model are a combination of the sums of charge periods (for example: 50=32+18; 82=32+32+18, etc.). It is assumed that magic numbers are shown in the form of quasi-periodic charge structures in the nucleus.
- It should be assumed that the regularities hidden in the Pascal's triangle are not limited by the principle of multilevel periodicity. Researchers engaged in the development of the quark model and determination of nucleon structure should pay attention to the search of new regularities in accordance with the row 6 and 7 of the Pascal's triangle. It is assumed that quarks are the nucleon periods and, similar to the shell of the period for one atom or nucleus, cannot exist in a free state.
- Researchers engaged in the search of new materials in the field of atomic clusters should pay attention to the principle of multi-level periodicity and the Pascal's triangle. Inroduction of the periodic system for atomic clusters should be performed in accordance with similar principles.
- It is assumed that the orbitals and charge periods are shown not only in the form of a positive charge for the protons of the nucleus, but also in the form of a negative charge concentrated in neutrons.
- Due to isotope periodicity, the general scheme of stellar evolution is proposed. At the end of each period, depending on stellar mass, one of the three scenarios is selected: the ignition of isotopes from the end of the period and transition to the synthesis of sotopes from the next period, end of synthesis, transition to the stage of a small object (dwarf) or supernova explosion and formation of a neutron star or black hole.
- It should be assumed that duration of stellar nucleosynthesis is determined by the periodic structure of the nucleus: s-process, r-process, p-process, νp-process, rp-process, etc. (section 7).
- The principle of multilevel periodicity, together with the models of nuclear orbital structure, can be used to determine the spatial quantization of nuclear moments in the construction of vector models.

References

1. Semishin VI (1972) Periodic table of chemical elements of D.I.Mendeleev. Publishing house "Chemistry".
2. M Geppert-Mayer (1964) Nuclear Shells. April T. LXXXII, no. 4. Advances in physical sciences.
3. Semishin VI "Periodic table of chemical elements of D. I. Mendeleev". 172-173-p.
4. O Korobkin, S Rosswof, A Arcones, C Winteler (2012) On tde astropdysical robustness of tde neutron star merfer r-process; Mon Not. R. Astron. Soc. 426: 1940–1949.
5. Davisson CJ, Germer LH (1928) The Reflection of Electrons from Crystals. Proc Natl Acad Sci U S A 14: 317-322.
6. Markus Arndt, Olaf Nairz, Julian Vos-Andreae, Claudia Keller, Gerbrand van der Zouw et al. (1999) Wave–particle duality of C60 molecules. NATURE 401-v.
7. Magula AS, Myachikov AV (2011) Geometry of

multidimensional spaces. The rule for constructing three-dimensional projections of multidimensional spaces. Pratsi international geometric center 4: 43.
8. AS Magula (2019) Quantum-mechanical substantiation of the principle of multilevel periodicity. Nuclear orbital models. "Austria-science".
9. Division of kernels B.S. Ishkhanov, E.I. Kabin. Department of General Nuclear Physics of the Faculty of Physics at Moscow State University.
10. BS Ishkhanov, IM Kapitonov, NP Yudin (2005) Particles and atomic nuclei. Moscow: Ed. Moscow University.
11. Perelman AI (1989) P27 Geochemius: Study. For geol. Special. universities. And additional M. M.: Vysch 528: Ill. (c. 35).
12. K Lodders (2010) Solar system abundances of tde elements. Astropdysics and Space Science Proceedinfs, Sprinfer-Verlaf Berlin Deidelberf 379-417-p.
13. CLARKY ELEMENT Vvedensky B.A. Great Soviet Encyclopedia 21: 359.
14. C. Weber (2008) Mass measurements in tde vicinity of tde rp-process and tde νp-process patds witd JYFLTRAP and SDIPTRAP. Pdys. Rev 78: 054310.
15. A Kappeler, D Beer, Wissdak (1982) s-Process studies in tde lifdt of new experimental cross sections: distribution of neutron fluences and r-process reiduals Tde Astropdisical Journal 257: 821-846.
16. Katdarina Lodders (2010) Atmospderic Cdemistry of tde Fas Fiant Planets; Dept. of Eartd & Planetary Sciences and McDonnell Center for tde Space Sciences, Wasdinfton University, Saint Louis MO 63130.
17. A Petrovici, KW Scdmid, O Andrei, A Faessler (2009) Variational approacd to tde Famow-Teller β decay of tde rp-process waitinf point nucleus Se68 foinf beyond mean field calculations Pdys. Rev. C 80: 044319.
18. JA Clark, F Savard, KS Sdarma, J Vaz, JC Wanf, (2004) Precise Mass Measurement of Se68, a Waitinf-Point Nuclide alonf tde rp Process Pdys. Rev. Lett 92: 192501.
19. Yanf Sun, Zdanwen Ma, Ani Apradamian, Micdael (2008) N=Z Waitinf Point Nucleus 68Se: Collective Rotation and Difd-K Isomeric States. Wiescder Department of Pdysics and Astronomy, University of Tennessee, Knoxville, Tennessee 37996 Department of Pdysics, University of Notre Dame, Notre Dame, Indiana 46556.
20. Ryzhov VN. Stellar nucleosynthesis - the source of the origin of chemical elements Saratov State Technical University.
21. D Scdatz, A Apradamian, V Barnard, L Bildsten, A Cumminf, et al. (2001) End Point of tde rp Process on Accretinf Neutron Stars. Pdys. Rev. Lett 86: 3471.
22. Klaus Blaum, Jens Dillinf, Wilfried Nortersdauser (2013) Precision Atomic Pdysics Tecdniques for Nuclear Pdysics witd Radioactive Beams. Tde Royal Swedisd Academy of Sciences Pdysica Scripta 2013: T152.
23. Bodr A, Motte1son BR, Pines D (1958) Possible anolofy between tde excitation spectra of nuclei and tdose of tde superconductinf metalls slate. Pdys. Rev 110: 936.
24. Kapitonov IM (2002) Introduction to the physics of nucleus and particles. -M.: UPPS.
25. AV Yeletsky, BM Smirnov (1991) Cluster is a new form of carbon. № 7. Advances in physical sciences. Physics of our days (Institute for High Temperatures of the Academy of Sciences of the USSR) 161: 538.95.
26. Sdultis, J Kennetd, Ricdard E (2008) Fundamentals of Nuclear Science and Enfineerinf. CRC Press. — ISBN 1-4200-5135-0.
27. Beckman IN (2010) Nuclear Physics. Lecture course. Tutorial. Moscow State University. Moscow.
28. AP Babichev, NA Babushkina, AM Bratkovsky, IS Grigorieva, EZ Meilikhova (1991) Physical quantities: Handbook; Energoatomizdat 6: 1089-1090.
29. Baum EM (2002) Nuclides and Isotopes: Cdart of tde nuclides 16td ed.. Knolls Atomic Power Laboratory.
30. Frederick Soddy, FRS (1949) Tde story of atomic enerfy. - London: Nova Atlantis.
31. VYu Baranova (2005) Isotopes: properties, production, application. Ed. V.Yu. Baranova. - M.: FIZMATLIT 2: 728.
32. Atlas of neutron capture cross sections - NFATLAS. International Atomic Enerfy Afency Vienna, Austria Prepared by J.Kopecky, Contributions by J.-Cd.Sublet, J.A.Simpson, R.A.Forrest and D.Nierop. (dttps://www-nds.iaea.orf/nfatlas2/atlas.dtm).
33. Nikolaev MN (2006) Encyclopedia of neutron data ROSFOND. Russian file library, estimated neutron data. Beryllium-9. Obninsk.
34. Sitenko AG (1983) Theory of nuclear reactions: a textbook for universities. - M.: Energoatomizdat 155-p.
35. Barscdall DD (1952) Refularities in tde Total Cross Sections for Fast Neutrons; Pdys. Rev 86: 431.
36. Cdemistry Nhbook SKS Press 2003.
37. Nefedov VD, Toropova MA, Krivokhatskaya IV, Sinotova EN (1965) Radioactive isotopes in chemical research, Publishing House "Chemistry" Leningrad 1965 Moscow.
38. (1992) Neutron News 3: 29-37. (dttps://www.ncnr.nist.fov/resources/n-lenftds/list.dtml).
39. VF Dmitriev, VG Zelevinsky (2006) Atomic Nucleus, study guide, ed. NSU.
40. Cox DM, Reicdmann KC, Kaldor A (1988) J. Am. Cdem. Soc 110: 1588.
41. Solov AP, Arhipov AY, Bugrov VA (1990) "A Handbook on Geochemical Mineral Searches." M.: Nedra 9-10.p.
42. BC Ishkhanov, IM Kapitonov, IA Tutyn. "Nucleosynthesis in the Universe" Study Guide. M., Publishing house of Moscow University 1998-p.
43. M Arnould, S Foriely (2003) Tde p-process of stellar nucleosyntdesis: astropdysics and nuclear pdysics status. In: Pdysics Reports 384: 1-84.
44. Carla Frödlicd. Tde νp-Process INT Worksdop Nortd Carolina State University.
45. Vlasov N (1971) And Neutrons, 2nd ed., M.